International School for Advanced Studies

Physics Area / Condensed Matter

Ph.D. thesis

Landau-Zener processes in out-of-equilibrium quantum physics

Candidate
Tommaso Zanca

Supervisor
Prof. Giuseppe E. Santoro

October 2017
Via Bonomea 265, 34136 Trieste - ITALY

Alla mia famiglia

Dicebat Bernardus Carnotensis nos esse quasi nanos,
gigantium humeris insidentes, ut possimus plura eis et remotiora videre,
non utique proprii visus acumine, aut eminentia corporis,
sed quia in altum subvehimur et extollimur magnitudine gigantea.

John of Salisbury

Omnia disce.
Videbis postea nihil esse superfluum.
Coartata scientia iucunda non est.

Hugh of Saint Victor

Acknowledgements

First of all I would like to thank my supervisor Prof. Giuseppe E. Santoro and Prof. Erio Tosatti for guiding me along my research projects with valuable advice, patience and encouragement. A special thank to Dr. Franco Pellegrini, who assisted me with his priceless help especially during the programming phase, he always had a solution! Thanks to my office mates and friends Maja, Francesco and Daniele: the working days in office "416" could not have been funnier. I am grateful to my friends Mariam, Caterina, Lorenzo, Simone and Kang for their support and encouragement throughout my Ph.D. Thanks to all the friends with whom I spent great time and shared wonderful experiences during my stay in Trieste. Finally, thanks to my family, that always supports me and believes in me.

Publications

The work of this thesis has been published in the following papers:

1. T. Zanca and G. E. Santoro, *Quantum annealing speedup over simulated annealing on random Ising chains*, Phys. Rev. B **93**, 224431 (2016)

2. T. Zanca, F. Pellegrini, G. E. Santoro and E. Tosatti, *Quantum lubricity*, arxiv.org/abs/1708.03362 (2017)

Contents

Introduction **1**

1 Quantum annealing versus simulated annealing on random Ising chains **5**
1.1 Model and methods for the classical problem 6
1.1.1 Glauber dynamics 6
1.1.2 Mapping into a quantum dynamics 7
1.1.3 Jordan-Wigner mapping 10
1.1.4 Diagonalization of Hamiltonian in the ordered case 12
1.1.5 Ground state and lowest excited states of the Ising model 15
1.2 Simulated and quantum annealing for ordered case 16
1.2.1 Simulated annealing 16
1.2.2 Quantum annealing 18
1.3 Results for the ordered case 21
1.4 Simulated and quantum annealing for disordered case 25
1.5 Results for the disordered case 27
1.5.1 Minimal gap distributions 27
1.5.2 Annealing results 27
1.6 Conclusions 35

2 Quantum lubricity **37**
2.1 Quantum model 38
2.1.1 Wannier functions basis 38
2.1.2 Dynamics 43
2.1.3 Quantum master equation 44
2.2 Classical model 48
2.2.1 Numerical integration 51
2.3 Results 53
2.4 Conclusions 57

3 Conclusions and perspectives **59**

A Landau-Zener problem **61**
A.1 The model 61
A.2 Derivation of Landau-Zener formula 62
A.3 Numerical solutions 65

B Computation of observables **69**
B.1 Ordered case 69
B.2 Disordered case 70

C The BCS-form of the ground state. **73**

D Derivation of the Green's functions **75**

E Quantum master equation **77**
E.0.1 Assumptions regarding the Bath 79
E.0.2 A perturbative derivation of the quantum Master equation. 80

Introduction

In out-of-equilibrium quantum physics the evolution of a system is generally described by a time-dependent Hamiltonian. Exact solutions to such problems are very rare, given the difficulty to solve the associated time-dependent partial differential equations. However, it is possible to obtain useful insights on the dynamics by analyzing it in terms of simplified descriptions of the single non-adiabatic processes that occur during the evolution.

A *non-adiabatic* process is a transition between quantum states governed by a time-dependent Hamiltonian. Its prototypical example is called *Landau-Zener* (LZ) problem. The model was introduced in 1932, when Zener published the exact solution to a one-dimensional semi-classical problem for non-adiabatic transitions [1]. In the model, nuclear motion is treated classically, in which case, it enters the electronic transition problem as an externally controlled parameter. As Landau had formulated and solved the same model independently (although in the perturbative limit and with an error of a factor of 2π) [2], it came to be known as the Landau-Zener model. Despite its limitations, it remains an important example of a non-adiabatic transition. Even in systems for which accurate calculations are possible, application of the LZ model can provide useful "first estimates" of non-adiabatic transition probabilities. Alternatively, for complex systems, it may offer the only feasible way to obtain transition probabilities. Landau-Zener problems are met in a large number of areas in physics including quantum optics, magnetic resonance, atomic collisions, solid state physics, etc. In this thesis we discuss two quantum problems for which the LZ process represents the basic paradigm of their evolutions.

First work: Simulated annealing vs quantum annealing

In the first problem we study the *quantum annealing* (QA) and *simulated annealing* (SA) of a one-dimensional random ferromagnetic Ising model. QA is the quantum counterpart of SA, where the time-dependent reduction of thermal fluctuations used to search for minimal energy states of complex problems are replaced by quantum fluctuations. Essentially, any optimization problem can be cast into a form of generalized Ising model [3] $\hat{H}_P = \sum_p \sum_{i_1 \ldots i_p} J_{i_1 \ldots i_p} \hat{\sigma}^z_{i_1} \ldots \hat{\sigma}^z_{i_p}$ in terms of N binary variables (Ising spins). In many cases, two-spin interactions are enough ($p = 2$), but some Boolean Satisfiability (SAT) problems involve $p = 3$ or larger. Quantum

fluctuations are often induced by a transverse field term $\hat{H}_D = -h_x \sum_i \hat{\sigma}_i^x$ by constructing a time-dependent quantum Hamiltonian interpolating the two terms: $\hat{H}(s(t)) = [1 - s(t)]\,\hat{H}_D + s(t)\hat{H}_P$ with $s(0) = 0$ and $s(\tau) = 1$, τ being a sufficiently long annealing time. Usually, the Hamiltonian as a function of s displays a *quantum phase transition* at $s = s_c$, separating the $s = 0$ (trivial) quantum paramagnetic phase from a complex, often glassy, phase close to $s = 1$. If the system is assumed to evolve unitarily, then one should solve the Schrödinger equation

$$i\hbar\,\partial_t\,|\psi(t)\rangle = \hat{H}(t)\,|\psi(t)\rangle \ . \tag{1}$$

The initial state is the simple ground state of $\hat{H_D}$:

$$|\psi(0)\rangle = \prod_i \left[|\uparrow\rangle_i + |\downarrow\rangle_i\right]/\sqrt{2}\,, \tag{2}$$

which is maximally disordered (any spin configuration has the same amplitude). The goal is to make the final state $|\psi(\tau)\rangle$ as close as possible to the optimal (classical) state of the problem Hamiltonian $\hat{H}_P$. The bottleneck in the adiabatic evolution is usually due to a spectral gap Δ above the instantaneous ground state which closes at $s = s_c$ either polynomially (for a 2nd-order critical point) or exponentially (for a 1st-order point or in some disordered cases) in the number of variables N. In this case, a short annealing time would give rise to excitations (*defects*) that can be easily explained and quantified in terms of LZ processes.

The idea of QA is more than two decades old [4–7], but it has recently gained momentum from the first commercially available quantum annealing programmable machines based on superconducting flux quantum bits [8,9]. Many problems remain open both on fundamental issues [10–13] and on the working of the quantum annealing machine [14–16]. Among them, if and when QA would provide a definite speedup over SA [17], and more generally, what is the potential of QA as an optimization strategy for hard combinatorial problems [18–20].

In this thesis we present our results on QA and SA of a one-dimensional ferromagnetic Ising model. The motivation for studying this problem is to determine whether the quantum evolution is faster in reaching the ground state than its classical counterpart in both ordered and disordered chains. Even though the problem is simple from the point of view of combinatorial optimization – the two classical ground states are trivial ferromagnetic states with all spins aligned –, it has a nontrivial annealing dynamics. Usually, the comparison is done by looking at classical Monte Carlo SA against path-integral Monte Carlo QA [7, 21–25], but that raises issues related to the stochastic nature of Monte Carlo technique. For this specific problem, we propose a direct comparison between QA and SA performing *deterministic* evolutions of both cases. The fact that SA does not encounter any phase transition during the evolution, contrary to the QA case, would lead to think that the excitations are reduced in the classical annealing, and therefore one intuitively expects that SA would overtake QA in reaching the ground state. This is in contradiction with the results of our simulations, which clearly demonstrate a *quadratic*

quantum speedup. Our machinery allows us to perform quantum annealing also in imaginary time, where an *exponential speedup* is visible. This remarkable result suggests that "quantum inspired" algorithms based on imaginary-time Schrödinger QA might be a valuable route in quantum optimization.

This work has been published in Physical Review B: T. Zanca and G. E. Santoro, *Quantum annealing speedup over simulated annealing on random Ising chains*, Phys. Rev. B **93**, 224431 (2016).

Second work: Quantum lubricity

The second problem we address is a model of *quantum nanofriction*. Quantum effects in sliding friction have not been discussed very thoroughly so far, except for some early work [26–28]. The reason is that in general the motion of atoms and molecules can be considered classically and the quantum effects that may arise at low temperatures are not deemed to be dramatic. Moreover, the scarcity of well defined frictional realizations where quantum effects might dominate and, on the theoretical side, the lack of easily implementable quantum dynamical simulation approaches are additional reasons for which this topic has received very little attention. Recently, new opportunities to explore the physics of sliding friction, including quantum aspects, are offered by cold atoms [29] and ions [30] in optical lattices.

In this work we show, anticipating experiment, that a first, massive quantum effect will appear already in the simplest sliding problem, which should also be realisable experimentally by a cold atom or ion dragged by an optical tweezer. The problem is that of a single particle forced by a spring k to move in a periodic potential:

$$\hat{H}_{\mathrm{Q}}(t) = \frac{\hat{p}^2}{2M} + U_0 \sin^2\left(\frac{\pi}{a}\hat{x}\right) + \frac{k}{2}\left(\hat{x} - vt\right)^2 \ . \tag{3}$$

The dissipation due to frictional force is provided by the interaction with a harmonic bath:

$$\hat{H}_{\mathrm{int}} = \sum_i \left[\frac{\hat{p}_i^2}{2m_i} + \frac{1}{2}m_i\omega_i^2\Big(\hat{x}_i - \frac{c_i}{m_i\omega_i^2}\hat{X}\Big)^2\right] \ , \tag{4}$$

where each oscillator position $\hat{x}_i$ is coupled to the periodic position of the particle $\hat{X} = \sin\left(\frac{2\pi}{a}\hat{x}\right)$. This problem is a quantum version of the renowned Prandtl-Tomlison model, where the dissipative dynamics is simulated by a classical Langevin equation:

$$M\ddot{x}(t) = -\gamma\,\dot{x}(t) - \frac{\partial}{\partial x}V[x(t),t] + \xi[x(t),t] \ , \tag{5}$$

with $V[x(t),t]$ the total potential, γ the dissipation factor and ξ the random force that simulates the thermostat. Conversely from the classical case, where the dynamics is simulated by means of stochastic processes, the quantum version is solved by a quantum master equation for the reduced matrix. Being a perturbative method, accurate results are available only for small system-bath

couplings. As we will show, the main quantum effect, amounting to a force-induced LZ tunnelling, is striking because it shows up preferentially for strong optical potentials and high barriers, where classical friction is large, but resonant tunnelling to a nearby excited state can cause it to drop – a phenomenon which we may call *quantum lubricity*. Moreover, at very low dragging velocities, LZ theory predicts a regime where friction vanishes non analytically $\sim \mathrm{e}^{-v^*/v}$, where v^* represents a velocity-scale for adiabaticity/non-adiabaticity transition. Despite its conceptual simplicity, this model provides theoretical results on quantum effects which have not been observed yet experimentally, but should be well within experimental reach for cold atoms/ions in optical lattices. Again, LZ process is the fundamental mechanism that describes the quantum evolution of sliding friction and explains the huge difference between classical and quantum results.

A paper about this work is available on arXiv.org: T. Zanca, F. Pellegrini, G. E. Santoro and E. Tosatti, *Quantum lubricity*, arxiv.org/abs/1708.03362 (2017).

Outline

This thesis is organized in the following way: in Chapter 1 we present the work on QA and SA problems. We start describing the mapping of the classical model into an imaginary-time quantum problem. We then derive the equations of motion for classical and quantum problems using the same structure for the Hamiltonians. Finally we present the results of the simulations, comparing the dynamics for SA and QA in real and imaginary time. Chapter 2 shows the second work on quantum lubricity. The first section of the chapter introduces the quantum model and the quantum master equation. In the second section we derive the classical Langevin equation from the same Hamiltonian used for the quantum model. Finally we compare the results of simulations for classical and quantum models, highlighting the difference between them originated by the quantum effects. In Chapter 3 we present a summary and conclusions. Technical details are contained in a number of final Appendices.

Chapter 1

Quantum annealing versus simulated annealing on random Ising chains

The first problem we studied is the dynamics of a one-dimensional ferromagnetic Ising model in classical (SA) and quantum (QA) annealing. As anticipated in the Introduction, the importance of this model is the possibility to obtain solutions of optimization problems by searching states of minimal energy through the reduction of thermal – for SA – or quantum – for QA – fluctuations.

For SA, the system consists in a ferromagnetic Ising spin chain in equilibrium at a certain high temperature. In this condition all the spins have random orientations. The aim is to drive the system towards minimal energy configurations by slowly decreasing the temperature, ending possibly in the ground state at the end of evolution when temperature vanishes.

The QA protocol is very similar to SA, with the only difference that temperature is replaced by a transverse magnetic field. In the same way, a high value of the magnetic field forces the spins to orient on the x-magnetic axis and therefore randomly on the quantized z-axis. Through a slow reduction of the magnetic field the system follows an adiabatic evolution remaining in its instantaneous ground state, that corresponds to the optimization problem solution at the end of evolution.

The question is whether SA or QA is more efficient – in terms of annealing time τ – in reaching the ground state. In fact, if the annealing time is too short, a non-adiabatic evolution takes place – as in the simple LZ problem – giving rise to excitations that spoils the final solution. This excitations emerge physically through the presence of defects – antiparallel spin configurations – that quantify the "distance" from the known ground state.

Results for real-time Schrödinger QA are known for the ordered [31,32] and disordered [33,34] Ising chain, already demonstrating the crucial role played by disorder, in absence of frustration: the Kibble-Zurek [35, 36] scaling $1/\sqrt{\tau}$ of the density of defects $\rho_{\rm def}$ generated by the annealing

of the ordered Ising chain [12,37,38], turning into a $\rho_{\rm def} \sim \ln^{-2} \gamma\tau$ for the real-time Schrödinger QA with disorder [33,34].

We addressed this problem and simulated the dynamics performing deterministic evolutions. The possibility to map the SA master equation into an imaginary-time Schrödinger equation allowed us to perform its evolution with the same strategy used for QA. In this way we could compare on equal-footing the two cases, without dealing with complications related to stochastic issues typical of Monte Carlo simulations.

For SA, we resort to studying a Glauber-type master equation with a "heat-bath" choice for the transition matrix. After a Jordan-Wigner fermionization, the problem is then translated into an imaginary-time Schrödinger equation with a quadratic – diagonalizable – Hamiltonian. The real (QA-RT) and imaginary (QA-IT) time Schrödinger equations are easier to derive, applying directly the Jordan-Wigner transformation.

At this point the three equations of motion have the same structure. Nevertheless, the classical dynamics is different from the quantum counterpart, with the main difference that the former does not encounter any phase transition during the evolution, differently from the quantum case. Despite that, it turns out that the QA-RT and QA-IT dynamics have a faster scaling laws for the density of defects, specifically a quadratic and exponentially speedup with respect to SA.

1.1 Model and methods for the classical problem

In this first section we describe the classical model and how to map the corresponding Glauber master equation into a quantum problem in imaginary time.

1.1.1 Glauber dynamics

The problem we deal with is that of classical Ising spins, $\sigma_j = \pm 1$, in 1d with nearest-neighbor ferromagnetic random couplings $J_j > 0$ (Fig. 1.1), with Hamiltonian

$$H = -\sum_{j=1}^{L} J_j \sigma_j \sigma_{j+1} \ . \tag{1.1}$$

Its classical annealing dynamics can be described by a Glauber master equation (ME) [39] that takes the form

$$\frac{\partial P(\sigma,t)}{\partial t} = \sum_j P(\bar{\sigma}_j,t) W_{\bar{\sigma}_j,\sigma} - \sum_j P(\sigma,t) W_{\sigma,\bar{\sigma}_j} \ , \tag{1.2}$$

where $\sigma = (\sigma_1, \cdots, \sigma_L)$ denotes a configuration of all L spins, with a probability of $P(\sigma,t)$ at time t, $\bar{\sigma}_j = (\sigma_1, \cdots, -\sigma_j, \cdots, \sigma_L)$ is a configuration with a single spin-flip at site j, and $W_{\sigma,\bar{\sigma}_j}$ is the transition matrix from σ to $\bar{\sigma}_j$.[1] The rates W will depend on the temperature T , which

[1] In Glauber's notation $W_{\sigma,\bar{\sigma}_j} = w_j(\sigma_j)$ and $W_{\bar{\sigma}_j,\sigma} = w_j(-\sigma_j)$.

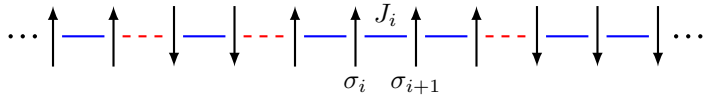

Figure 1.1: Sketch of the ferromagnetic Ising chain. Dashed red links represent the *defects*.

is in turn decreased as a function of time, $T(t)$, to perform a "thermal annealing". The detailed balance (DB) condition, which is a sufficient condition to reach equilibrium, restricts the possible forms of W to the following:

$$P_{\rm eq}(\bar{\sigma}_j)W_{\bar{\sigma}_j,\sigma} = P_{\rm eq}(\sigma)W_{\sigma,\bar{\sigma}_j} \ , \tag{1.3}$$

where $P_{\rm eq}(\sigma) = {\rm e}^{-\beta H(\sigma)}/Z$ is the Gibbs distribution at fixed $\beta = 1/(k_B T)$ and Z the canonical partition function. However, many possible choices of W are compatible with DB, and we can exploit that freedom. Let us denote by $\Delta E = H(\bar{\sigma}_j) - H(\sigma)$ the energy change upon flipping a spin at site j. One of the most common choices is the *Metropolis choice* $W^{(M)}_{\sigma,\bar{\sigma}_j} = \alpha \, \min[1, {\rm e}^{-\beta\Delta E}]$, α being an arbitrary rate constant (which can always be reabsorbed in our units of time). Although very popular in numerical Monte Carlo work, this choice is not ideal for our purposes, because it is not an analytical function of ΔE: we will not consider it further. Another popular choice (also in numerical work) is the so-called *heat bath*:

$$W^{(\rm hb)}_{\sigma,\bar{\sigma}_j} = \frac{\alpha \, {\rm e}^{-\beta H(\bar{\sigma}_j)}}{{\rm e}^{-\beta H(\sigma)} + {\rm e}^{-\beta H(\bar{\sigma}_j)}} = \frac{\alpha \, {\rm e}^{-\beta\Delta E}}{1 + {\rm e}^{-\beta\Delta E}} = \frac{\alpha \, {\rm e}^{-\beta\Delta E/2}}{{\rm e}^{\beta\Delta E/2} + {\rm e}^{-\beta\Delta E/2}} \ . \tag{1.4}$$

From the first form the validity of DB is immediately obvious (the denominator is symmetric), while the last form is the most useful one. Another possible choice of W is what Glauber does in its original paper: it is similar to the heat bath, with the omission of the denominator: [2]

$$W^{(\rm G)}_{\sigma,\bar{\sigma}_j} = \alpha \, {\rm e}^{-\beta\Delta E/2} \ . \tag{1.5}$$

1.1.2 Mapping into a quantum dynamics

Our target now is to map the classical Glauber ME into a quantum imaginary-time (IT) Schrödinger problem. The general idea is that DB can be used to *symmetrize* the transition matrix W, thus making it a legitimate "kinetic energy operator". More precisely, with our previous notation, it is easily to show that DB implies that:

$$K_{\sigma,\bar{\sigma}_j} = W_{\sigma,\bar{\sigma}_j}\sqrt{\frac{P_{\rm eq}(\sigma)}{P_{\rm eq}(\bar{\sigma}_j)}} = W_{\sigma,\bar{\sigma}_j}{\rm e}^{\beta\Delta E/2} = K_{\bar{\sigma}_j,\sigma} \ . \tag{1.6}$$

To exploit this observation, it is useful to work in terms of a new function $\psi(\sigma,t)$ defined by:

$$P(\sigma,t) = \sqrt{P_{\rm eq}(\sigma)}\,\psi(\sigma,t) \ . \tag{1.7}$$

[2] Glauber writes it in a form which looks different but equivalent to ours, in view of Eq. (1.16) below.

At this point, the ME in Eq. (1.2) can be rewritten as:

$$-\frac{\partial\psi(\sigma,t)}{\partial t} = -\sum_j K_{\bar{\sigma}_j,\sigma}\psi(\bar{\sigma}_j,t) + V(\sigma)\psi(\sigma,t)\ , \tag{1.8}$$

where

$$V(\sigma) = \sum_j W_{\sigma,\bar{\sigma}_j}\ . \tag{1.9}$$

This looks like a Schrödinger problem in imaginary time ($i\partial/\partial t \to -\partial/\partial t$) with a "kinetic energy" matrix $-K$ and a potential energy V. In principle the previous mapping holds in the present form only if the temperature T does not depend on time, i.e., we are not annealing the system. Otherwise, we should add an extra term to the potential in the form

$$V(\sigma) = \sum_j W_{\sigma,\bar{\sigma}_j} + \frac{\dot{P}_{\rm eq}}{2P_{\rm eq}} = \sum_j W_{\sigma,\bar{\sigma}_j} - \frac{\dot{\beta}}{2}\Big(H(\sigma) - \langle H\rangle_{\rm eq}\Big)\ . \tag{1.10}$$

Nevertheless, as argued in Ref. [40], the additional potential term proportional to $\dot{\beta}$ is likely not important in the limit of a very large many-body system: we will hence neglect it. Let us see how these "operators" look for the two choices of W proposed above, $W^{(\rm hb)}$ and $W^{(\rm G)}$. We start with the Glauber case $W^{(\rm G)}_{\sigma,\bar{\sigma}_j} = \alpha\ {\rm e}^{-\beta\Delta E/2}$. Then, we immediately get:

$$K^{(\rm G)}_{\sigma,\bar{\sigma}_j} = W^{(\rm G)}_{\sigma,\bar{\sigma}_j}{\rm e}^{\beta\Delta E/2} = \alpha\ . \tag{1.11}$$

Correspondingly, the potential energy is:

$$V^{(\rm G)}(\sigma) = \sum_j W^{(\rm G)}_{\sigma,\bar{\sigma}_j} = \alpha\sum_j {\rm e}^{-2\beta h_j\sigma_j}\ . \tag{1.12}$$

where $h_j \equiv (J_{j-1}\sigma_{j-1} + J_j\sigma_{j+1})/2$.

Using Pauli matrices to represent the spins and a ket-notation for the state $\psi(\sigma,t) = \langle\sigma|\psi(t)\rangle$, the state $\psi(\bar{\sigma}_j,t)$ takes the form

$$\psi(\bar{\sigma}_j,t) = \langle\bar{\sigma}_j|\psi(t)\rangle = \langle\sigma|\,\hat{\sigma}^x_j\,|\psi(t)\rangle\ . \tag{1.13}$$

Hence the IT Schrödinger problem for the Glauber dynamics can be written as:

$$-\frac{\partial}{\partial t}|\psi(t)\rangle = \widehat{H}^{(\rm G)}|\psi(t)\rangle\ , \tag{1.14}$$

where the quantum Hamiltonian is:

$$\widehat{H}^{(\rm G)} = -\widehat{K}^{(\rm G)} + \widehat{V}^{(\rm G)} = -\alpha\sum_j \hat{\sigma}^x_j + \alpha\sum_j {\rm e}^{-2\beta\hat{h}_j\hat{\sigma}^z_j}\ . \tag{1.15}$$

The exponential can be considerably simplified using the fact that powers of Pauli matrices are linearly related to the Pauli matrices: recall that $(\hat{\sigma}^\alpha)^2 = 1$. Indeed, we can show that

$${\rm e}^{\pm 2\beta\hat{h}_j\hat{\sigma}^z_j} = \big[\cosh(\beta J_j) \pm \hat{\sigma}^z_j\hat{\sigma}^z_{j+1}\sinh(\beta J_j)\big]\ \big[\cosh(\beta J_{j-1}) \pm \hat{\sigma}^z_{j-1}\hat{\sigma}^z_j\sinh(\beta J_{j-1})\big]\ . \tag{1.16}$$

Unfortunately, the potential energy contains not only nearest-neighbor terms like $\hat{\sigma}^z_j\hat{\sigma}^z_{j+1}$, but also *next-nearest-neighbor* ones $\hat{\sigma}^z_{j-1}\hat{\sigma}^z_{j+1}$. These terms do not have a simple Jordan-Wigner form.

The heat-bath case is, in this respect, much more interesting: indeed, while the spin-flip term is a bit more complicated, the dangerous $\hat{\sigma}^z_{j-1}\hat{\sigma}^z_{j+1}$ terms cancel out everywhere. First, observe that

$$K^{(\mathrm{hb})}_{\sigma,\bar{\sigma}_j} = W^{(\mathrm{hb})}_{\sigma,\bar{\sigma}_j}\mathrm{e}^{\beta\Delta E/2} = \frac{\alpha}{\mathrm{e}^{\beta\Delta E/2}+\mathrm{e}^{-\beta\Delta E/2}} \; . \tag{1.17}$$

Using Eq. (1.16) it is simple to show that the energy denominator is:

$$\mathrm{e}^{2\beta\hat{h}_j\hat{\sigma}^z_j} + \mathrm{e}^{-2\beta\hat{h}_j\hat{\sigma}^z_j} = 2\left[\cosh(\beta J_{j-1})\cosh(\beta J_j) + \sinh(\beta J_{j-1})\sinh(\beta J_j)\hat{\sigma}^z_{j-1}\hat{\sigma}^z_{j+1}\right] \; . \tag{1.18}$$

Since $\hat{\sigma}^z_{j-1}\hat{\sigma}^z_{j+1} = \pm 1$, this allows us to write:

$$\hat{K}^{(\mathrm{hb})}_{\sigma,\bar{\sigma}_j} = \frac{\alpha}{4}\left[\frac{1-\hat{\sigma}^z_{j-1}\hat{\sigma}^z_{j+1}}{\cosh\beta(J_j-J_{j-1})} + \frac{1+\hat{\sigma}^z_{j-1}\hat{\sigma}^z_{j+1}}{\cosh\beta(J_j+J_{j-1})}\right] = \Gamma^{(0)}_j - \Gamma^{(2)}_j\hat{\sigma}^z_{j-1}\hat{\sigma}^z_{j+1} \; , \tag{1.19}$$

with

$$\Gamma^{(0/2)}_j = \frac{\alpha}{4}\left[\frac{1}{\cosh\beta(J_j-J_{j-1})} \pm \frac{1}{\cosh\beta(J_j+J_{j-1})}\right] \; , \tag{1.20}$$

where the + (−) sign applies to $\Gamma^{(0)}_j$ ($\Gamma^{(2)}_j$). We can rewrite $\Gamma^{(0/2)}_j$ as

$$\Gamma^{(0/2)}_j = \frac{\alpha}{2D_j}\left\{\begin{array}{ll}\cosh(\beta J_{j-1})\cosh(\beta J_j) & (\text{for } 0)\\ \sinh(\beta J_{j-1})\sinh(\beta J_j) & (\text{for } 2)\end{array}\right. \tag{1.21}$$

where the denominators D_j read:

$$D_j = \cosh\beta(J_j+J_{j-1})\cosh\beta(J_j-J_{j-1}) = \sinh^2(\beta J_{j-1}) + \cosh^2(\beta J_j) \; . \tag{1.22}$$

The potential term can be written as:

$$\begin{aligned}\widehat{V}^{(\mathrm{hb})}(\hat{\sigma}) &= -\alpha\sum_j\left[\frac{\sinh(\beta J_{j-1})\cosh(\beta J_{j-1})}{2D_j}\hat{\sigma}^z_{j-1}\hat{\sigma}^z_j + \frac{\sinh(\beta J_j)\cosh(\beta J_j)}{2D_j}\hat{\sigma}^z_j\hat{\sigma}^z_{j+1}\right] + C\\ &= -\sum_j\Gamma^{(1)}_j\hat{\sigma}^z_j\hat{\sigma}^z_{j+1} + C \; ,\end{aligned} \tag{1.23}$$

where the unwanted next-neighbor-terms $\hat{\sigma}^z_{j-1}\hat{\sigma}^z_{j+1}$ disappeared. To make the notation shorter we have defined here:

$$\Gamma^{(1)}_j = \alpha\sinh(\beta J_j)\cosh(\beta J_j)\left[\frac{1}{2D_j} + \frac{1}{2D_{j+1}}\right] \; , \tag{1.24}$$

while the constant C is given by:

$$C = \alpha\sum_j\frac{\cosh^2(\beta J_{j-1})\cosh^2(\beta J_j) - \sinh^2(\beta J_{j-1})\sinh^2(\beta J_j)}{2D_j} = \frac{\alpha}{2}L \; . \tag{1.25}$$

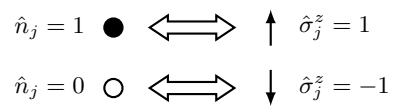

Figure 1.2: Fermion-spin correspondence in Jordan-Wigner mapping.

In operator form, the quantum Hamiltonian corresponding to the heat-bath choice is therefore:

$$\widehat{H}^{(\mathrm{hb})} = -\widehat{K}^{(\mathrm{hb})} + \widehat{V}^{(\mathrm{hb})} = -\sum_j \Gamma^{(0)}_j \hat{\sigma}^x_j + \sum_j \Gamma^{(2)}_j \hat{\sigma}^z_{j-1}\hat{\sigma}^x_j\hat{\sigma}^z_{j+1} - \sum_j \Gamma^{(1)}_j \hat{\sigma}^z_j\hat{\sigma}^z_{j+1} + C \;, \quad (1.26)$$

and this is the Hamiltonian governing the corresponding imaginary-time dynamics, i.e.,

$$-\frac{\partial}{\partial t}|\psi(t)\rangle = \widehat{H}^{(\mathrm{hb})}|\psi(t)\rangle \;. \quad (1.27)$$

Notice the seemingly more complicated transverse-field term, in which terms of the form $\hat{\sigma}^z_{j-1}\hat{\sigma}^x_j\hat{\sigma}^z_{j+1}$ appear: a Jordan-Wigner study of these terms shows that they are indeed simple to fermionize, as opposed to the plain $\hat{\sigma}^z_{j-1}\hat{\sigma}^z_{j+1}$ terms.

Let us consider the simplified case in which we have a uniform Ising chain with periodic boundary conditions (PBC), i.e., $J_j = J$. The Hamiltonian then reads:

$$\widehat{H}^{(\mathrm{hb})} = -\frac{\Gamma^{(0)}}{2}\sum_j \hat{\sigma}^x_j + \frac{\Gamma^{(2)}}{2}\sum_j \hat{\sigma}^z_{j-1}\hat{\sigma}^x_j\hat{\sigma}^z_{j+1} - \frac{\Gamma^{(1)}}{2}\sum_j \hat{\sigma}^z_j\hat{\sigma}^z_{j+1} + C \;, \quad (1.28)$$

with $C = \alpha L/2$. The couplings are (with an explicit factor 2 in the denominator pulled out, for later convenience):

$$\Gamma^{(0)} = \alpha\frac{\cosh^2(\beta J)}{\cosh(2\beta J)} \;, \qquad \Gamma^{(2)} = \alpha\frac{\sinh^2(\beta J)}{\cosh(2\beta J)} \;, \qquad \Gamma^{(1)} = \alpha\tanh(2\beta J) \;. \quad (1.29)$$

1.1.3 Jordan-Wigner mapping

The Glauber ME has been translated into a quantum problem, but the form of its Hamiltonian requires additional manipulation in order to be diagonalized. This is accomplished by the Jordan-Wigner transformation. Essentially, the Jordan-Wigner mapping allows us to map spin-1/2 Pauli operators into *hard-core bosons* $\hat{b}_j$ (in any dimension) and then hard-core bosons into *spinless fermions* $\hat{c}_j$ (Fig. 1.2), but only in one-dimension. The latter part of the mapping is the most useful one for solving problems, if the resulting Hamiltonian is quadratic in the fermions. This is precisely what happens for $\widehat{H}^{(\mathrm{hb})}$, after a spin-rotation that exchanges $\hat{\sigma}^x \leftrightarrow \hat{\sigma}^z$.

As well known, a few spin operators transform in a simple way into local fermionic operators. Here is a short summary:

$$\begin{aligned}
\hat{\sigma}^z_j &= 2\hat{n}_j - 1 \\
\hat{\sigma}^x_j\hat{\sigma}^x_{j+1} &= \left(\hat{b}^\dagger_j\hat{b}^\dagger_{j+1} + \hat{b}^\dagger_j\hat{b}_{j+1} + H.c.\right) = \left(\hat{c}^\dagger_j\hat{c}^\dagger_{j+1} + \hat{c}^\dagger_j\hat{c}_{j+1} + H.c.\right) \\
\hat{\sigma}^y_j\hat{\sigma}^y_{j+1} &= -\left(\hat{b}^\dagger_j\hat{b}^\dagger_{j+1} - \hat{b}^\dagger_j\hat{b}_{j+1} + H.c.\right) = -\left(\hat{c}^\dagger_j\hat{c}^\dagger_{j+1} - \hat{c}^\dagger_j\hat{c}_{j+1} + H.c.\right) \;.
\end{aligned} \quad (1.30)$$

Concerning our problem, we can show that, away from the borders of the chain:

$$\hat{\sigma}^x_{j-1}\hat{\sigma}^z_j\hat{\sigma}^x_{j+1} = (\hat{c}^\dagger_{j-1} + \hat{c}_{j-1})(2\hat{n}_j - 1)(1 - 2\hat{n}_{j-1})(1 - 2\hat{n}_j)(\hat{c}^\dagger_{j+1} + \hat{c}_{j+1}) \,, \tag{1.31}$$

where the terms $(1-2\hat{n}_{j-1})(1-2\hat{n}_j)$ originate from the Jordan-Wigner string due to $(\hat{c}^\dagger_{j+1}+\hat{c}_{j+1})$. Taking into account that $(2\hat{n}_j - 1)(1 - 2\hat{n}_j) = -1$, and that the factor $(1 - 2\hat{n}_{j-1})$ contributes a -1 sign when combined with $\hat{c}_{j-1}$ and a $+1$ sign with $\hat{c}^\dagger_{j-1}$, we readily conclude that:

$$\hat{\sigma}^x_{j-1}\hat{\sigma}^z_j\hat{\sigma}^x_{j+1} = -\Big(\hat{c}^\dagger_{j-1}\hat{c}_{j+1} + \hat{c}^\dagger_{j+1}\hat{c}_{j-1} + \hat{c}^\dagger_{j-1}\hat{c}^\dagger_{j+1} + \hat{c}_{j+1}\hat{c}_{j-1}\Big) \,. \tag{1.32}$$

It is now important to take care of boundary conditions. It is customary to assume periodic boundary conditions (PBC) for the spin operators, which in turns immediately implies the same PBC conditions for the hard-core bosons, that is, e.g., $\hat{b}^\dagger_L\hat{b}_{L+1} \equiv \hat{b}^\dagger_L\hat{b}_1$. But when we rewrite a term of this form using spinless fermions we get:

$$\hat{b}^\dagger_L\hat{b}_1 = \mathrm{e}^{i\pi\sum_{j'=1}^{L-1}\hat{n}_{j'}}\hat{c}^\dagger_L\hat{c}_1 = -\mathrm{e}^{i\pi\sum_{j'=1}^{L}\hat{n}_{j'}}\hat{c}^\dagger_L\hat{c}_1 = -(-1)^{N_F}\hat{c}^\dagger_L\hat{c}_1 \,, \tag{1.33}$$

where the second equality follows because, to the left of $\hat{c}^\dagger_L$ we certainly have $\hat{n}_L = 1$, and therefore the factor $-\mathrm{e}^{i\pi\hat{n}_L} \equiv 1$. Similarly, we can verify that:

$$\hat{b}^\dagger_L\hat{b}^\dagger_1 = \mathrm{e}^{i\pi\sum_{j'=1}^{L-1}\hat{n}_{j'}}\hat{c}^\dagger_L\hat{c}^\dagger_1 = -\mathrm{e}^{i\pi\sum_{j'=1}^{L}\hat{n}_{j'}}\hat{c}^\dagger_L\hat{c}^\dagger_1 = -(-1)^{N_F}\hat{c}^\dagger_L\hat{c}^\dagger_1 \,. \tag{1.34}$$

This shows that boundary conditions are affected by the *fermion parity* $(-1)^{N_F}$, and PBC become antiperiodic boundary condition (ABC) when N_F is *even*. No problem whatsoever is present, instead, when the boundary conditions are *open*, OBC, because there is no link, in the Hamiltonian, between operators at site L and operators at site $L + 1 \equiv 1$.

Let us see what happens to our term $\hat{\sigma}^x_{j-1}\hat{\sigma}^z_j\hat{\sigma}^x_{j+1}$ for $j = L$. Using spin-PBC, $\hat{\sigma}^\alpha_{L+1} \equiv \hat{\sigma}^\alpha_1$, we have:

$$\begin{aligned}
\hat{\sigma}^x_{L-1}\hat{\sigma}^z_L\hat{\sigma}^x_{L+1} &= \hat{\sigma}^x_{L-1}\hat{\sigma}^z_L\hat{\sigma}^x_1 \\
&= (\hat{b}^\dagger_{L-1} + \hat{b}_{L-1})(2\hat{n}_L - 1)(\hat{b}^\dagger_1 + \hat{b}_1) \\
&= -\mathrm{e}^{i\pi\sum_{j'=1}^{L-2}\hat{n}_{j'}}(\hat{c}^\dagger_{L-1} + \hat{c}_{L-1})\mathrm{e}^{i\pi\hat{n}_L}(\hat{c}^\dagger_1 + \hat{c}_1) \\
&= -\mathrm{e}^{i\pi\sum_{j'=1}^{L-2}\hat{n}_{j'}}(-\mathrm{e}^{i\pi\hat{n}_{L-1}}\hat{c}^\dagger_{L-1} + \mathrm{e}^{i\pi\hat{n}_{L-1}}\hat{c}_{L-1})\mathrm{e}^{i\pi\hat{n}_L}(\hat{c}^\dagger_1 + \hat{c}_1) \\
&= -[-(-1)^{N_F}]\Big(\hat{c}^\dagger_{L-1}\hat{c}_1 + \hat{c}^\dagger_1\hat{c}_{L-1} + \hat{c}^\dagger_{L-1}\hat{c}^\dagger_1 + \hat{c}_1\hat{c}_{L-1}\Big) \,.
\end{aligned} \tag{1.35}$$

Similarly:

$$\hat{\sigma}^x_0\hat{\sigma}^z_1\hat{\sigma}^x_2 = \hat{\sigma}^x_L\hat{\sigma}^z_1\hat{\sigma}^x_2 = -[-(-1)^{N_F}]\Big(\hat{c}^\dagger_L\hat{c}_2 + \hat{c}^\dagger_2\hat{c}_L + \hat{c}^\dagger_L\hat{c}^\dagger_2 + \hat{c}_2\hat{c}_L\Big) \,. \tag{1.36}$$

These rather contorted final expressions are meant to show that these terms possess an overall factor $-(-1)^{N_F}$ with respect to the corresponding bulk terms in Eq. (1.32), exactly as every Hamiltonian term: in essence, the choice of boundary conditions can be made consistently for all the Hamiltonian terms.

The case of open boundary conditions (OBC) is recovered by setting $J_0 = J_L = 0$. By considering that $\hat{h}_1 = J_1\hat{\sigma}_2^z/2$ and $\hat{h}_L = J_{L-1}\hat{\sigma}_{L-1}^z/2$, it is simple to show, from Eq. (1.16) and related ones, that the anomalous flipping term does not enter the Hamiltonian. [3]

Let us start studying the fermionised version of the *ordered* Ising model quantum-mapped dynamics.

1.1.4 Diagonalization of Hamiltonian in the ordered case

In the ordered case, all $J_j = J$, and it is useful to consider spin-PBC so that translational invariance is not broken by the boundaries. When written in terms of JW-fermions, the quantum heat-bath Hamiltonian in Eq. (1.28) is:

$$\begin{aligned}\widehat{H} &= -\frac{\Gamma^{(0)}}{2}\sum_{j=1}^{L}(2\hat{n}_j - 1) - \frac{\Gamma^{(2)}}{2}\sum_{j=1}^{L}\left(\hat{c}_{j+1}^\dagger\hat{c}_{j-1} + \hat{c}_{j-1}^\dagger\hat{c}_{j+1}^\dagger + H.c.\right) \\ &\quad -\frac{\Gamma^{(1)}}{2}\sum_{j=1}^{L}\left(\hat{c}_{j+1}^\dagger\hat{c}_j + \hat{c}_j^\dagger\hat{c}_{j+1}^\dagger + H.c.\right) + C\,, \end{aligned} \tag{1.37}$$

where the first line originates from kinetic energy term, while the second line from the potential one. So, in the PBC case, if the number of fermions N_F is odd, then all couplings are the same, and it is possible (and convenient) to retain PBC for the fermions as well, i.e., indeed take $\hat{c}_{L+1} = \hat{c}_1$ and $\hat{c}_0 = \hat{c}_L$. If, on the contrary, N_F is even, then the boundary bonds have an opposite sign with respect to the remaining ones: translational invariance can then be exploited only if antiperiodic boundary conditions (ABC) are enforced on the fermions, taking $\hat{c}_{L+1} = -\hat{c}_1$ and $\hat{c}_0 = -\hat{c}_L$. Since the Hamiltonian conserves the fermion parity, both the even and the odd sector of the fermionic Hilbert space have to be considered when diagonalizing the model, i.e., $\widehat{H} = \widehat{H}^{\mathrm{e}} + \widehat{H}^{\mathrm{o}}$, where $\widehat{H}^{\mathrm{e/o}}$ denote the even/odd subspace restrictions. However, the fact that the Hamiltonian conserves the fermion parity also guarantees that if we start from a state with N_F-even (requiring ABC) we will always remain in that subsector in the subsequent dynamics, which is quite useful.

In order to diagonalize the Hamiltonian we introduce the fermion operators in k-space, $\hat{c}_k$ and $\hat{c}_k^\dagger$, in terms of which:

$$\begin{cases} \hat{c}_j &= \dfrac{\mathrm{e}^{i\phi}}{\sqrt{L}}\displaystyle\sum_k \mathrm{e}^{+ikj}\hat{c}_k \\ \hat{c}_k &= \dfrac{\mathrm{e}^{-i\phi}}{\sqrt{L}}\displaystyle\sum_j \mathrm{e}^{-ikj}\hat{c}_j \end{cases},$$

where we have included an overall phase $\mathrm{e}^{i\phi}$ which is irrelevant for the canonical anti-commutation relationships, but will turn out useful in eliminating an imaginary unit i from the final k-space

[3] An equivalent way of appreciating this fact comes from $\Gamma_L^{(2)} = \sinh(\beta J_{L-1})\sinh(\beta J_L)/(2D_L) = 0$, which follows from $\sinh(0) = 0$.

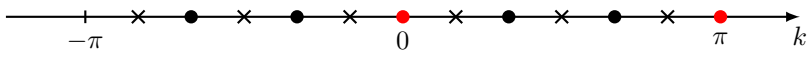

Figure 1.3: k-points for N_F-even (cross) and N_F-odd (circle) sectors with $L = 6$. The choice of k-points automatically enforces periodic and anti-periodic boundary conditions. Notice the unpaired points at $k = 0$ and $k = \pi$ in the N_F-odd sector.

Hamiltonian. If N_F is odd we should take PBC for the fermions, $\hat{c}_{L+1} \equiv \hat{c}_1$ and $\hat{c}_0 \equiv \hat{c}_L$: this in turn implies for the k's the usual choice $k = \frac{2\pi n}{L}$, with $n = -\frac{L}{2} + 1, \cdots, \frac{L}{2}$ (assuming L even, for definiteness) (Fig. 1.3):

$$N_F \text{ odd} \iff \text{PBC} \implies k = \frac{2\pi n}{L} \quad \text{with} \quad n = -\frac{L}{2} + 1, \cdots, \frac{L}{2} \,. \tag{1.38}$$

If N_F is even, then we have to take ABC for the fermions, $\hat{c}_{L+1} \equiv -\hat{c}_1$ and $\hat{c}_0 \equiv -\hat{c}_L$, if we want to exploit translational invariance. This in turn requires a different choice for the k's: $k = \pm\frac{\pi(2n+1)}{L}$ with $n = 0, \cdots, \frac{L}{2} - 1$:

$$N_F \text{ even} \iff \text{ABC} \implies k = \pm\frac{\pi(2n+1)}{L} \quad \text{with} \quad n = 0, \cdots, \frac{L}{2} - 1 \,. \tag{1.39}$$

In terms of $\hat{c}_k$ and $\hat{c}_k^\dagger$, $\widehat{H}^{\mathrm{e/o}}$ becomes (with the appropriate choice of the k-vectors):

$$\begin{aligned} \widehat{H}^{\mathrm{e/o}} \;=\; & -\frac{\Gamma^{(0)}}{2}\sum_k (2\hat{c}_k^\dagger \hat{c}_k - 1) - \frac{\Gamma^{(2)}}{2}\sum_k \Big[2\cos 2k\; \hat{c}_k^\dagger \hat{c}_k + (\mathrm{e}^{2ik}\mathrm{e}^{-2i\phi}\hat{c}_k^\dagger \hat{c}_{-k}^\dagger + H.c.)\Big] \\ & -\frac{\Gamma^{(1)}}{2}\sum_k \Big[2\cos k\; \hat{c}_k^\dagger \hat{c}_k + (\mathrm{e}^{ik}\mathrm{e}^{-2i\phi}\hat{c}_k^\dagger \hat{c}_{-k}^\dagger + H.c.)\Big] + C \,, \end{aligned} \tag{1.40}$$

Notice the coupling of $-k$ with k in the anomalous term, with the exceptions of $k = 0$ and $k = \pi$ for the PBC-case, which do not have a separate $-k$ partner. By grouping together terms with k and $-k$, the Hamiltonian is decoupled into a sum of independent terms acting in the 4-dimensional Hilbert spaces generated by k and $-k$:

$$\widehat{H}^{\mathrm{e}} = \sum_{k>0}^{\mathrm{ABC}} \widehat{H}_k + C \qquad \text{and} \qquad \widehat{H}^{\mathrm{o}} = \sum_{k>0}^{\mathrm{PBC}} \widehat{H}_k + \widehat{H}_{k=0} + \widehat{H}_{k=\pi} + C \,, \tag{1.41}$$

where we have singled-out $\widehat{H}_{k=0}$ and $\widehat{H}_{k=\pi}$ for the N_F-odd (PBC) case:

$$\widehat{H}_k = a_k\big(\hat{c}_k^\dagger \hat{c}_k - \hat{c}_{-k}\hat{c}_{-k}^\dagger\big) + b_k\big(-i\mathrm{e}^{-2i\phi}\hat{c}_k^\dagger \hat{c}_{-k}^\dagger + i\mathrm{e}^{2i\phi}\hat{c}_{-k}\hat{c}_k\big) \,, \tag{1.42}$$

$$\widehat{H}_{k=0} = -\Big(\Gamma^{(0)} + \Gamma^{(1)} + \Gamma^{(2)}\Big)\,\hat{c}_{k=0}^\dagger\,\hat{c}_{k=0} + \frac{\Gamma^{(0)}}{2} \,, \tag{1.43}$$

$$\widehat{H}_{k=\pi} = \Big(-\Gamma^{(0)} + \Gamma^{(1)} - \Gamma^{(2)}\Big)\,\hat{c}_{k=\pi}^\dagger\,\hat{c}_{k=\pi} + \frac{\Gamma^{(0)}}{2} \,, \tag{1.44}$$

where we have defined the shorthand:

$$a_k \;=\; -\big(\Gamma^{(0)} + \Gamma^{(1)}\cos k + \Gamma^{(2)}\cos 2k\big) \tag{1.45}$$

$$b_k \;=\; \Gamma^{(1)}\sin k + \Gamma^{(2)}\sin 2k \,. \tag{1.46}$$

Notice the transformation of the $-k$ cosine-term, where we used $\sum_{k>0}\cos k = 0$, whose usefulness will be appreciated in a moment. Notice also that

$$(2\hat{c}_k^\dagger\hat{c}_k - 1) + (2\hat{c}_{-k}^\dagger\hat{c}_{-k} - 1) = 2(\hat{c}_k^\dagger\hat{c}_k - \hat{c}_{-k}\hat{c}_{-k}^\dagger) \; .$$

We see that a critical point occurs for $T \to 0$ and $k \to \pi$. In fact at zero temperature the parameters entering the Hamiltonian assume the values $\Gamma^{(0)} = 1/2$, $\Gamma^{(1)} = 1$ and $\Gamma^{(2)} = 1/2$ (Eq. 1.29), yielding to vanishing a_k and b_k coefficients.

We can still make use of the freedom we have in choosing the overall phase ϕ to eliminate the i appearing in $\widehat{H}_k$ and choosing the sign of the anomalous BCS-like terms. In particular, with the choice $\phi = -\pi/4$ we end up writing:

$$\widehat{H}_k = a_k\big(\hat{c}_k^\dagger\hat{c}_k - \hat{c}_{-k}\hat{c}_{-k}^\dagger\big) + b_k\big(\hat{c}_k^\dagger\hat{c}_{-k}^\dagger + \hat{c}_{-k}\hat{c}_k\big) \; . \tag{1.47}$$

With the Nambu formalism, we define the fermionic two-component spinor

$$\widehat{\Psi}_k = \begin{pmatrix} \hat{c}_k \\ \hat{c}_{-k}^\dagger \end{pmatrix} \; , \qquad \widehat{\Psi}_k^\dagger = (\hat{c}_k^\dagger \; \hat{c}_{-k}) \tag{1.48}$$

with commutation relations ($\alpha = 1, 2$ stands for the two components of $\widehat{\Psi}$)

$$\{\widehat{\Psi}_{k\alpha}, \widehat{\Psi}_{k'\alpha'}^\dagger\} = \delta_{\alpha,\alpha'}\delta_{k,k'} \; . \tag{1.49}$$

We can then rewrite each $\widehat{H}_k$ as:

$$\widehat{H}_k = \widehat{\Psi}_k^\dagger\mathbb{H}^{(k)}\widehat{\Psi}_k = \sum_{\alpha,\beta}\widehat{\Psi}_{k\alpha}^\dagger\mathbb{H}_{\alpha\beta}^{(k)}\widehat{\Psi}_{k\beta} = (\hat{c}_k^\dagger \; \hat{c}_{-k}) \begin{pmatrix} a_k & b_k \\ b_k & -a_k \end{pmatrix} \begin{pmatrix} \hat{c}_k \\ \hat{c}_{-k}^\dagger \end{pmatrix} \; . \tag{1.50}$$

In short, we could write $\mathbb{H}^{(k)} = a_k\tau^z + b_k\tau^x$, with $\tau^{z,x}$ standard Pauli matrices (in Nambu space). By solving the 2×2 eigenvalue problem for $\mathbb{H}^{(k)}$ we find the eigenvalues

$$\epsilon_{k\pm} = \pm\epsilon_k \qquad \text{with} \qquad \epsilon_k = \sqrt{a_k^2 + b_k^2} \tag{1.51}$$

with corresponding eigenvectors $(u_{k\pm} \; v_{k\pm})^T$. For the positive energy eigenvector, we have:

$$\begin{pmatrix} u_{k+} \\ v_{k+} \end{pmatrix} \equiv \begin{pmatrix} u_k \\ v_k \end{pmatrix} = \frac{1}{\sqrt{2\epsilon_k(\epsilon_k + a_k)}} \begin{pmatrix} \epsilon_k + a_k \\ b_k \end{pmatrix} \; , \tag{1.52}$$

where we have introduced the shorthands $u_k = u_{k+}$ and $v_k = v_{k+}$, both *real*. Note, in passing, that $u_{-k} = u_k$, while $v_{-k} = -v_k$, since b_k is odd. The negative-energy eigenvector $(u_{k-} \; v_{k-})^T$ is:

$$\begin{pmatrix} u_{k-} \\ v_{k-} \end{pmatrix} = \begin{pmatrix} -v_k \\ u_k \end{pmatrix} = \frac{1}{\sqrt{2\epsilon_k(\epsilon_k + a_k)}} \begin{pmatrix} -b_k \\ \epsilon_k + a_k \end{pmatrix} \; . \tag{1.53}$$

The (real) unitary matrix $\mathbb{U}_k$ having the two previous eigenvectors as columns:

$$\mathbb{U}_k = \begin{pmatrix} u_k & -v_k \\ v_k & u_k \end{pmatrix} \; , \tag{1.54}$$

diagonalizes $\mathbb{H}^{(k)}$:

$$\mathbb{U}_k^\dagger \, \mathbb{H}^{(k)} \, \mathbb{U}_k = \mathrm{diag}(\epsilon_k, -\epsilon_k) = \begin{pmatrix} \epsilon_k & 0 \\ 0 & -\epsilon_k \end{pmatrix} . \tag{1.55}$$

So, we define new fermion Nambu operators Φ_k through

$$\widehat{\Phi}_k = \mathbb{U}_k^\dagger \widehat{\Psi}_k = \begin{pmatrix} u_k \hat{c}_k + v_k \hat{c}_{-k}^\dagger \\ -v_k \hat{c}_k + u_k \hat{c}_{-k}^\dagger \end{pmatrix} = \begin{pmatrix} \hat{\gamma}_k \\ \hat{\gamma}_{-k}^\dagger \end{pmatrix} , \tag{1.56}$$

where, in the second term, we have made use of the fact that $u_{-k} = u_k$ and $v_{-k} = -v_k$. It is straightforward to verify that $\hat{\gamma}_k$ is indeed a fermionic operator, i.e.

$$\begin{aligned} \{\hat{\gamma}_k, \hat{\gamma}_k^\dagger\} &= \{u_k \hat{c}_k + v_k \hat{c}_{-k}^\dagger, u_k \hat{c}_k^\dagger + v_k \hat{c}_{-k}\} \\ &= u_k^2 \{\hat{c}_k, \hat{c}_k^\dagger\} + v_k^2 \{\hat{c}_{-k}^\dagger, \hat{c}_{-k}\} = u_k^2 + v_k^2 = 1 , \end{aligned} \tag{1.57}$$

the last equality following from the normalisation condition for the eigenvectors. In terms of $\widehat{\Phi}_k = (\hat{\gamma}_k \; \hat{\gamma}_{-k}^\dagger)^T$ and $\widehat{\Phi}_k^\dagger = \widehat{\Psi}_k^\dagger \mathbb{U}_k = (\hat{\gamma}_k^\dagger \; \hat{\gamma}_{-k})$, we have:

$$\begin{aligned} \widehat{H}_k &= \widehat{\Psi}_k^\dagger \, \mathbb{U}_k \, \mathbb{U}_k^\dagger \, \mathbb{H}^{(k)} \, \mathbb{U}_k \, \mathbb{U}_k^\dagger \widehat{\Psi}_k = \widehat{\Phi}_k^\dagger \begin{pmatrix} \epsilon_k & 0 \\ 0 & -\epsilon_k \end{pmatrix} \widehat{\Phi}_k \\ &= \epsilon_k \left(\hat{\gamma}_k^\dagger \hat{\gamma}_k - \hat{\gamma}_{-k} \hat{\gamma}_{-k}^\dagger \right) = \epsilon_k \left(\hat{\gamma}_k^\dagger \hat{\gamma}_k + \hat{\gamma}_{-k}^\dagger \hat{\gamma}_{-k} - 1 \right) . \end{aligned} \tag{1.58}$$

The total Hamiltonians in the ABC and PBC sectors then reads:

$$\widehat{H}^{\mathrm{e}} = \sum_k^{\mathrm{ABC}} \epsilon_k \hat{\gamma}_k^\dagger \hat{\gamma}_k - \sum_{k>0}^{\mathrm{ABC}} \epsilon_k + C , \tag{1.59}$$

$$\widehat{H}^{\mathrm{o}} = \sum_k^{\mathrm{PBC}} \epsilon_k \hat{\gamma}_k^\dagger \hat{\gamma}_k - \sum_{k>0}^{\mathrm{PBC}} \epsilon_k + \Gamma^{(0)} + C , \tag{1.60}$$

where we have transformed the first term using $\epsilon_{-k} = \epsilon_k$.

1.1.5 Ground state and lowest excited states of the Ising model

Having obtained a quadratic Hamiltonian in the new fermion operators $\hat{\gamma}_k$, the next step is to identify the ground state and the excited states. The expression (1.58) allows to immediately conclude that the ground state of the Hamiltonian must be the state $|\emptyset\rangle_\gamma$ which annihilates the $\hat{\gamma}_k$ for all k — the so-called *Bogoliubov vacuum*:

$$\hat{\gamma}_k \, |\emptyset\rangle_\gamma = 0 \quad \forall k . \tag{1.61}$$

In principle, one can define two such states, one in the N_F-even (ABC) sector, and one in the N_F-odd (PBC). However, comparing Eqs. 1.59 and 1.60 it turns out that the actual global ground state is the one in the N_F-even sector, with an energy

$$E_0^{\mathrm{ABC}} = -\sum_{k>0}^{\mathrm{ABC}} \epsilon_k + C . \tag{1.62}$$

The ground state can be obtained explicitly as:

$$|\emptyset\rangle_\gamma^{\rm ABC} \propto \prod_{k>0} \hat{\gamma}_{-k}\hat{\gamma}_k|0\rangle \tag{1.63}$$

where $|0\rangle$ is the vacuum for the original fermions, $\hat{c}_k|0\rangle = 0$. So

$$\begin{aligned}\prod_{k>0} \hat{\gamma}_{-k}\hat{\gamma}_k|0\rangle &= \prod_{k>0}\Big(u_k\hat{c}_{-k} - v_k\hat{c}_k^\dagger\Big)\Big(u_k\hat{c}_k + v_k\hat{c}_{-k}^\dagger\Big)|0\rangle \\ &= \prod_{k>0} v_k\Big(u_k - v_k\hat{c}_k^\dagger\hat{c}_{-k}^\dagger\Big)|0\rangle\ ,\end{aligned} \tag{1.64}$$

and by normalizing the state, we arrive at a standard BCS expression:

$$|\emptyset\rangle_\gamma^{\rm ABC} = \prod_{k>0}^{\rm ABC}\Big(u_k - v_k\hat{c}_k^\dagger\hat{c}_{-k}^\dagger\Big)|0\rangle = \mathcal{N}\ {\rm e}^{-\sum_{k>0}^{\rm ABC}\lambda_k\hat{c}_k^\dagger\hat{c}_{-k}^\dagger}|0\rangle\ , \tag{1.65}$$

where $\lambda_k = v_k/u_k$ and the normalisation constant is

$$\mathcal{N} = \prod_{k>0}^{\rm ABC}\left[1+\lambda_k^2\right]^{-\frac{1}{2}}\ . \tag{1.66}$$

The PBC-sector ground state must contain an odd number of particles. Since a BCS-paired state is always fermion-even, the unpaired Hamiltonian terms $\widehat{H}_{k=0} + \widehat{H}_{k=\pi}$ must have exactly an odd number of fermions in the ground state.

Regarding the excited states, the situation is simple enough within the N_F-even (ABC) sector. Here excited states are obtained by applying an *even* number of $\hat{\gamma}_k^\dagger$ to $|\emptyset\rangle_{\rm ABC}$, each $\hat{\gamma}_k^\dagger$ costing an energy ϵ_k:

$$\begin{aligned}|\psi_{\{n_k\}}\rangle &= \prod_k^{\rm ABC}[\hat{\gamma}_k^\dagger]^{n_k}|\emptyset\rangle_\gamma^{\rm ABC} \qquad \text{with} \quad n_k = 0,1 \quad \text{and} \quad \sum_k^{\rm ABC} n_k = \text{even} \\ E_{\{n_k\}} &= \sum_k^{\rm ABC} n_k\epsilon_k + E_0^{\rm ABC}\ .\end{aligned} \tag{1.67}$$

In the N_F-odd (PBC) sector, the situation is a bit more tricky. One could apply an even number of $\gamma_k^\dagger$ to the ground state $|\emptyset\rangle_{\rm PBC}$, or, alternatively, change by one the fermion occupation of the unpaired states at $k = 0$ and $k = \pi$, and apply only an odd number of $\gamma_k^\dagger$'s.

1.2 Simulated and quantum annealing for ordered case

1.2.1 Simulated annealing

We want now to study the imaginary time dynamics which "simulates" the correct classical ME dynamics. For generality, assume that we anneal the system by driving the temperature as

a function of time, $T(t)$. This in general requires further terms in the quantum Hamiltonian, but in all cases the resulting quantum Hamiltonian is quadratic in the fermions. If the system is ordered, we essentially have an Hamiltonian as the one studied in the previous subsection, except that in general we can allow the Hamiltonian to depend on time, through its parameters and $T(t)$. Let us write a general BCS state for the ordered system as:

$$|\psi(t)\rangle = \mathcal{N}(t)\, \mathrm{e}^{-\sum_{k>0}^{\mathrm{ABC}} \lambda_k(t) \hat{c}_k^\dagger \hat{c}_{-k}^\dagger} |0\rangle \;, \tag{1.68}$$

where $\lambda_k(t)$ depends on time and $\mathcal{N}(t)$ is an overall factor. One important aspect of the imaginary-time dynamics is that the normalisation of a state is *not conserved*: therefore, even if at $t = 0$ we take an initial state which is normalised, i.e., such that $\mathcal{N}(0) = \prod_{k>0}[1+\lambda_k^2(0)]^{-1/2}$, the resulting dynamics will make in general $\mathcal{N}(t)$ not simply related to the $\lambda_k(t)$. In principle, we will be able to write an equation governing $\mathcal{N}(t)$ but the actual value of $\mathcal{N}(t)$ is not important: what we have to do is to calculate averages with a correctly normalised state, i.e., effectively using $\mathcal{N}(t) = \prod_{k>0}[1+\lambda_k^2(t)]^{-1/2}$.

The imaginary time Scrödinger equation we want to solve is:

$$-\frac{\partial}{\partial t}|\psi(t)\rangle = \widehat{H}(t)|\psi(t)\rangle \;, \tag{1.69}$$

where $\widehat{H}(t)$ is a quadratic fermion Hamiltonian which can be parameterized with the usual $a_k(t)$ and $b_k(t)$. First of all, we notice that:

$$-\frac{\partial}{\partial t}|\psi(t)\rangle = -\Big[-\sum_{k>0}^{\mathrm{ABC}} \dot{\lambda}_k \hat{c}_k^\dagger \hat{c}_{-k}^\dagger + \frac{\dot{\mathcal{N}}}{\mathcal{N}} \Big] |\psi(t)\rangle \;. \tag{1.70}$$

Regarding the right-hand side, all constant terms in $\widehat{H}$ are trivial to account for: let us disregard them for a while. Consider therefore the general ordered form we have previously used:

$$\widehat{H}(t) = \sum_{k>0}^{\mathrm{ABC}} \Big[a_k(t)(\hat{c}_k^\dagger \hat{c}_k - \hat{c}_{-k}\hat{c}_{-k}^\dagger) + b_k(t)(\hat{c}_k^\dagger \hat{c}_{-k}^\dagger + \hat{c}_{-k}\hat{c}_k) \Big] \;, \tag{1.71}$$

where both $a_k(t)$ and $b_k(t)$ can in general depend on time through the dependence of $T(t)$. The k-th term of $\widehat{H}$, $\widehat{H}_k$, will act on the k-th component of $|\psi(t)\rangle$, essentially $\mathrm{e}^{-\lambda_k(t)\hat{c}_k^\dagger \hat{c}_{-k}^\dagger}|0\rangle$, ignoring all other $k' \neq k$ components. When $\widehat{H}_k$ acts on $\mathrm{e}^{-\lambda_k(t)\hat{c}_k^\dagger \hat{c}_{-k}^\dagger}|0\rangle$ we obtain:

$$\widehat{H}_k \mathrm{e}^{-\lambda_k \hat{c}_k^\dagger \hat{c}_{-k}^\dagger}|0\rangle = \Big[(-2\lambda_k a_k + b_k - \lambda_k^2 b_k)\hat{c}_k^\dagger \hat{c}_{-k}^\dagger + (-a_k - b_k\lambda_k) \Big] \mathrm{e}^{-\lambda_k \hat{c}_k^\dagger \hat{c}_{-k}^\dagger}|0\rangle \;. \tag{1.72}$$

Recalling that the other components with $k' \neq k$ are present, but not acted upon, we can then write:

$$\widehat{H}(t)|\psi(t)\rangle = \sum_{k>0}^{\mathrm{ABC}} \Big[(-2\lambda_k a_k + b_k - \lambda_k^2 b_k)\hat{c}_k^\dagger \hat{c}_{-k}^\dagger + (-a_k - b_k\lambda_k) \Big] |\psi(t)\rangle \;. \tag{1.73}$$

By equating term-by-term the left and right-hand side of the imaginary time Schrödinger equation we finally obtain an equation of λ_k in the form:

$$\dot{\lambda}_k = -2\lambda_k a_k + b_k - \lambda_k^2 b_k \ . \tag{1.74}$$

Concerning the rather unimportant equation for $\mathcal{N}(t)$, we have:

$$\frac{\dot{\mathcal{N}}}{\mathcal{N}} = \frac{d}{dt}\log\mathcal{N} = \sum_{k>0}^{\text{ABC}} (a_k + b_k\lambda_k) - \text{Constants} \ , \tag{1.75}$$

where we have reinserted all the possible constant terms appearing in the Hamiltonian. It is interesting to notice that all the Hamiltonian constants enter the (irrelevant) equation for $\mathcal{N}(t)$, but they do not influence at all the important equation for $\lambda_k(t)$.

At this point one can study two types of problems: *1)* the relaxation towards equilibrium after a sudden quench of the temperature from T_0 to T, or *2)* a slow annealing of the temperature. In the case of a sudden quench, the final $\widehat{H}$ governing the dynamics is time-independent, and appropriate to describe the classical dynamics at T_f, but the initial state $|\psi_0\rangle$ is the ground state of a different Hamiltonian, $\widehat{H}_0$, appropriate to describe the dynamics at T_0. In the second case, we have a genuinely time-dependent $\widehat{H}(t)$.

The first case is quite simple to analyze: the coefficients a_k and b_k are time-independent, and one readily shows that the non-linear equation $\dot{\lambda}_k = -2\lambda_k a_k + b_k - \lambda_k^2 b_k$ has two fixed points at the values of λ_k which satisfy $-2\lambda_k a_k + b_k - \lambda_k^2 b_k = 0$:

$$\lambda_{k,\pm} = \frac{-a_k \pm \sqrt{a_k^2 + b_k^2}}{b_k} \ .$$

Simple algebra shows that the fixed point $\lambda_{k,+} = \lambda_k^{\text{gs}} = v_k^{\text{gs}}/u_k^{\text{gs}}$ is attractive, and corresponds to the ground state solution of $\widehat{H}$, while $\lambda_{k,-}$ is unstable and not relevant to our discussion.

1.2.2 Quantum annealing

We move now to the quantum annealing for ordered Ising chains. Here the temperature is replaced by an external transverse magnetic field $\Gamma(t)$ that allows for quantum fluctuations (Fig. 1.4).

The Hamiltonian governing a quantum annealing process is the following:

$$\hat{H}_Q(t) = -J\sum_j \hat{\sigma}_j^z\hat{\sigma}_{j+1}^z - \Gamma(t)\sum_j \hat{\sigma}_j^x \ . \tag{1.76}$$

The diagonalization of the Hamiltonian follows the same calculations as in the simulated annealing case: we first perform a Jordan-Wigner transformation on the exchanged spins $\hat{\sigma}^x \leftrightarrow \hat{\sigma}^z$, followed by a Fourier transform with the usual rules on the determination of k-points according

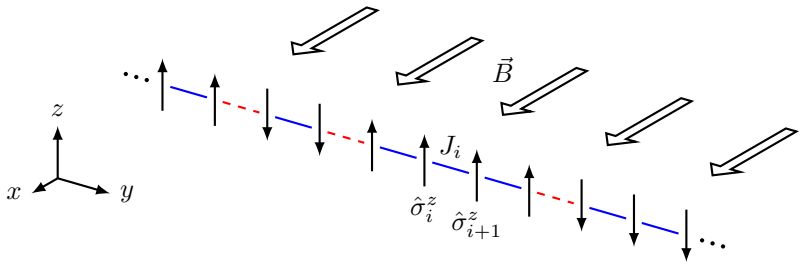

Figure 1.4: Sketch of the transverse field ferromagnetic Ising model.

to periodic and anti-periodic boundary conditions. In this section we will assume an even number of fermions, so we deal with ABC. The Hamiltonian is then rewritten as:

$$\hat{H}_k(t) = a_k(t)\left(\hat{c}_k^\dagger \hat{c}_k - \hat{c}_{-k}\hat{c}_{-k}^\dagger\right) + b_k\left(\hat{c}_k^\dagger \hat{c}_{-k}^\dagger + \hat{c}_{-k}\hat{c}_k\right) \ , \tag{1.77}$$

where the coefficients $a_k(t)$ and b_k are redefined as:

$$a_k(t) = -2\left(\Gamma(t) + J\cos k\right) \ , \tag{1.78}$$

$$b_k = 2J\sin k \ , \tag{1.79}$$

with $k = \dfrac{\pi}{L}, \dfrac{3\pi}{L}, \ldots, \dfrac{\pi(L-1)}{L}$. From Eqs. 1.78 and 1.79 it is easy to see that a quantum critical point occurs at $\Gamma(t) = J$ in the limit $k \to \pi$ (for infinite chain length L). This translates into zero-energy cost for excitations leading to a non-adiabatic dynamics. For a finite system, the minimum energy gap occurs at $k = k_{\max} \equiv \pi(L-1)/L$ and $\Gamma(t) = -J\cos(k_{\max})$:

$$\Delta_{k_{\max}} = \sqrt{a_{k_{\max}}^2 + b_{k_{\max}}^2} = 2J\sin(k_{\max}) \ . \tag{1.80}$$

The dynamics of the system can be studied in both *real* and *imaginary* time. The imaginary-time QA-IT dynamics is governed by the same non-linear differential equation as in the SA (Eq. 1.74):

$$\dot{\lambda}_k = -2\lambda_k a_k(t) + b_k - \lambda_k^2 b_k \ , \tag{1.81}$$

while for the real-time QA-RT evolution the differential equation takes the form:

$$-i\dot{\lambda}_k = -2\lambda_k a_k(t) + b_k - \lambda_k^2 b_k \ . \tag{1.82}$$

In our study we considered a linear decreasing of annealing time τ:

$$\Gamma(t) = \Gamma_0\left(1 - \frac{t}{\tau}\right) \ . \tag{1.83}$$

This particular choice allows us to make predictions on the annealing time τ at which the QA-RT dynamics has a transition between non-adiabatic and adiabatic evolutions. In fact, the

Hamiltonian can be rewritten in terms of a Landau-Zener process, on which we can evaluate the correspondent excitation probability.

As detailed in Appendix A, the Landau-Zener model is a two-state quantum problem governed by a time-dependent Hamiltonian and described by the following Schrödinger equation:

$$i\hbar\frac{\partial}{\partial t}\begin{pmatrix} c_1(t) \\ c_2(t) \end{pmatrix} = \begin{bmatrix} at & b \\ b^* & -at \end{bmatrix}\begin{pmatrix} c_1(t) \\ c_2(t) \end{pmatrix} , \tag{1.84}$$

where c_1 and c_2 are the probability amplitudes of the eigenstates at $t \to \infty$. Starting in the ground state at $t \to -\infty$, the probability to have a transition at the end of the evolution is given by the Landau-Zener formula:

$$P_{\text{ex}}(t \to +\infty) = \mathrm{e}^{-\pi|b|^2/\hbar a} . \tag{1.85}$$

Let us study the quantum annealing in terms of Landau-Zener process. First we write the Hamiltonian $\hat{H}_k(t)$ in matrix form as in Eq. 1.50:

$$\widehat{H}_k = (\hat{c}_k^\dagger \ \hat{c}_{-k})\begin{pmatrix} -2\left(\Gamma(t) + J\cos k\right) & 2J\sin k \\ 2J\sin k & 2\left(\Gamma(t) + J\cos k\right) \end{pmatrix}\begin{pmatrix} \hat{c}_k \\ \hat{c}_{-k}^\dagger \end{pmatrix} . \tag{1.86}$$

At this point we can manipulate the matrix to make it in LZ standard form:

$$\begin{pmatrix} -2\left(\Gamma(t) + J\cos k\right) & 2J\sin k \\ 2J\sin k & 2\left(\Gamma(t) + J\cos k\right) \end{pmatrix} = \begin{pmatrix} \frac{2\Gamma_0}{\tau}\left(t - \tilde{t}\right) & 2J\sin k \\ 2J\sin k & \frac{2\Gamma_0}{\tau}(t - \tilde{t}) \end{pmatrix} , \tag{1.87}$$

where we have defined the time $\tilde{t} = \tau + J\tau\cos k/\Gamma_0$. The form of the matrix is now suitable for applying Eq. 1.85 for LZ excitation:

$$P_k^{\text{ex}} = \mathrm{e}^{-2\pi J^2\tau\sin^2 k/\Gamma_0} = \mathrm{e}^{-\tau/\tau_k^*} , \tag{1.88}$$

where the time-scale $\tau_k^* = \Gamma_0/2\pi J^2\sin^2 k$ defines the annealing time at which excitation in k-state can happen with a probability $1/e$. Since we are interested in predicting the transition between non-adiabatic and adiabatic dynamics, we need to consider the most probable excitation, hence correspondent to minimal gap $\Delta_{k_{\max}}$. For sufficiently large L we can approximate $\sin(k_{\max}) \approx \pi/L$, leading to a probability

$$P_{k_{\max}}^{\text{ex}} = \mathrm{e}^{-2\pi^3 J^2\tau/\Gamma_0 L^2} . \tag{1.89}$$

Therefore $\tau^* = \Gamma_0 L^2/2\pi^3 J^2$ defines the annealing time of "adiabaticity breaking".

The same consideration can not be done in SA since the critical point occurs at the end of evolution – at zero temperature – and it is never crossed during annealing. Moreover, the gap decreases exponentially fast approaching $T \to 0$. Let us see how. The parameters of SA Hamiltonian take the form

$$\Gamma^{(0)} = \alpha\frac{\cosh^2(\beta J)}{\cosh(2\beta J)} , \qquad \Gamma^{(1)} = \alpha\tanh(2\beta J) , \qquad \Gamma^{(2)} = \alpha\frac{\sinh^2(\beta J)}{\cosh(2\beta J)} . \tag{1.90}$$

In the limit $T \to 0$ we obtain the asymptotic behaviours:

$$\Gamma^{(0)} = \frac{\alpha}{2}\left[1 + 2\mathrm{e}^{-2\beta J} + \mathcal{O}\left(\mathrm{e}^{-4\beta J}\right)\right] , \tag{1.91}$$

$$\Gamma^{(1)} = \alpha\left[1 - 2\mathrm{e}^{-4\beta J} + \mathcal{O}\left(\mathrm{e}^{-8\beta J}\right)\right] , \tag{1.92}$$

$$\Gamma^{(2)} = \frac{\alpha}{2}\left[1 - 2\mathrm{e}^{-2\beta J} + \mathcal{O}\left(\mathrm{e}^{-4\beta J}\right)\right] . \tag{1.93}$$

The coefficients a_k and b_k close to the critical point behave as

$$a_k \approx -2\alpha\mathrm{e}^{-4\beta J} + \frac{\alpha\pi^2}{2L^2}\left(1 - 4\mathrm{e}^{-2\beta J}\right) + \mathcal{O}\left(\mathrm{e}^{-6\beta J}\right) , \tag{1.94}$$

$$b_k \approx \frac{2\alpha\pi}{L}\mathrm{e}^{-2\beta J} + \mathcal{O}\left(\frac{\mathrm{e}^{-4\beta J}}{L}\right) . \tag{1.95}$$

From last equations we see that the gap decreases exponentially fast for $t \to 0$, making the problem different from standard LZ.

1.3 Results for the ordered case

In this section we show the results obtained for ordered Ising chains. The evolutions have been simulated solving the following equation through a Runge-Kutta 4th-order method:

$$\xi\dot{\lambda}_k = -2\lambda_k\, a_k(t) + b_k(t) - \lambda_k^2\, b_k(t) , \tag{1.96}$$

with $\xi = 1$ for SA and QA-IT, while $\xi = -i$ for QA-RT.

The coefficients a_k and b_k are the following:

$$\text{SA:} \begin{cases} a_k(t) &= -\alpha\left(\dfrac{\cosh^2(\beta(t)J)}{\cosh(2\beta(t)J)} + \tanh(2\beta(t)J)\cos k + \dfrac{\sinh^2(\beta(t)J)}{\cosh(2\beta(t)J)}\cos 2k\right) \\ b_k(t) &= \alpha\left(\tanh(2\beta(t)J)\sin k + \dfrac{\sinh^2(\beta(t)J)}{\cosh(2\beta(t)J)}\sin 2k\right) \end{cases} , \tag{1.97}$$

$$\text{QA:} \begin{cases} a_k(t) &= -2\left(\Gamma(t) + J\cos k\right) \\ b_k &= 2J\sin k \end{cases} . \tag{1.98}$$

The evolutions start in the ground state at reasonably high temperature for SA and transverse field for QA, and then they are decreased linearly to zero in an annealing time τ:

$$\text{SA: } T(t) = T_0\left(1 - \frac{t}{\tau}\right) , \qquad \text{QA: } \Gamma(t) = \Gamma_0\left(1 - \frac{t}{\tau}\right) , \tag{1.99}$$

with $T_0 = 10\, J/k_\mathrm{B}$ and $\Gamma_0 = 10\, J$.

The variables $\lambda_k = v_k/u_k$ are initialized to the ground state condition (Eq. 1.52):

$$\lambda_k(t=0) = \frac{b_k(0)}{a_k(0) + \epsilon_k(0)} . \tag{1.100}$$

The interesting observable is the density of defects $\rho_{\rm def}$ at the end of the annealing. This measure is an indicator of the adiabaticity/non-adiabaticity level of the evolution, since it counts the number of excitations and therefore the "distance" from the true ground state at the end of the dynamics. The defect density operator is defined as:

$$\hat{\rho}_{\rm def} = \frac{1}{L}\sum_j \frac{1-\hat{\sigma}_j^z\hat{\sigma}_{j+1}^z}{2} \ . \tag{1.101}$$

Its average can be computed in terms of λ_k coefficients with the following formula (see Appendix B.1 for derivation):

$$\rho_{\rm def}(t) = \frac{2}{L}\sum_{k>0} \frac{\left|\lambda_k(t)\sin\left(k/2\right)-\cos\left(k/2\right)\right|^2}{1+\left|\lambda_k(t)\right|^2} \ . \tag{1.102}$$

Another important observable is the residual energy $\epsilon_{\rm res}$, defined as the extra energy with respect to the ground state level. In the ordered case it does not give us additional information since it is proportional to $\rho_{\rm def}$:

$$\epsilon_{\rm res} \equiv -J\sum_j \hat{\sigma}_j^z\hat{\sigma}_{j+1}^z + JL = 2J\rho_{\rm def} \ . \tag{1.103}$$

In figure 1.5 we show the results of the final density of defects $\rho_{\rm def}(t=\tau)$ for the three dynamics.

The behavior of $\rho_{\rm def}$ for real-time QA follows the Kibble-Zurek power-law $\rho_{\rm def}^{\rm QA-RT}(\tau) \sim 1/\sqrt{\tau}$ associated to crossing the Ising critical point [31, 32]. As predicted from LZ theory, finite-size deviations are revealed by an exponential drop of $\rho_{\rm def}(\tau)$, occurring for annealing times larger than $\tau_L^* \approx \Gamma_0 L^2/2\pi^3 J^2$ due to a LZ probability of excitation across a small gap $\Delta_k = 2J\sin k \approx \pi/L$ close to the critical wave-vector $k_c = \pi$, $P_{\rm ex} = {\rm e}^{-2\pi^3 J^2\tau/\Gamma_0 L^2}$. We note that, for any finite L, the exponential drop of $\rho_{\rm def}^{\rm QA-RT}(\tau)$ eventually turns into a $1/\tau^2$, due to finite-time corrections to LZ [41, 42].

The QA-IT case is very different from QA-RT for $L \to \infty$. We find $\rho_{\rm def}^{\rm QA-IT}(\tau) \sim a/\tau^2 + \mathcal{O}({\rm e}^{-b\tau})$, with $a \approx 0.784$, where the first term is due to non-critical modes, while the exponentially decreasing term (see Fig. 1.6) is due to critical modes with $k = \pi - q$ at small q: their LZ dynamics, see Fig. 1.7, shows that IT follows a standard LZ up to the critical point, but then *filters the ground state* (GS) exponentially fast as the gap resurrects after the critical point.
That IT evolution gives different results from RT for $L \to \infty$ is not obvious. From the study of toy problems [43], it was conjectured that QA-IT might have the same asymptotic behavior as QA-RT, as later shown more generally [44] from adiabatic perturbation theory estimates. That is what happens in our Ising case too for *finite* L and $\tau \to \infty$, with a common $1/\tau^2$ asymptotic. Moreover, IT gives the same critical exponents as RT for QA ending at the critical point [45]. The deviation of QA-IT from QA-RT for Ising chains *in the thermodynamic limit* $L \to \infty$ is due to the non-perturbative LZ nature when the annealing proceeds beyond the critical point.

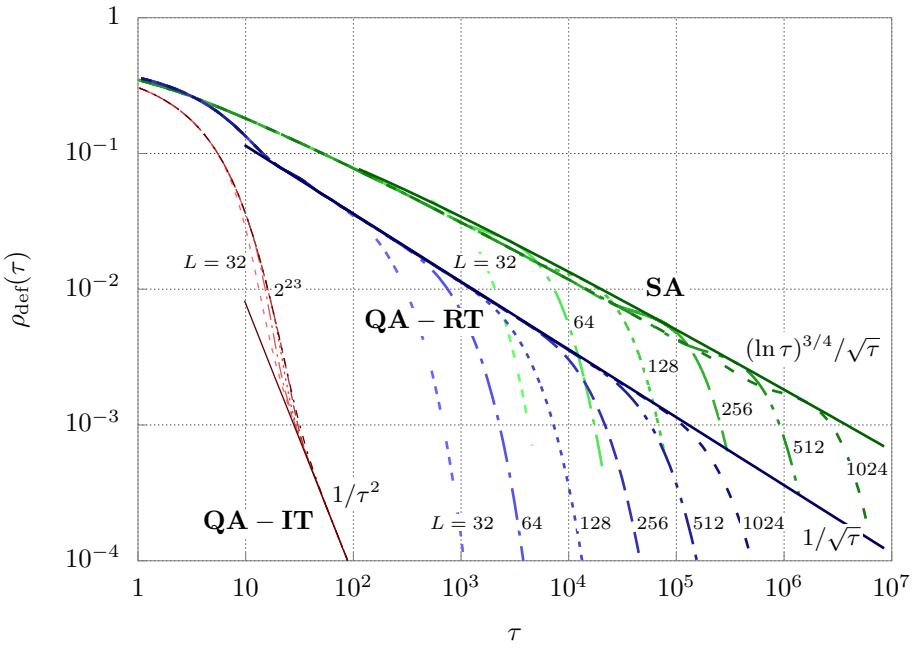

Figure 1.5: Density of defects after the annealing, $\rho_{\rm def}(\tau)$, versus the annealing time τ for the *ordered* Ising chain. Results for simulated annealing (SA) and for quantum annealing (QA) in real time (QA-RT) and in imaginary time (QA-IT).

The SA result, Fig. 1.5, is marginally worse than QA-RT due to logarithmic corrections, $\rho_{\rm def}^{\rm SA}(\tau) \sim (\ln\tau)^{\nu}/\sqrt{\tau}$, where we find $\nu \approx 3/4$. As discussed in the previous section, two aspects make the SA dynamics different from the standard LZ dynamics behind QA-RT, and are at the origin of the logarithmic corrections: first, the critical point occurs at $T = 0$ (for $k = \pi$) and is never crossed during the annealing; second, the coefficients a_k and b_k, which behave as $a_k \approx -2\alpha e^{-4\beta J} + \frac{\alpha\pi^2}{2L^2}\left(1 - 4e^{-2\beta J}\right) + \mathcal{O}\left(e^{-6\beta J}\right)$ and $b_k \approx \frac{2\alpha\pi}{L} e^{-2\beta J} + \mathcal{O}\left(\frac{e^{-4\beta J}}{L}\right)$ close to the critical point, lead to an energy gap which decreases exponentially fast for $T \to 0$.

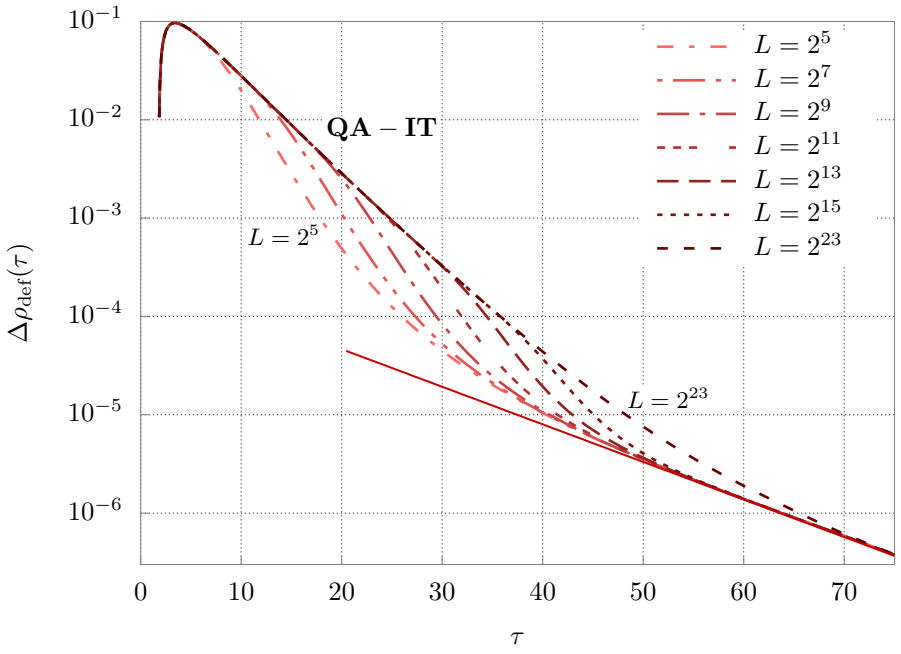

Figure 1.6: Log-linear plot of the deviation $\Delta\rho_{\rm def} = \rho_{\rm def} - a/\tau^2$, with $a \approx 0.784$, for QA-IT, showing a clear exponential approach to the leading $1/\tau^2$.

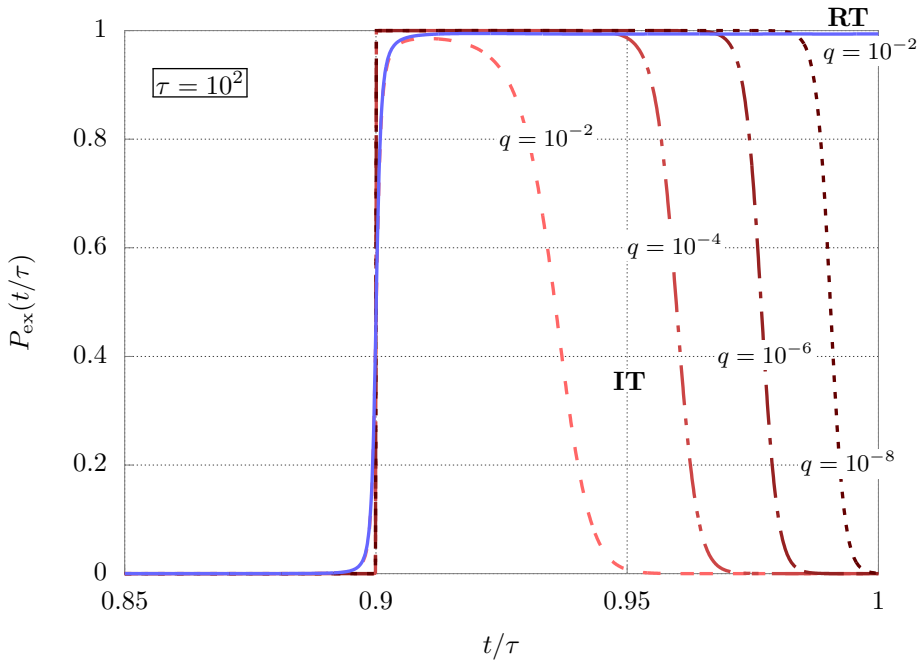

Figure 1.7: Landau-Zener dynamics in real and imaginary time for modes close to the critical wave vector, $k = \pi - q$, with small q. Notice the excitations happening at the critical point $\Gamma_c = 1$ (in units of coupling J) for $t/\tau = 1 - 1/\Gamma_0 = 0.9$.

1.4 Simulated and quantum annealing for disordered case

The general disordered case can be tackled along similar lines as we did for ordered case. The heat-bath quantum Hamiltonian will be in the end quadratic in the JW-fermions. Apart from constants, we can always rewrite it in the general Nambu form:

$$\hat{H}(t) = \widehat{\mathbf{\Psi}}^\dagger \cdot \mathbb{H}(t) \cdot \widehat{\mathbf{\Psi}} = \begin{pmatrix} \hat{\mathbf{c}}^\dagger & \hat{\mathbf{c}} \end{pmatrix} \begin{pmatrix} \mathbf{A}(t) & \mathbf{B}(t) \\ -\mathbf{B}^*(t) & -\mathbf{A}^*(t) \end{pmatrix} \begin{pmatrix} \hat{\mathbf{c}} \\ \hat{\mathbf{c}}^\dagger \end{pmatrix} . \tag{1.104}$$

For a general quadratic fermionic Hamiltonian the $2L \times 2L$ matrix $\mathbb{H}$ should be Hermitean, and its $L \times L$ blocks $\mathbf{A}$ and $\mathbf{B}$ should be, respectively, Hermitean ($\mathbf{A} = \mathbf{A}^\dagger$) and antisymmetric ($\mathbf{B} = -\mathbf{B}^T$). In the Ising case we are considering, where all couplings are *real*, $\mathbb{H}$ is a $2L \times 2L$ real symmetric matrix, $\mathbf{A}$ is real and symmetric ($\mathbf{A} = \mathbf{A}^* = \mathbf{A}^T$), and $\mathbf{B}$ is real and anti-symmetric ($\mathbf{B} = \mathbf{B}^* = -\mathbf{B}^T$) hence we can write:

$$\mathbb{H}(t) = \begin{pmatrix} \mathbf{A}(t) & \mathbf{B}(t) \\ -\mathbf{B}(t) & -\mathbf{A}(t) \end{pmatrix} . \tag{1.105}$$

The structure of the two blocks $\mathbf{A}$ and $\mathbf{B}$ is given, in SA case (omitting any t-dependence), by:

$$\begin{cases} \mathbf{A}_{j,j} = -\Gamma_j^{(0)} \\ \mathbf{A}_{j,j+1} = \mathbf{A}_{j+1,j} = -\dfrac{\Gamma_j^{(1)}}{2} \\ \mathbf{A}_{j,j+2} = \mathbf{A}_{j+2,j} = -\dfrac{\Gamma_{j+1}^{(2)}}{2} \end{cases} \qquad \begin{cases} \mathbf{B}_{j,j} = 0 \\ \mathbf{B}_{j,j+1} = -\mathbf{B}_{j+1,j} = -\dfrac{\Gamma_j^{(1)}}{2} \\ \mathbf{B}_{j,j+2} = -\mathbf{B}_{j+2,j} = -\dfrac{\Gamma_{j+1}^{(2)}}{2} \end{cases} , \tag{1.106}$$

while in the QA case:

$$\begin{cases} \mathbf{A}_{j,j} = -\Gamma \\ \mathbf{A}_{j,j+1} = \mathbf{A}_{j+1,j} = -\dfrac{J_j}{2} \end{cases} \qquad \begin{cases} \mathbf{B}_{j,j} = 0 \\ \mathbf{B}_{j,j+1} = -\mathbf{B}_{j+1,j} = -\dfrac{J_j}{2} \end{cases} . \tag{1.107}$$

In the PBC-spin case, we have additional matrix elements in both A and B connecting neighbors across the boundary, with an overall extra factor $-(-1)^{N_F}$ depending on the fermion parity: $(-1)^{N_F} = +1$ for the ABC-fermion case ($\hat{c}_{L+1} = -\hat{c}_1$, corresponding to even N_F) and $(-1)^{N_F} = -1$ for the PBC-fermion case ($\hat{c}_{L+1} = \hat{c}_1$, corresponding to odd N_F). In SA:

$$\begin{cases} \mathbf{A}_{L,1} = \mathbf{A}_{1,L} = (-1)^{N_F} \dfrac{\Gamma_L^{(1)}}{2} \\ \mathbf{A}_{L-1,1} = \mathbf{A}_{1,L-1} = (-1)^{N_F} \dfrac{\Gamma_L^{(2)}}{2} \\ \mathbf{A}_{L,2} = \mathbf{A}_{2,L} = (-1)^{N_F} \dfrac{\Gamma_1^{(2)}}{2} \end{cases} \qquad \begin{cases} \mathbf{B}_{L,1} = -\mathbf{B}_{1,L} = (-1)^{N_F} \dfrac{\Gamma_L^{(1)}}{2} \\ \mathbf{B}_{L-1,1} = -\mathbf{B}_{1,L-1} = (-1)^{N_F} \dfrac{\Gamma_L^{(2)}}{2} \\ \mathbf{B}_{L,2} = -\mathbf{B}_{2,L} = (-1)^{N_F} \dfrac{\Gamma_1^{(2)}}{2} . \end{cases} , \tag{1.108}$$

and QA:

$$\mathbf{A}_{L,1} = \mathbf{A}_{1,L} = (-1)^{N_F} \frac{J_L}{2} \qquad \mathbf{B}_{L,1} = -\mathbf{B}_{1,L} = (-1)^{N_F} \frac{J_L}{2} , \tag{1.109}$$

As detailed in Appendix C, the most general BCS-paired state one can write will have the Gaussian form:

$$|\psi(t)\rangle = \mathcal{N}(t)\, \mathrm{e}^{\mathcal{Z}(t)}\, |0\rangle = \mathcal{N}(t)\, \mathrm{e}^{\frac{1}{2}(\hat{\mathbf{c}}^\dagger)^T\cdot\mathbf{Z}(t)\cdot(\hat{\mathbf{c}}^\dagger)}\, |0\rangle = \mathcal{N}(t)\, \exp\Big(\frac{1}{2}\sum_{j_1 j_2}\mathbf{Z}_{j_1 j_2}(t)\hat{c}^\dagger_{j_1}\hat{c}^\dagger_{j_2}\Big)\, |0\rangle\ , \tag{1.110}$$

where $\mathcal{Z}(t)$ will be our shorthand notation for the quadratic fermion form we exponentiate. Clearly, since $\hat{c}^\dagger_{j_1}\hat{c}^\dagger_{j_2} = -\hat{c}^\dagger_{j_2}\hat{c}^\dagger_{j_1}$ we can take the matrix $\mathbf{Z}$ to be *antisymmetric* (complex, in general, but real for the problem we are considering, since imaginary-time dynamics does not bring in any imaginary numbers): any symmetric part of $\mathbf{Z}$ would give 0 contribution. The time-derivative of such a state will be simply:

$$\frac{\partial}{\partial t}|\psi(t)\rangle = \Big[\Big(\frac{1}{2}\sum_{j_1 j_2}\dot{\mathbf{Z}}_{j_1 j_2}(t)\hat{c}^\dagger_{j_1}\hat{c}^\dagger_{j_2}\Big) + \frac{\dot{\mathcal{N}}}{\mathcal{N}}\Big]|\psi(t)\rangle\ . \tag{1.111}$$

Using Eq. (C.5) we immediately derive that:

$$\hat{c}_j \mathrm{e}^{\mathcal{Z}}|0\rangle = \sum_{j'}\mathbf{Z}_{jj'}\hat{c}^\dagger_{j'}\mathrm{e}^{\mathcal{Z}}|0\rangle\ . \tag{1.112}$$

which immediately implies that the normal terms of the Hamiltonian bring:

$$\sum_{j_1 j_2}\hat{c}^\dagger_{j_1}\mathbf{A}_{j_1 j_2}\hat{c}_{j_2}\mathrm{e}^{\mathcal{Z}}|0\rangle = \sum_{j_1 j_2}\hat{c}^\dagger_{j_1}(\mathbf{A}\cdot\mathbf{Z})_{j_1 j_2}\hat{c}^\dagger_{j_2}\mathrm{e}^{\mathcal{Z}}|0\rangle\ . \tag{1.113}$$

With similar manipulations, we can deal with all terms of $\widehat{H}$, obtaining:

$$\widehat{H}(t)|\psi(t)\rangle = \Big[\sum_{j_1 j_2}\hat{c}^\dagger_{j_1}\Big(\mathbf{A}\cdot\mathbf{Z} + \mathbf{Z}\cdot\mathbf{A} + \mathbf{B} + \mathbf{Z}\cdot\mathbf{B}\cdot\mathbf{Z}\Big)_{j_1 j_2}\hat{c}^\dagger_{j_2} - \mathrm{Tr}\,\mathbf{A} - \mathrm{Tr}(\mathbf{B}\cdot\mathbf{Z})\Big]|\psi(t)\rangle\ . \tag{1.114}$$

Equating term-by-term left and right-hand side of the Scrödinger equation, and omitting the time-dependence of all quantities, we finally get:

$$\xi\dot{\mathbf{Z}} = -2\Big(\mathbf{A}\cdot\mathbf{Z} + \mathbf{Z}\cdot\mathbf{A} + \mathbf{B} + \mathbf{Z}\cdot\mathbf{B}\cdot\mathbf{Z}\Big)\ , \tag{1.115}$$

with $\xi = 1$ for SA and QA-IT, and $\xi = -i$ for QA-RT. Notice that the right-hand side is manifestly antisymmetric. In principle we can write an equation for $\mathcal{N}(t)$ as well, although not particularly useful here:

$$\xi\,\frac{\dot{\mathcal{N}}}{\mathcal{N}} = \frac{d}{dt}\log\mathcal{N} = \mathrm{Tr}\,\mathbf{A} + \mathrm{Tr}(\mathbf{B}\cdot\mathbf{Z}) - \text{Constants}\ , \tag{1.116}$$

where "Constants" denotes all possible constant terms appearing in the Hamiltonian, omitted from the Nambu quadratic form.

As already mentioned, all we really need to do is to properly normalize the state in calculating the averages. All the information regarding the normalization is contained in the antisymmetric matrix $\mathbf{Z}(t)$.

1.5 Results for the disordered case

We now discuss the results for disordered Ising chains with open BC, and couplings J_j chosen from a flat distribution, $J_j \in [0,1]$. First we focus on the minimal gap distributions for SA and QA. In the second subsection we present the results on SA, QA-RT and QA-IT dynamics.

1.5.1 Minimal gap distributions

The smallest instantaneous gap that occurs during the total evolution of the annealing is the key element for the dynamics, since it directly affects the adiabaticity (or non-adiabaticity) of the process. For QA, given a random realization of energy interactions J_j, there is not a unique critical value of the transverse field Γ at which the minimal gap occurs. Indeed, the transverse field random Ising model is known to possess an *infinite randomness critical point* whose average is given by the known relation $\ln \Gamma_c = \langle \ln J_i \rangle$ [46]. In our case:

$$\langle \ln J_i \rangle = \int_0^1 \mathrm{d}J_i \; \mathrm{P}(J_i) \ln J_i = \int_0^1 \mathrm{d}J_i \; \ln J_i = -1 \qquad \Longrightarrow \qquad \Gamma_c = 1/\mathrm{e} \; . \tag{1.117}$$

In Figure 1.8 we show the lowest instantaneous gaps for a particular realization of the chain, with a minimal gap slightly shifted from Γ_c.

At the critical point the distribution of the equilibrium gaps Δ becomes a universal function [47] of $g = -(\ln \Delta)/\sqrt{L}$, as we can see in Figure 1.9, where g-distributions for different chain length L collapse into a single curve.

The SA Hamiltonian $\widehat{H}_{\mathrm{SA}}$ shows different physics: the smallest typical equilibrium gaps are seen at the end of the annealing, $T \to 0$, where they vanish Arrhenius-like, $\Delta_{\mathrm{typ}}(T) \sim \mathrm{e}^{-B/T}$ with $B/J \sim 2$ (Fig. 1.10 and 1.11). We expect that $B/J = 2$ is a finite size effect, turning into $B/J = 4$ in the thermodynamic limit, as suggested from the ordered case (Eqs. 1.94 and 1.95). In fact, in ordered case, the leading term $b_k \sim \mathrm{e}^{-2\beta J}/L$ is replaced by $-2\alpha \mathrm{e}^{-4\beta J}$ for $L \to +\infty$.

1.5.2 Annealing results

Turning to dynamics, we calculate $\rho_{\mathrm{def}}(\tau)$ and $\epsilon_{\mathrm{res}}(\tau)$ by integrating numerically the equation for $\mathbf{Z}$:

$$\xi \dot{\mathbf{Z}} = -2\Big(\mathbf{A} \cdot \mathbf{Z} + \mathbf{Z} \cdot \mathbf{A} + \mathbf{B} + \mathbf{Z} \cdot \mathbf{B} \cdot \mathbf{Z}\Big) \tag{1.118}$$

with $\xi = 1$ for SA and QA-IT, while $\xi = -i$ for QA-RT. This is feasible for L up to $O(1000)$. Given the need for a good statistics, we will present data up to $L = 128$. The $\mathbf{A}$ and $\mathbf{B}$ matrices take the values as in Eqs. 1.106 and 1.107 with open BC. The annealing schedule is the same as in the ordered case:

$$\text{SA: } T(t) = T_0 \left(1 - \frac{t}{\tau}\right) \; , \qquad \text{QA: } \Gamma(t) = \Gamma_0 \left(1 - \frac{t}{\tau}\right) \; , \tag{1.119}$$

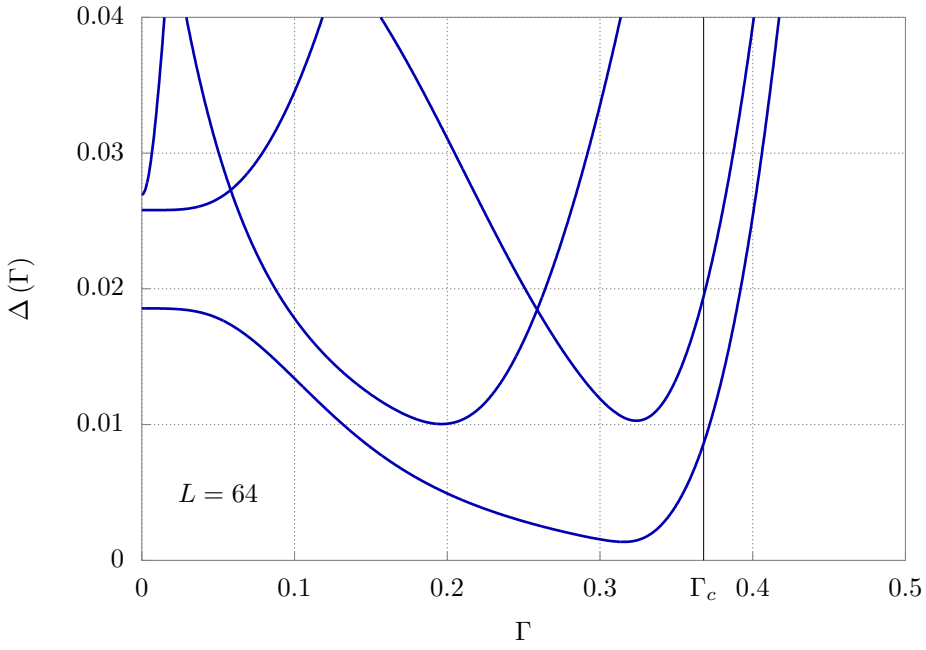

Figure 1.8: Lowest-lying instantaneous spectral gaps Δ_n as a function of Γ for QA with $L = 64$. Notice the minimal gap located close to $\Gamma_c = 1/\mathrm{e}$.

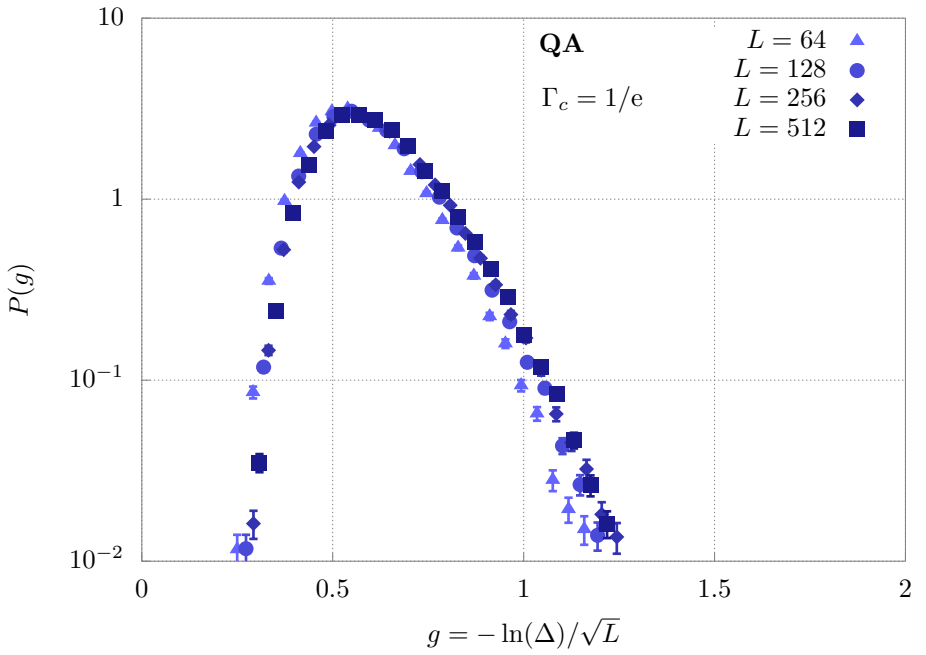

Figure 1.9: Distributions of $g = -(\ln \Delta)/\sqrt{L}$, Δ being the equilibrium gap at the critical point $\Gamma_c = 1/\mathrm{e}$, in the QA case for different chain lengths L.

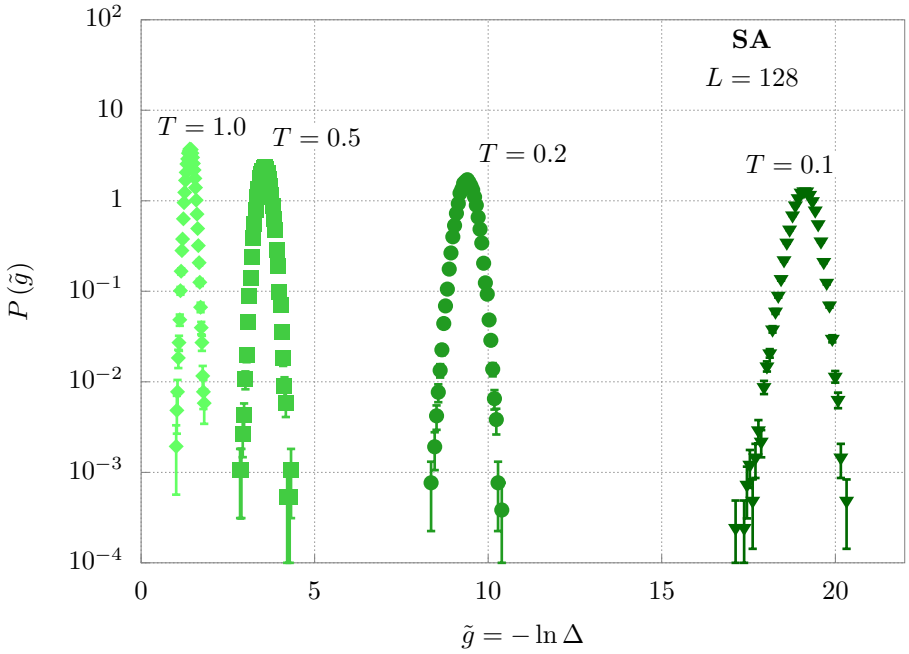

Figure 1.10: Distributions of equilibrium gaps $\tilde{g} = -\ln \Delta$ in the SA case at temperatures $k_B T/J = 1, 0.5, 0.2, 0.1$ for a chain length $L = 128$.

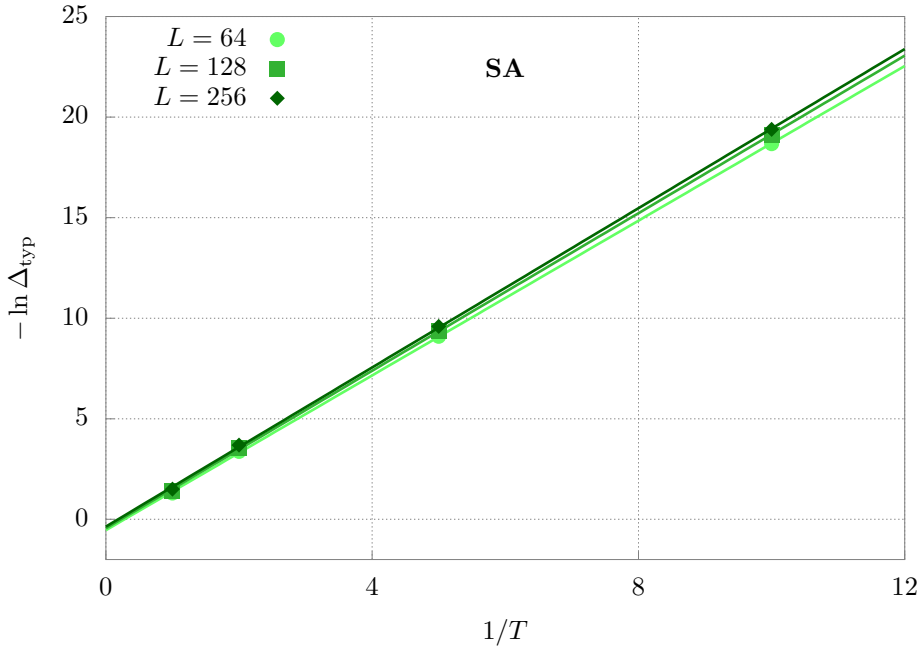

Figure 1.11: Arrhenius-like behavior of the typical minimum gap Δ_{typ} in the SA case vs. $1/T$ for different chain lengths.

with $T_0 = 5\,J/k_{\rm B}$ and $\Gamma_0 = 5\,J$. The system is initialized in its ground state, correspondent to $\mathbf{Z}(t=0) = -(\mathbf{U}^\dagger)^{-1}\cdot\mathbf{V}^\dagger$. For any given τ, we considered many disorder realizations, obtaining distributions for $\rho_{\rm def}(\tau)$ and $\epsilon_{\rm res}(\tau)$. The observables can be computed in terms of $\mathbf{Z}$ matrix through the following relations (see Appendix B.2):

$$\rho_{\rm def} = \frac{1}{2} - \frac{1}{2\,(L-1)}\sum_{j=1}^{L-1}\left(G_{j+1,j} + F_{j,j+1} + c.\,c.\right)\ , \tag{1.120}$$

$$E_{\rm res} = \sum_{j=1}^{L-1} J_j\left[1 - \left(G_{j+1,j} + F_{j,j+1} + c.\,c.\right)\right]\ . \tag{1.121}$$

where matrices $\mathbf{F}$ and $\mathbf{G}$ are expressed in terms of $\mathbf{Z}$ (see Appendix D for derivation):

$$\mathbf{F} = (\mathbf{1} + \mathbf{Z}\mathbf{Z}^\dagger)^{-1}\mathbf{Z}\ , \tag{1.122}$$

$$\mathbf{G} = (\mathbf{1} + \mathbf{Z}\mathbf{Z}^\dagger)^{-1}\mathbf{Z}\mathbf{Z}^\dagger\ . \tag{1.123}$$

For SA these distributions are approximately log-normal (Fig. 1.12), as previously found for QA-RT [34], with a width decreasing as $1/\sqrt{L}$, implying that the average $[\rho_{\rm def}]_{\rm av}$ approaches the *typical* value $[\rho_{\rm def}]_{\rm typ} = \mathrm{e}^{[\ln\rho_{\rm def}]_{\rm av}}$ for large L, and similarly for $\epsilon_{\rm res}$.

QA-IT behaves differently: the distributions of both $\rho_{\rm def}(\tau)$ and $\epsilon_{\rm res}(\tau)$ show marked deviations from log-normal, see Fig. 1.13, hence typical and average values are rather different. Fig. 1.14 shows $[\rho_{\rm def}(\tau)]_{\rm typ/av}$ (a) and $[\epsilon_{\rm res}(\tau)]_{\rm typ/av}$ (b) for the three annealings performed.

The SA results are nearly size-independent, with a clear logarithmic behaviour [48] for large τ:

$$\begin{aligned}\left[\rho_{\rm def}\right]^{\rm SA} &\sim \log^{-1}(\gamma_{\rm SA}\tau)\ ,\\ \left[\epsilon_{\rm res}\right]^{\rm SA} &\sim \log^{-2}(\gamma_{\rm SA}\tau)\ ,\end{aligned} \tag{1.124}$$

with $\gamma_{\rm SA} \approx 6.5$. Notice that a residual energy of the form $\epsilon_{\rm res} \sim \log^{-\zeta_{\rm SA}}(\gamma_{\rm SA}\tau)$ with $\zeta_{\rm SA} = 2$ saturates the bound $\zeta_{\rm SA} \le 2$ for thermal annealing in glassy systems [49]. Concerning the QA-RT case, results are well established from Ref. [34] where larger systems were tackled by the linear BdG equations:

$$\begin{aligned}\left[\rho_{\rm def}\right]^{\rm QA-RT} &\sim \log^{-2}(\gamma\tau)\ ,\\ \left[\epsilon_{\rm res}\right]^{\rm QA-RT} &\sim \log^{-\zeta}(\gamma\tau)\ ,\end{aligned} \tag{1.125}$$

with $\gamma \approx 0.13$, and $\zeta \approx 3.4$. Finally, we again find QA-IT very different from QA-RT, with a faster, power-law, decrease of $\rho_{\rm def}$ and $\epsilon_{\rm res}$. The size-dependence of the data is revealing: the "typical" data move upwards with increasing L, but, luckily, the "average" data show the opposite tendency — they move towards lower values, with an increasing slope vs τ. It is fair to

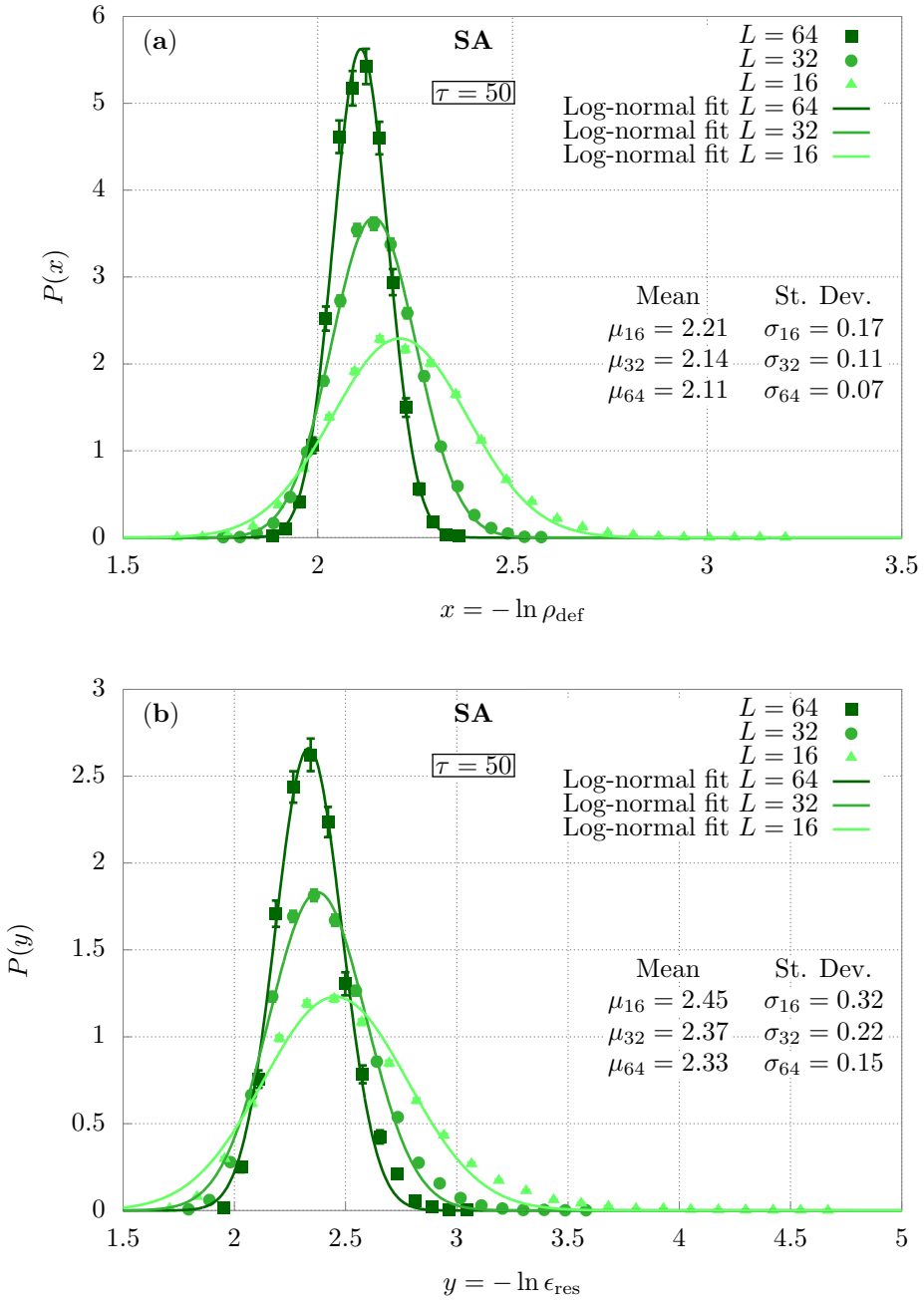

Figure 1.12: (**a**) Probability distribution for the logarithm of the density of defects $x = -\ln \rho_{\text{def}}$ and (**b**) residual energy $y = -\ln \epsilon_{\text{res}}$ for a SA evolution with annealing time $\tau = 50$ for $L = 32$ and 64.

conclude that our data support a power-law for both $\rho_{\rm def}$ and $\epsilon_{\rm res}$:

$$\begin{aligned} [\rho_{\rm def}]^{\rm QA-IT}_{\rm typ/av} &\sim \tau^{-\mu_\rho} \, , \\ [\epsilon_{\rm res}]^{\rm QA-IT}_{\rm typ/av} &\sim \tau^{-\mu_\epsilon} \, , \end{aligned} \tag{1.126}$$

where we estimate $\mu_\rho \sim 1 \div 2$ and $\mu_\epsilon \sim 1.5 \div 2$.

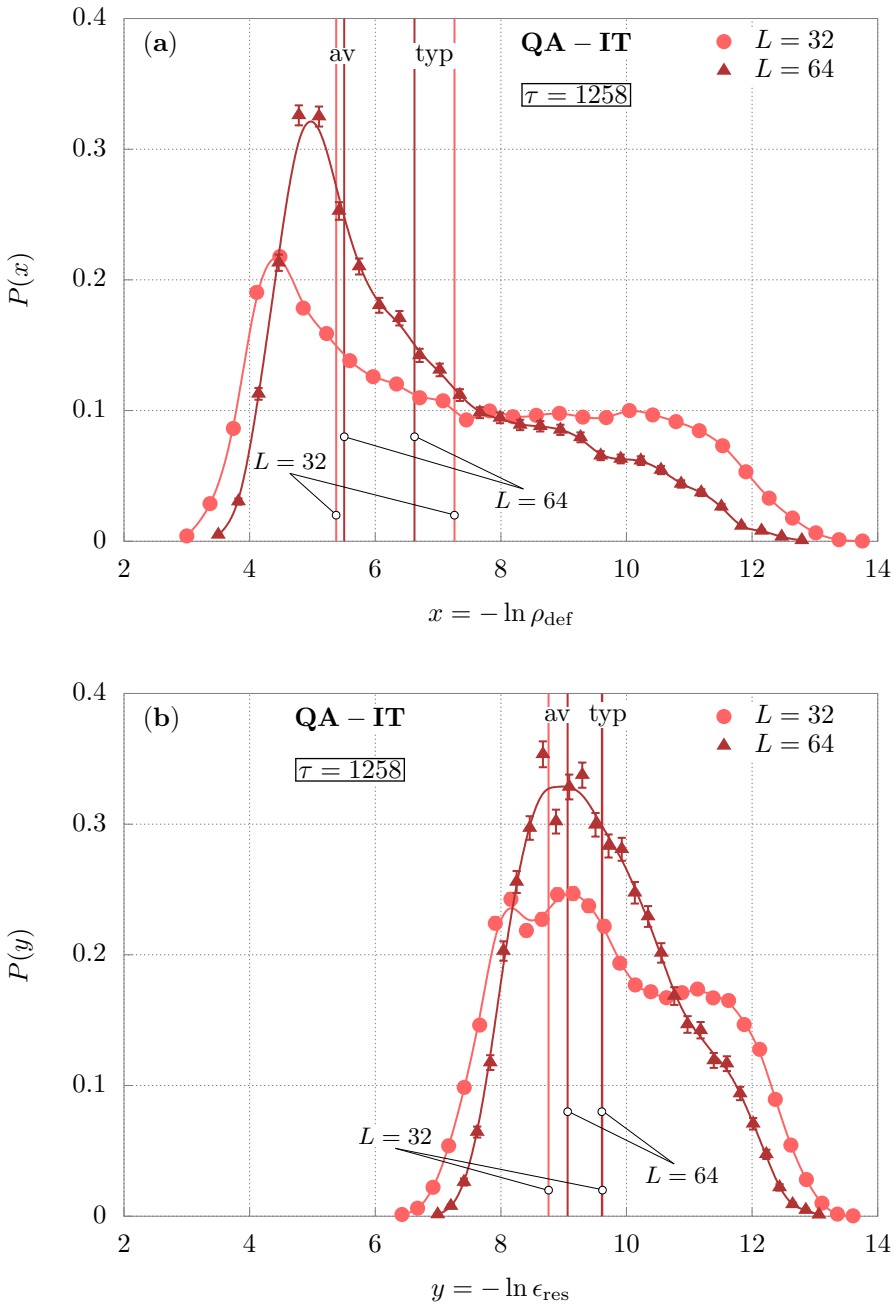

Figure 1.13: (**a**) Probability distribution of $x = -\ln \rho_{\rm def}$ and (**b**) residual energy $y = -\ln \epsilon_{\rm res}$ for QA-IT with $\tau = 1258$ for $L = 32$ and 64. Notice the deviation from log-normal distribution. Increasing L the average and typical values tend to a common value.

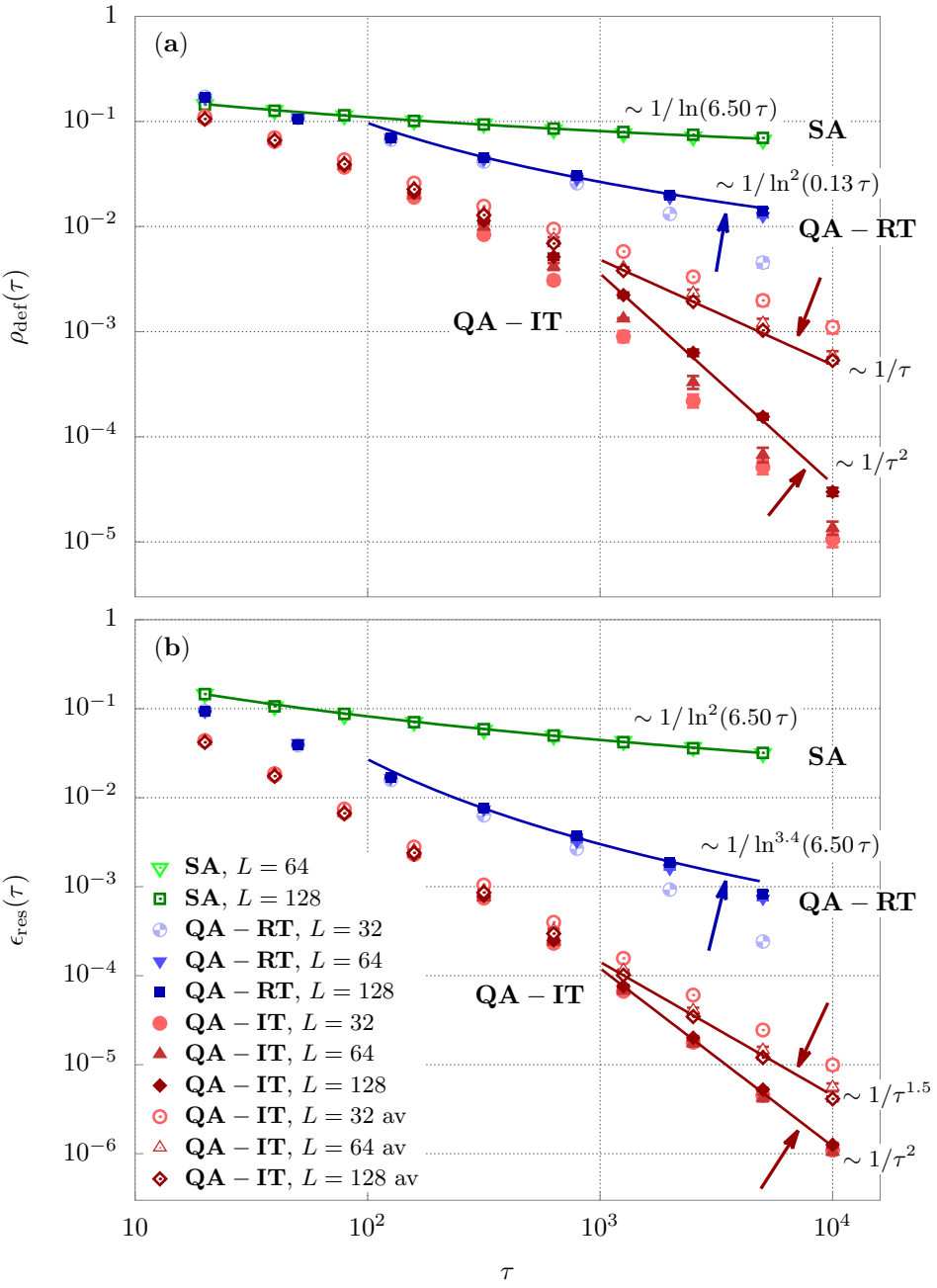

Figure 1.14: (**a**) Density of defects $[\rho_{\rm def}(\tau)]_{\rm typ}$ and (**b**) residual energy $[\epsilon_{\rm def}(\tau)]_{\rm typ}$ versus τ for SA, QA-RT and QA-IT (for which average data are also shown). The lines are fits of the data. Solid arrows are guides to the eye for the size dependence towards $L \to +\infty$.

1.6 Conclusions

We have presented a non-trivial example of a quantum speedup of real-time Schrödinger QA over master-equation SA on an equal-footing single-flip deterministic dynamics. Our second important result is that a "fictitious" imaginary-time QA behaves very differently from the "physical" real-time QA, providing a much faster annealing, with an asymptotic behavior compatible with $\tau^{-\mu}$, with $\mu \approx 1 \div 2$, i.e., an *exponential speedup*. Hence, provocatively, "quantum inspired" is here better than "quantum", a point that deserves further studies. Results on the fully-connected Ising ferromagnet confirm that this IT-speedup is not specific to the present 1d problem [50].

The specific problem we addressed — a random ferromagnetic Ising chain — is "easy" in many respects: *i)* it does not possess frustration, the ingredient that makes optimization problems generally hard [18], *ii)* it can be reduced to a quadratic fermionic problem, and *iii)* is also a case where SA does not encounter any phase transition for $T \to 0$, while the QA dynamics goes through a critical point at $\Gamma_c > 0$. This, as discussed in Ref. [19] for the spin-glass case, might in principle give an unfair advantage to SA over QA: but, remarkably, it doesn't, in the present case. Our study provides a useful benchmark for many possible developments, like the role of thermal effects, or the comparison with QA simulated by path-integral MC [51]. Our QA-IT results suggest also to pursue the application of diffusion quantum MC to simulate the imaginary-time Schrödinger QA, likely a very good "quantum-inspired" classical optimization algorithm [52].

Chapter 2

Quantum lubricity

In this chapter we deal with a different out-of-equilibrium quantum problem. We present a nanofriction model – a quantum version of the classical Prandtl-Tomlinson model – that aims to describe quantum effects in the sliding problem. In the classical model, a particle is pulled by a harmonic spring over a one-dimensional sinusoidal potential. The dissipation is introduced by adding a viscous term, proportional to the particle velocity, and a random force, that provides thermal equilibrium with the environment. The dynamics is then solved for a single stochastic evolution through a Langevin equation, and then averaged over many realizations. In the quantum version, the dissipation is provided by introducing an interaction with a bosonic bath, composed of a large number of harmonic oscillators. Given the huge complexity in dealing with a large number of degrees of freedom in quantum mechanics, the problem is tackled by solving a quantum master equation on the reduced matrix, where the bath degrees of freedom are traced out. A comparison between classical and quantum results shows a huge difference in the average dissipated energy per period, with a much higher amount of heat generated by the classical evolution. This can be explained in terms of LZ theory, that predicts a resonant tunneling to a nearby excited state, responsible for a significative drop of frictional force – a phenomenon which we may call quantum lubricity. This phenomenon is responsible also for the discontinuous particle transfer to the next well, happening in correspondence of avoided crossings of energy levels. Moreover, the theory predicts an adiabatic regime of low velocities where the frictional force drops to zero non-analytically in the particle velocity with a $e^{-v^*/v}$ behavior.

In Section 2.1 We present the quantum model and the method for solving its dynamics. In Section 2.2 we derive the classical equations of motion from the Hamiltonian used for the quantum case. In Section 2.3 we present the results comparing classical and quantum dynamics using the same physical parameters, and finally in Section 2.4 we draw some conclusions.

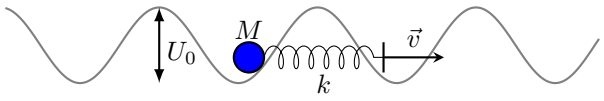

Figure 2.1: Pictorial sketch of the nanofriction model. A particle is pulled by a moving spring over a sinusoidal potential.

2.1 Quantum model

Our model consists of a single quantum particle of mass M in the one-dimensional periodic potential created, for instance, by an optical lattice, of strength U_0 and lattice spacing a. The particle is set in motion by the action of a harmonic spring k, representing for instance an optical tweezer, which moves with constant velocity v (Fig. 2.1):

$$\hat{H}_{\mathrm{Q}}(t) = \frac{\hat{p}^2}{2M} + U_0 \sin^2\left(\frac{\pi}{a}\hat{x}\right) + \frac{k}{2}\left(\hat{x} - vt\right)^2 \ . \tag{2.1}$$

The forced motion gives the particle an energy that, in a frictional steady state, is removed by dissipation in a thermostat. As pioneered by Feynman and Vernon [53], such a dissipation can be introduced by means of a harmonic bath [54]

$$\hat{H}_{\mathrm{int}} = \sum_i \left[\frac{\hat{p}_i^2}{2m_i} + \frac{1}{2}m_i\omega_i^2\Big(\hat{x}_i - \frac{c_i}{m_i\omega_i^2}\hat{X}\Big)^2\right] \ , \tag{2.2}$$

where each oscillator $\hat{x}_i$ couples, through an interaction coefficient c_i, to the "periodic position" of the particle $\hat{X} = \sin\left(\frac{2\pi}{a}\hat{x}\right)$. The coefficients c_i determine the coupling strength of the bath, through the spectral function $J(\omega) = \hbar\sum_i \frac{c_i^2}{2m_i\omega_i}\,\delta(\omega - \omega_i)$, which we choose of the standard Caldeira-Leggett ohmic form $J(\omega) = 2\alpha\hbar^2\omega \mathrm{e}^{-\omega/\omega_c}$, where ω_c sets the high-energy cutoff.

2.1.1 Wannier functions basis

In order to simulate the problem we need, first of all, to restrict the space to few wells of the lattice potential and set periodic boundary conditions. This is straightforward for periodic function $\sin^2(\pi x/a)$, while parabolic potential needs to be manipulated a bit:

$$\frac{k}{2}\left(\hat{x} - vt\right)^2 \quad \Longrightarrow \quad \frac{k}{2}\left[\ \mathrm{mod}\ \left(\hat{x} - vt - \frac{L}{2}, L\right) - \frac{L}{2}\right]^2 \ , \tag{2.3}$$

with L the length of lattice. Our choice is to set the number of wells equal four ($N = 4$), taking care to have reasonable high parabolic potential at the boundary with almost zero probability for the particle to cross it. A sketch of the new total potential is represented in Figure 2.2.

The second step is to set a wavefunctions basis. This is done by considering the time-independent part of the Hamiltonian constituted by the solely lattice potential, $\hat{H}_{\mathrm{V}} = \frac{\hat{p}^2}{2M} +$

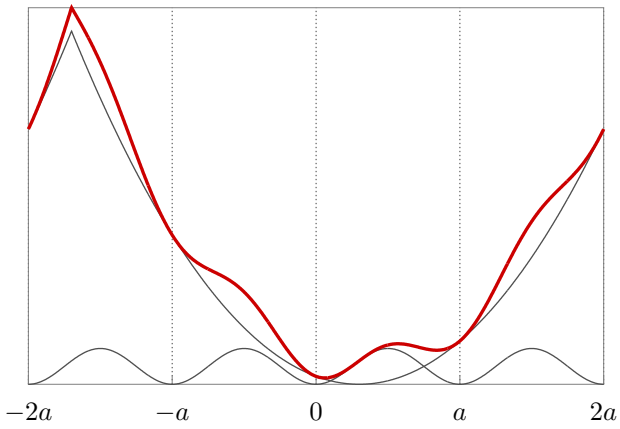

Figure 2.2: Total periodic potential as sum of lattice and parabolic contributions.

$U_0 \sin^2\left(\frac{\pi}{a}\hat{x}\right)$. The correspondent Schrödinger equation can be cast into a Mathieu equation[1] after a rescaling of the position $\zeta \equiv \frac{\pi}{a}x$:

$$-\frac{\hbar^2}{2M}\frac{d^2}{dx^2}\psi(x) + U_0 \sin^2\left(\frac{\pi}{a}\hat{x}\right)\psi(x) = E\psi(x) \tag{2.5}$$

$$\Downarrow$$

$$\frac{d^2}{d\zeta^2}\psi_{\mathrm{m}}(\zeta) + \left[a_{\mathrm{m}} - 2q_{\mathrm{m}}\cos(2\zeta)\,\psi_{\mathrm{m}}(\zeta)\right] = 0\ , \tag{2.6}$$

with adimensional parameters

$$a_{\mathrm{m}} = \frac{2Ma^2}{\pi^2\hbar^2}E - \frac{Ma^2}{\pi^2\hbar^2}U_0 = \frac{E}{E_R} - \frac{U_0}{2E_R}\ , \tag{2.7}$$

$$q_{\mathrm{m}} = -\frac{Ma^2}{2\pi^2\hbar^2}U_0 = -\frac{U_0}{4E_R}\ , \tag{2.8}$$

where we have introduced the *recoil energy* $E_R = \pi^2\hbar^2/2Ma^2$.

Mathieu functions (Fig 2.3) are solutions of Eq. 2.6, and therefore they are eigenfunctions of $\hat{H}_{\mathrm{V}}$:

$$\hat{H}_{\mathrm{V}}\,\psi_{\mathrm{m}}^{(l,n)}(x) = E_{l,n}\,\psi_{\mathrm{m}}^{(l,n)}(x)\ , \tag{2.9}$$

where n is the energy band and l spans from 1 to N. Notice that the functions are two-fold degenerate, except for $l = 1$ and $l = N$. Mathieu functions are real functions and form an

[1] Mathieu equation takes the general form:

$$\frac{d^2y(x)}{dx^2} + \left[a_{\mathrm{m}} - 2q_{\mathrm{m}}\cos(2x)\right]y(x) = 0\ . \tag{2.4}$$

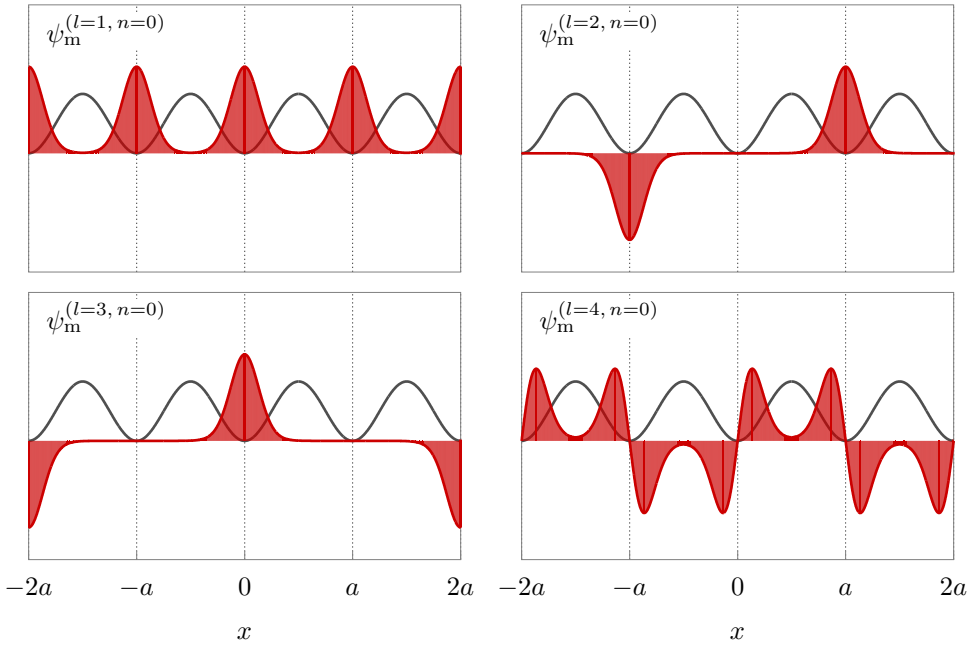

Figure 2.3: Mathieu functions for the first band. Notice that the two degenerate functions ($l = 2$ and $l = 3$) differ just by a shift.

orthonormal basis:

$$\int_{-L/2}^{L/2} \psi_{\mathrm{m}}^{(l,n)}(x)\, \psi_{\mathrm{m}}^{(l',n')}(x) = \delta_{l,l'}\, \delta_{n,n'} \ . \tag{2.10}$$

They are related to Bloch functions $\psi_{\mathrm{b}}^{(k,n)}(x) = \mathrm{e}^{ikx} u_{k,n}(x)$ by linear combinations:

$$\psi_{\mathrm{b}}^{(k=0,\,n)}(x) = \psi_{\mathrm{m}}^{(l=1,\,n)}(x) \tag{2.11}$$

$$\psi_{\mathrm{b}}^{(k=\pm 2\pi(l-1)/Na,\,n)}(x) = \frac{1}{\sqrt{2}} \left(\psi_{\mathrm{m}}^{(l,n)}(x) \pm i\, \psi_{\mathrm{m}}^{(l+1,\,n)}(x) \right) \qquad \text{with } l \neq 1, N \tag{2.12}$$

$$\psi_{\mathrm{b}}^{(k=\pi/a,\,n)}(x) = \psi_{\mathrm{m}}^{(l=N,\,n)}(x) \ , \tag{2.13}$$

with correspondent eigenenergies $E_{k,n}$ shown in Figure 2.4, for parameter $U_0 = 38.5\, E_R$. Notice that Bloch functions correspondent to $k = 0$ and $k = \pi/a$ are real. The (delocalized) Bloch waves can be transformed into localized states called *Wannier* states (Fig. 2.5):

$$W_{j,n}(x) = \frac{1}{\sqrt{N}} \sum_{k}^{\mathrm{BZ}} \mathrm{e}^{-ikaj} \psi_{\mathrm{b}}^{(k,n)}(x) \ , \tag{2.14}$$

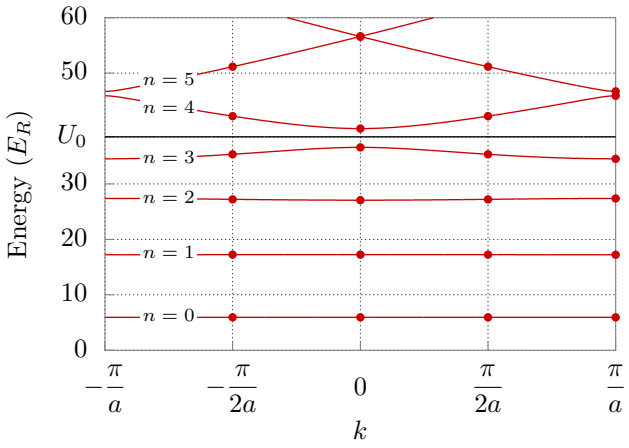

Figure 2.4: Energy spectrum of the first six bands for the infinite lattice potential. Dots are the energies for the reduced system $L = 4$. $U_0 = 38.5\, E_R$ is the height of lattice potential.

where BZ indicates sum over all the Brillouin zone. From this definition it follows that[2]

$$W_{j,n}(x + ma) = W_{j-m,n}(x) \; . \tag{2.15}$$

Moreover, they form an orthonormal basis:

$$\int_{-L/2}^{L/2} dx \, W^*_{j,n}(x) \, W_{j',n'}(x) = \delta_{j,j'} \, \delta_{n,n'} \; . \tag{2.16}$$

Our choice is to set Wannier states as wavefunctions basis for our problem, since they are localized and therefore more physically intuitive than delocalized states.

The $\hat{H}_{\mathrm{V}}$ matrix elements are readily computed:

$$\langle W_{j,n}| \, \hat{H}_{\mathrm{V}} \, |W_{j',n'}\rangle = \frac{1}{N} \sum_{k,k'} \mathrm{e}^{ia(kj-k'j')} \left\langle \psi_{\mathrm{b}}^{(k,n)} \right| \hat{H}_{\mathrm{V}} \left| \psi_{\mathrm{b}}^{(k',n')} \right\rangle = \frac{1}{N} \, \delta_{n,n'} \sum_{k} E_{k,n} \, \mathrm{e}^{ika(j-j')} \; . \tag{2.17}$$

[2] From Bloch functions property $\psi_{\mathrm{b}}^{(k,n)}(x + ma) = \mathrm{e}^{ikma} \, \psi_{\mathrm{b}}^{(k,n)}(x)$ we have:

$$\begin{aligned} W_{j,n}(x + ma) &= \frac{1}{\sqrt{N}} \sum_{k}^{\mathrm{BZ}} \mathrm{e}^{-ikaj} \, \psi_{\mathrm{b}}^{(k,n)}(x + ma) \\ &= \frac{1}{\sqrt{N}} \sum_{k}^{\mathrm{BZ}} \mathrm{e}^{-ika(j-m)} \, \psi_{\mathrm{b}}^{(k,n)}(x) \\ &= W_{j-m,n}(x) \; . \end{aligned}$$

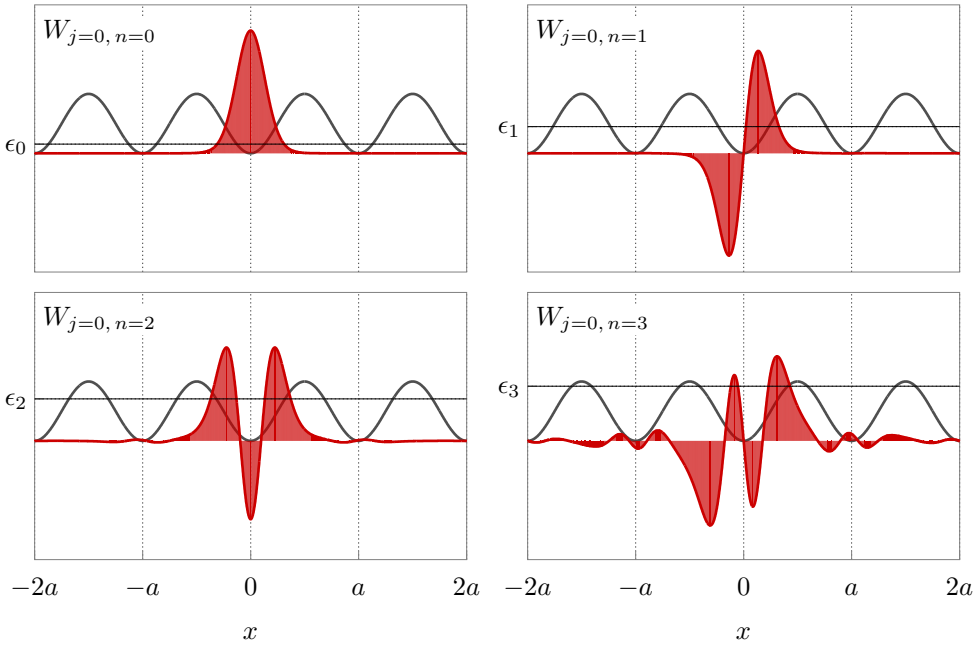

Figure 2.5: First four Wannier states for central well $j = 0$ of the lattice potential with the correspondent onsite energy ϵ_n.

From Eq. 2.17 we see that $[\hat{H}_{\mathrm{V}}]_{j,n;j',n'}$ is a block matrix. For $N = 4$ it takes the form:

$$[\hat{H}_{\mathrm{V}}]_{j,n;j',n'} = \begin{pmatrix} \epsilon_0 & t_{1,0} & t_{2,0} & t_{1,0} & & & & & \\ t_{1,0} & \epsilon_0 & t_{1,0} & t_{2,0} & & & & & \\ t_{2,0} & t_{1,0} & \epsilon_0 & t_{1,0} & & & & & \\ t_{1,0} & t_{2,0} & t_{1,0} & \epsilon_0 & & & & & \\ & & & & \epsilon_1 & t_{1,1} & t_{2,1} & t_{1,1} & \\ & & & & t_{1,1} & \epsilon_1 & t_{1,1} & t_{2,1} & \\ & & & & t_{2,1} & t_{1,1} & \epsilon_1 & t_{1,1} & \\ & & & & t_{1,1} & t_{2,1} & t_{1,1} & \epsilon_1 & \\ & & & & & & & & \ddots \end{pmatrix} , \tag{2.18}$$

with onsite energies:

$$\epsilon_n = \frac{1}{N} \sum_k E_{k,n} \, , \tag{2.19}$$

and hopping terms:

$$t_{r,n} = \frac{1}{N} \left[E_{k=0,n} + (-1)^r E_{k=\pi/a,n} + \sum_{k>0}^{k \neq \pi/a} 2\cos\left(kar\right) \right] \, , \tag{2.20}$$

with $r = j - j'$.

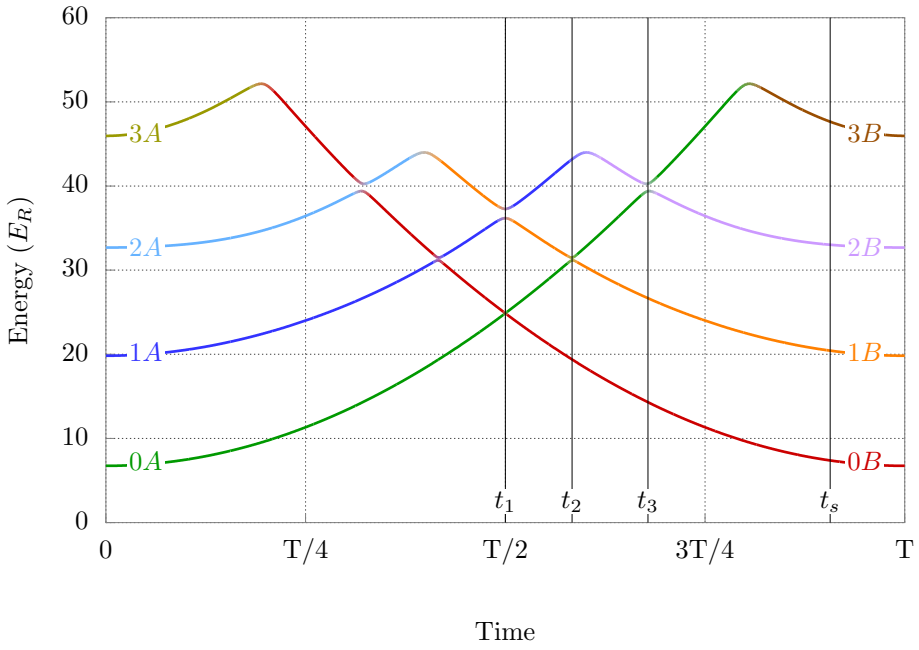

Figure 2.6: The four lowest instantaneous eigenvalues of a particle that is adiabatically driven by the harmonic trap from a periodic potential minimum to the nearest one. Note the avoided-crossing gaps associated with tunnelling events encountered during the dynamics at times t_1, t_2 and t_3. At time t_s a classical particle would be pushed to the next well after the disappearance of the rising local minimum.

2.1.2 Dynamics

Having set the Wannier basis, we introduce the time-dependent harmonic potential $(k/2)\,(\hat{x}-vt)^2$. The coherent part of dynamics is governed by

$$\hat{H}_{\rm Q}(t) = \frac{\hat{p}^2}{2M} + U_0 \sin^2\left(\frac{\pi}{a}\hat{x}\right) + \frac{k}{2}\,(\hat{x}-vt)^2 \ , \tag{2.21}$$

whose matrix elements are given by:

$$\langle W_{j,n}|\,\hat{H}_{\rm Q}\,|W_{j',n'}\rangle = \langle W_{j,n}|\,\hat{H}_{\rm V}\,|W_{j',n'}\rangle + \int_{-L/2}^{L/2} dx\, W^*_{j,n}(x)\,(x-vt)^2\,W_{j',n'}(x)\ . \tag{2.22}$$

We can understand the basic mechanism leading to quantum frictional dissipation by considering the instantaneous eigenstates of $\hat{H}_{\rm Q}(t)$, shown in Fig. 2.6 for a reduced Hilbert space with 4 states per well. Denote by $\mathrm{T} = a/v$ the time period in which the driving spring moves by one lattice spacing: at $t = 0$, when the harmonic potential is centered at $x = 0$, the lowest eigenstate is essentially coincident with the lowest Wannier state in the $x = 0$ potential well, that we call "$0A$". As the harmonic spring moves forward, at $t = t_1 = \mathrm{T}/2$, the particle negotiates the perfect double-well state between $x = 0$ and $x = a$ ("0B"), where all pairs of left and right

levels anticross. The LZ "diabatic" transition rate (population of the excited state after the anticrossing) between levels $E_n(t)$ and $E_{n'}(t)$ is given by LZ formula A.5:

$$P_{n\to n'} = \mathrm{e}^{-\frac{\pi\Delta^2_{nn'}}{2\hbar v\alpha_{nn'}}} = \mathrm{e}^{-\frac{v_{n\to n'}}{v}} \ , \tag{2.23}$$

where $\alpha_{nn'}$ is the relative slope of the two eigenvalues involved, E_n and $E_{n'}$, $\Delta_{nn'}$ their anticrossing gap, and v is the speed.

At the anticrossing at $t_1 = \mathrm{T}/2$ between ground states at $x = 0$ and $x = a$, due to the large barrier the states are very localized and the gap, here Δ_{01}, is exceedingly small. For very small velocity, nonetheless,

$$v \ll v_{0\to 1} = \frac{\pi\Delta^2_{01}}{2\hbar\partial_x \left|E_1 - E_0\right|} \ , \tag{2.24}$$

the LZ transition rate $P_{0\to 1}$ (2.23), which as we shall see is proportional to the frictional dissipation, is negligible. In that low velocity case, a quantum particle is transmitted adiabatically without friction. This is therefore a regime, which one might designate of *quantum superlubricity*, where friction vanishes non analytically as in Eq. (2.23) in the limit of zero speed – totally unlike the classical case, where friction vanishes linearly with v (viscous friction). Quantum superlubricity should be realized at sufficiently low temperature, to be thermally destroyed in favor of viscous lubricity as soon as temperature T is large enough to upset the LZ physics behind the mechanism. This, however, is not expected to occur until T becomes considerably larger than the tunnelling gap Δ_{01}, as a recent study on the dissipative LZ problem has confirmed [55].

Moving on to larger speeds $v \gg v_{0\to 1}$, the particle, unable to negotiate tunnelling adiabatically, remains diabatically trapped with large probability $P_{0\to 1}$ in the lowest $0A$ Wannier state even for $t > \mathrm{T}/2$. Only at a later time, $t = t_2^{(0)}$, the rising level becomes resonant with the first excited state 1B of the $x = a$ well (Fig. 2.7). As this second gap Δ_{12} is now much larger, the LZ diabatic rate drops and the particle transfers with large adiabatic probability from the A to the B well for driving speeds $v_{0\to 1} \ll v \ll v_{1\to 2}$. Once the first excited $1B$ state in the $x = a$ well is occupied, the bath exponentially sucks out the excess energy and thermalizes the particle to lowest $0B$ level. That amounts to dissipation which is paid for by frictional work done by the external force. The $0A \to 1B$ quantum slip between neighboring wells preempts by far the classical slip, which would take place when the rising classical minimum disappears, at

$$t_s = \frac{\pi U_0}{kva}\sqrt{1 - \left(\frac{ka^2}{2\pi^2 U_0}\right)^2} + \frac{a}{2\pi v}\cos^{-1}\left(-\frac{ka^2}{2\pi^2 U_0}\right) > t_2 \ . \tag{2.25}$$

2.1.3 Quantum master equation

To calculate the frictional dissipation rate, we describe the particle motion by means of a weak coupling Born-Markov quantum master equation (QME), based on a time-evolving density matrix (DM) $\hat{\rho}_Q(t)$ [55, 56], whose equation of motion is (see Appendix E for details on derivation)

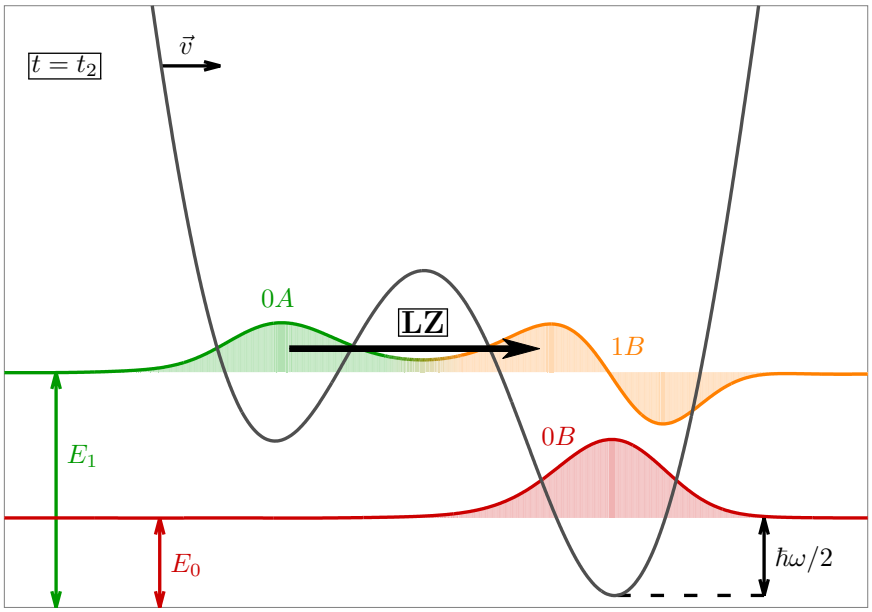

Figure 2.7: A pictorial sketch of the tunnelling event in which a particle in the ground level of the left well (A) resonantly tunnels into the first excited level of the right well (B). This process occurs in correspondence of the avoided crossing energy levels at $t = t_2$.

$$\frac{d}{dt}\hat{\rho}_Q(t) = \frac{1}{i\hbar}\left[\hat{H}_X(t), \hat{\rho}_Q(t)\right] - \left(\left[\hat{X}, \hat{S}(t)\hat{\rho}_Q(t)\right] + \text{H.c.}\right) , \tag{2.26}$$

where

$$\hat{H}_X(t) = \hat{H}_Q(t) + 2\hbar\alpha\omega_c\hat{X}^2 . \tag{2.27}$$

The operator $\hat{X} = \sin(2\pi\hat{x}/a)$ mediates the dissipation by connecting Wannier states with different parity within the same well. In this way, the dissipative process takes place by de-excitation of a Wannier state into the lower one in the same well. In Fig. 2.8 we show a graphical representation of $\hat{X}$ matrix elements, where we can appreciate the main contribution to dissipation given by the de-excitations between consecutive Wannier energy levels. The counterterm $2\hbar\alpha\omega_c\hat{X}^2$ is needed in order to compensate a renormalization of the potential which is caused by the bath interaction. Nevertheless, its contribution is very small, since it is proportional to the coupling constant α of the interaction. The operator $\hat{S}(t)$ is a bath-convoluted $\hat{X}$ given by [56]

$$\hat{S}(t) = \frac{1}{\hbar^2}\int_0^t d\tau\, C(\tau)\, \hat{U}_X(t, t-\tau)\, \hat{X}\, \hat{U}_X^\dagger(t, t-\tau) , \tag{2.28}$$

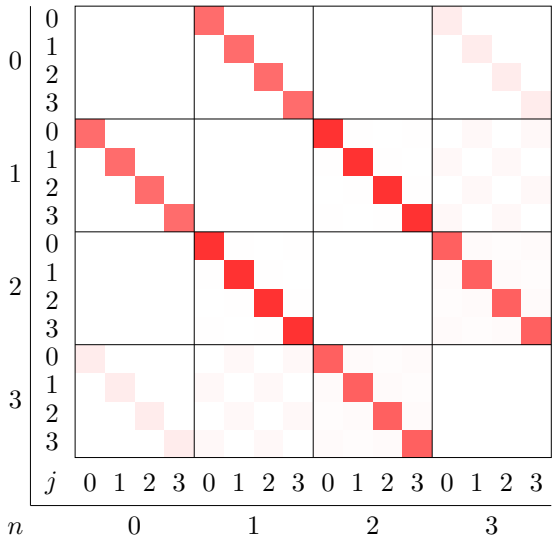

Figure 2.8: Graphical representation of matrix $\langle W_{j,n}| \hat{X} |W_{j',n'}\rangle$. The color intensity is proportional to the absolute value of matrix elements. The operator $\hat{X}$, "mediator" of the dissipation process, connects Wannier states with different parity within the same well.

with $C(\tau)$ the bath correlator:

$$\begin{aligned} C(\tau) &= \sum_{ij} c_i c_j \langle \hat{x}_i(\tau)\hat{x}_j(0)\rangle_{\text{eq}} \\ &= \sum_i \frac{\hbar\, c_i^2}{2m_i\omega_i} \left\langle b_i(\tau)b_i^\dagger(0) + b_i^\dagger(\tau)b_i(0)\right\rangle \\ &= \int_0^{+\infty} d\omega\, J(\omega) \left[\mathrm{e}^{i\omega\tau} f_B(\omega) + \mathrm{e}^{-i\omega\tau}\left[f_B(\omega)+1\right]\right] , \end{aligned} \tag{2.29}$$

and $\hat{U}_X(t, t-\tau)$ the time evolution operator:

$$\hat{U}_X(t, t-\tau) = T\left\{\mathrm{e}^{-\frac{i}{\hbar}\int_{t-\tau}^{t} dt'\, \hat{H}_X(t')}\right\} . \tag{2.30}$$

The operators b_i and $b_i^\dagger$ are annihilation and creation operators of the i-th harmonic oscillator of the bath, while $f_B(\omega) = 1/(\mathrm{e}^{\beta\hbar\omega} - 1)$ is the Bose-Einstein distribution function. Since the time-scale of the bath decorrelation is much smaller than the time-scale of the dynamics of the system, the contribution to the integral of $\hat{S}(t)$ is given by small values of τ for which $\hat{H}_X(t)$ remains approximately constant. We can then write:

$$\hat{U}_X(t, t-\tau)|_{\tau \ll a/v} \approx \mathrm{e}^{-\frac{i}{\hbar}\hat{H}_X(t)\tau} . \tag{2.31}$$

At this point, $\hat{S}(t)$ takes the form:

$$\hat{S}(t) \approx \int_0^t d\tau\, C(\tau)\, \mathrm{e}^{-\frac{i}{\hbar}\hat{H}_X(t)\tau}\, \hat{X}\, \mathrm{e}^{\frac{i}{\hbar}\hat{H}_X(t)\tau} \,. \tag{2.32}$$

In order to evaluate the term $\mathrm{e}^{-\frac{i}{\hbar}\hat{H}_X(t)\tau}\, \hat{X}\, \mathrm{e}^{\frac{i}{\hbar}\hat{H}_X(t)\tau}$ we insert the identity expressed in the basis of instantaneous eigenstates:

$$\begin{aligned} \mathrm{e}^{-\frac{i}{\hbar}\hat{H}_X(t)\tau}\, \hat{X}\, \mathrm{e}^{\frac{i}{\hbar}\hat{H}_X(t)\tau} &= \sum_{k,k'} \mathrm{e}^{-\frac{i}{\hbar}\hat{H}_X(t)\tau}\, |\psi_k(t)\rangle \langle\psi_k(t)|\, \hat{X}\, |\psi_{k'}(t)\rangle \langle\psi_{k'}(t)|\, \mathrm{e}^{\frac{i}{\hbar}\hat{H}_X(t)\tau} \\ &= \sum_{k,k'} \mathrm{e}^{-\frac{i}{\hbar}[E_k(t)-E_{k'}(t)]\tau} \langle\psi_k(t)|\, \hat{X}\, |\psi_{k'}(t)\rangle\, |\psi_k(t)\rangle \langle\psi_{k'}(t)| \,, \end{aligned} \tag{2.33}$$

with $\hat{H}_X(t)\,|\psi_k(t)\rangle = E_k(t)\,|\psi_k(t)\rangle$. Hence we can rewrite $\hat{S}(t)$ as:

$$\hat{S}(t) \approx \sum_{k,k'} \langle\psi_k(t)|\, \hat{X}\, |\psi_{k'}(t)\rangle\, |\psi_k(t)\rangle \langle\psi_{k'}(t)| \int_0^t d\tau\, C(\tau)\, \mathrm{e}^{\frac{i}{\hbar}[E_{k'}(t)-E_k(t)]\tau} \,. \tag{2.34}$$

We can further simplify the integral letting t tend to infinity (*Markov approximation*), since $C(\tau)$ is assumed to rapidly decrease after a (small) time-scale τ_B:

$$\int_0^t d\tau\, C(\tau)\, \mathrm{e}^{\frac{i}{\hbar}[E_{k'}(t)-E_k(t)]\tau} \to \int_0^{+\infty} d\tau\, C(\tau)\, \mathrm{e}^{\frac{i}{\hbar}[E_{k'}(t)-E_k(t)]\tau} \equiv \Gamma(E_{k'}(t) - E_k(t)) \,. \tag{2.35}$$

Finally, $\hat{S}(t)$ can be approximated, in the basis of the instantaneous eigenstates $|\psi_k(t)\rangle$ of the system Hamiltonian $\hat{H}_X(t)$, as

$$\hat{S}(t) = \sum_{k,k'} S_{k,k'}(t)\, |\psi_k(t)\rangle \langle\psi_{k'}(t)| \,, \tag{2.36}$$

with

$$S_{k,k'}(t) \approx \frac{1}{\hbar^2} \langle\psi_k(t)|\, \hat{X}\, |\psi_{k'}(t)\rangle\, \Gamma\left[E_{k'}(t) - E_k(t)\right] \,, \tag{2.37}$$

where

$$\Gamma(E^+) \equiv \int_0^{+\infty} d\tau\, C(\tau)\, \mathrm{e}^{i\left(E+i0^+\right)\tau/\hbar} \tag{2.38}$$

is the rate for a bath-induced transition at energy E, and $E_k(t)$ is the instantaneous eigenvalue associated to $|\psi_k(t)\rangle$. Recent work on the dissipative LZ problem [55] has shown that this approximation is perfectly safe, when the coupling to the bath is weak, in an extended regime of driving velocities v. The QME is then solved in the basis of the Wannier orbitals of the unperturbed particle in the periodic potential.

We focus now on the integral

$$\Gamma(\omega^+) = \frac{1}{2}\gamma(\omega) + i\sigma(\omega) \,, \tag{2.39}$$

where we have separated the real and imaginary components. The real part takes a simple form:

$$\gamma(\omega) = \begin{cases} 2\pi J(|\omega|) f_B(|\omega|) & \text{for } \omega < 0 \\ 2\pi J(\omega)(f_B(\omega) + 1) & \text{for } \omega > 0 \, , \end{cases} \tag{2.40}$$

while the imaginary part involves a principal value integral:

$$\sigma(\omega) = \fint_0^{+\infty} d\omega' \, J(\omega') \left[\frac{f_B(\omega')}{\omega + \omega'} + \frac{f_B(\omega') + 1}{\omega - \omega'} \right] \, . \tag{2.41}$$

For an ohmic spectral function $J(\omega) \sim \omega \, \mathrm{e}^{-\omega/\omega_c}$ the two quantities take simple forms in the limit $\omega \to 0$:

$$\gamma(\omega \to 0) = \frac{4\pi}{\beta} \, , \tag{2.42}$$

$$\sigma(\omega \to 0) = -2\omega_c \, . \tag{2.43}$$

2.2 Classical model

The same problem can be simulated with a classical approach – the well-known Prandtl-Tomlinson model –, where the bath interaction contribution is introduced by a dissipative term proportional to particle velocity, plus a thermostat that provides thermalization through random forces acting on the particle. The equation of motion, known as *Langevin equation*, can be derived from the Hamiltonian used in the quantum model. Let us proceed with its derivation. The classical Hamiltonian is:

$$H(t) = \frac{p^2}{2M} + V[x(t), t] + \sum_i \left[\frac{p_i^2}{2m_i} + \frac{1}{2} m_i \omega_i^2 \left(x_i - \frac{c_i}{m_i \omega_i^2} X \right)^2 \right] \, , \tag{2.44}$$

where

$$V[x(t), t] = U_0 \sin^2 \left(\frac{\pi}{a} x \right) + \frac{k}{2} \left(x - vt \right)^2 \, , \tag{2.45}$$

$$X(x) = \sin \left(\frac{2\pi}{a} x \right) \, . \tag{2.46}$$

The subscript i refers to the degrees of freedom of the bath. As in quantum model, the energy exchange with the environment is provided by the interaction with an infinite set of harmonic oscillators, classical in this case. From the Hamilton equations we obtain the equations of motion:

$$\begin{cases} M\ddot{x} + \dfrac{\partial}{\partial x} V[x(t), t] + \displaystyle\sum_i \frac{c_i^2}{m_i \omega_i^2} X(x) X'(x) = \sum_i c_i x_i X'(x) \\ m_i \ddot{x}_i + m_i \omega_i^2 x_i = c_i X(x) \end{cases} \, , \tag{2.47}$$

where $X'(x) \equiv \frac{\partial}{\partial x} X(x)$. The dynamical equation for $x(t)$ alone is found to read [54]:

$$M\ddot{x}(t) + X'[x(t)] \int_0^t dt' \sum_i \frac{c_i^2}{m_i \omega_i^2} \cos[\omega_i (t-t')] X'[x(t')] \dot{x}(t') + \frac{\partial}{\partial x} V[x(t), t] =$$

$$-X'[x(t)] \sum_i \frac{c_i^2}{m_i \omega_i^2} \cos[\omega_i t] X[x(0)] + X'[x(t)] \sum_i c_i \left[x_i^{(0)} \cos(\omega_i t) + \frac{p_i^{(0)}}{m_i \omega_i} \sin(\omega_i t) \right] , \quad (2.48)$$

where $x_i^{(0)}$ and $p_i^{(0)}$ are the initial positions and momenta. The first term in Eq. (2.48) is the total force acting on the particle, the second term is a viscous term since it involves the velocity of the particle, the third term is the deterministic force due to the potential and finally we interpret the last two terms as the random force due to the bath interaction. We rename the last two terms as ξ:

$$\xi(t) = -X'[x(t)] \sum_i \frac{c_i^2}{m_i \omega_i^2} \cos[\omega_i t] X[x(0)] + X'[x(t)] \sum_i c_i \left[x_i^{(0)} \cos(\omega_i t) + \frac{p_i^{(0)}}{m_i \omega_i} \sin(\omega_i t) \right] . \quad (2.49)$$

Let us now check if our interpretation is correct by evaluating the average $\langle \xi(t) \rangle$ and correlation $\langle \xi(t) \xi(t') \rangle$. This requires to take the averages of $x_i^{(0)}$ and $p_i^{(0)}$ with respect to the *shifted* canonical equilibrium distribution of the reservoir:

$$\rho_R = Z^{-1} \exp \left\{ -\beta \sum_i \frac{\left(p_i^{(0)} \right)^2}{2m_i} + \frac{m_i \omega_i^2}{2} \left(x_i^{(0)} - \frac{c_i}{m_i \omega_i^2} X[x(0)] \right)^2 \right\} . \quad (2.50)$$

The shift $c_i X[x(0)]/m_i \omega_i^2$ is the new equilibrium position for the i-th bath oscillator after the renormalization of the potential due to the coupling of the bath with the system. We have:

$$\langle \xi(t) \rangle = \left\langle -X'[x(t)] \sum_i \frac{c_i^2}{m_i \omega_i^2} \cos[\omega_i t] X[x(0)] + X'[x(t)] \sum_i c_i \left[x_i^{(0)} \cos(\omega_i t) + \frac{p_i^{(0)}}{m_i \omega_i} \sin(\omega_i t) \right] \right\rangle , \quad (2.51)$$

$$\langle \xi(t) \xi(t') \rangle = \left\langle \left\{ -X'[x(t)] \sum_i \frac{c_i^2}{m_i \omega_i^2} \cos[\omega_i t] X[x(0)] + X'[x(t)] \sum_i c_i \left[x_i^{(0)} \cos(\omega_i t) + \frac{p_i^{(0)}}{m_i \omega_i} \sin(\omega_i t) \right] \right\} \right.$$
$$\left. \cdot \left\{ -X'[x(t')] \sum_i \frac{c_i^2}{m_i \omega_i^2} \cos[\omega_i t] X[x(0)] + X'[x(t')] \sum_i c_i \left[x_i^{(0)} \cos(\omega_i t') + \frac{p_i^{(0)}}{m_i \omega_i} \sin(\omega_i t') \right] \right\} \right\rangle . \quad (2.52)$$

The important quantities to compute are:

$$\left\langle x_i^{(0)} \right\rangle = \frac{c_i}{m_i \omega_i^2} X[x(0)] , \quad (2.53)$$

$$\left\langle p_i^{(0)} \right\rangle = 0 , \quad (2.54)$$

$$\left\langle x_i^{(0)} x_j^{(0)} \right\rangle = \frac{c_i c_j}{m_i m_j \omega_i^2 \omega_j^2} \left[X[x(0)] \right]^2 + \delta_{ij} \left(\frac{k_B T}{m_i \omega_i^2} \right) , \quad (2.55)$$

$$\left\langle p_i^{(0)} p_j^{(0)} \right\rangle = \delta_{ij} \, k_B T \, m_i . \quad (2.56)$$

Using these relations we obtain:

$$\langle \xi(t) \rangle = 0 \ , \tag{2.57}$$

$$\langle \xi(t)\xi(t') \rangle = X'[x(t)]X'[x(t')] \sum_i \frac{c_i^2 \, k_B T}{m_i \omega_i^2} \cos[\omega_i (t-t')] \ . \tag{2.58}$$

We see that Eqs. (2.57) and (2.58) describe a multiplicative colored noise[3]. Let us check the limit of delta-correlated noise for the spectral function:

$$\sum_i \frac{c_i^2}{m_i \omega^2} \, \delta(\omega - \omega_i) = c_0 \ , \tag{2.59}$$

with c_0 constant[4]. Hence we obtain:

$$\begin{aligned} \langle \xi(t)\xi(t') \rangle &= X'[x(t)]X'[x(t')] \sum_i \frac{c_i^2 \, k_B T}{m_i \omega_i^2} \cos[\omega_i (t-t')] \\ &= X'[x(t)]X'[x(t')] \int_0^{+\infty} d\omega \sum_i \frac{c_i^2 \, k_B T}{m_i \omega^2} \delta(\omega - \omega_i) \cos[\omega (t-t')] \\ &= X'[x(t)]X'[x(t')] \, c_0 \, k_B T \int_0^{+\infty} d\omega \cos[\omega (t-t')] \\ &= \pi c_0 \, k_B T \ \left(X'[x(t)] \right)^2 \ \delta(t-t') \ . \end{aligned} \tag{2.60}$$

If we instead set an exponential decay:

$$\sum_i \frac{c_i^2}{m_i \omega^2} \, \delta(\omega - \omega_i) = c_0 \, \mathrm{e}^{-\omega/\omega_c} \ , \tag{2.61}$$

we obtain the case of *ohmic* bath[5] , and the force correlation reads:

$$\begin{aligned} \langle \xi(t)\xi(t') \rangle &= X'[x(t)]X'[x(t')] \, c_0 \, k_B T \int_0^{+\infty} d\omega \, \mathrm{e}^{-\omega/\omega_c} \cos[\omega (t-t')] \\ &= X'[x(t)]X'[x(t')] \frac{c_0 \, k_B T \, \omega_c}{1 + \omega_c^2 (t-t')^2} \ . \end{aligned} \tag{2.62}$$

This time the 2-point correlation function takes the form of a Lorentzian, that still approximates a delta-function in case of very large cutoff frequency $\omega_c \gg 1/\tau_S$, with τ_S referring to the time scale of the system:

$$\langle \xi(t)\xi(t') \rangle = \pi c_0 \, k_B T \ \left(X'[x(t)] \right)^2 \ \delta(t-t') \ . \tag{2.63}$$

We now focus on the second term of Eq. (2.48):

$$X'[x(t)] \int_0^t dt' \sum_i \frac{c_i^2}{m_i \omega_i^2} \cos[\omega_i (t-t')] X'[x(t')] \dot{x}(t') \ . \tag{2.64}$$

[3] A multiplicative noise is a space-dependent noise, while colored means that its correlation at different times does not vanish.

[4] The dimensions of c_0 are $[M] \left[L^2\right] \left[T^{-1}\right] = [E] \, [T]$.

[5] This corresponds to a spectral function $J(\omega) \sim \omega \, \mathrm{e}^{-\omega/\omega_c}$.

We interpreted this term as the viscous part of the Langevin equation. Let us choose an ohmic spectral function (2.61):

$$\begin{aligned} & X'[x(t)] \int_0^t dt' \sum_i \frac{c_i^2}{m_i \omega_i^2} \cos[\omega_i (t-t')] X'[x(t')] \dot{x}(t') \\ = & X'[x(t)] \int_0^t dt' \int_0^{+\infty} d\omega \, c_0 \, \mathrm{e}^{-\omega/\omega_c} \cos[\omega (t-t')] X'[x(t')] \dot{x}(t') \\ = & X'[x(t)] \int_0^t dt' \frac{c_0 \, \omega_c}{1+\omega_c^2 (t-t')^2} \, X'[x(t')] \dot{x}(t') \, . \end{aligned} \tag{2.65}$$

Making the assumption $\omega_c \gg 1/\tau_S$ we obtain:

$$\frac{\pi c_0}{2} \, \left(X'[x(t)] \right)^2 \dot{x}(t) \, . \tag{2.66}$$

Finally the dynamical equation (Eq. 2.48) can be simplified into the standard form of Langevin equation:

$$M \ddot{x}(t) = -\gamma \, \dot{x}(t) - \frac{\partial}{\partial x} V[x(t), t] + \xi[x(t), t] \, , \tag{2.67}$$

where we have defined:

$$\gamma \equiv \frac{\pi c_0}{2} \, \left(X'[x(t)] \right)^2 \, . \tag{2.68}$$

The *fluctuation-dissipation* theorem is satisfied:

$$\left\langle \xi^2[x(t), t] \right\rangle = 2 \, k_B T \gamma[x(t)] \, . \tag{2.69}$$

Let us now evaluate the damping factor γ using the power spectrum chosen in the quantum model:

$$J(\omega) = \sum_i \frac{\hbar c_i^2}{2 m_i \omega_i} \delta(\omega - \omega_i) = 2 \hbar^2 \alpha \omega \mathrm{e}^{-\omega/\omega_c} \, . \tag{2.70}$$

This corresponds to set the parameter $c_0 = 4\hbar\alpha$. Hence we have:

$$\gamma = 2\pi\hbar\alpha \, \left(X'[x(t)] \right)^2 = \frac{(2\pi)^3 \hbar \alpha}{a^2} \left(\cos \left[\frac{2\pi}{a} x(t) \right] \right)^2 \, . \tag{2.71}$$

Now we have all elements to simulate a classical dynamics with the same physical parameters used in quantum model, useful to compare both evolutions results.

2.2.1 Numerical integration

Langevin equation is simulated by the *Euler-Maruyama* method as follows:

$$\begin{cases} x(t+\Delta t) = x(t) + \dfrac{p(t)}{M} \Delta t \\ p(t+\Delta t) = p(t) + F[x(t)] \Delta t - \gamma[x(t)] \dfrac{p(t)}{M} \Delta t + \Delta W[x(t), t] \end{cases} \, , \tag{2.72}$$

where $F[x(t)]$ is the force acting on the particle due to the potential:

$$F[x(t)] \equiv -\frac{\partial V[x(t),t]}{\partial x} \ , \tag{2.73}$$

and $\Delta W[x(t),t]$ is a Wiener process drawn by:

$$P(\Delta W) = \frac{\mathrm{e}^{-\frac{(\Delta W)^2}{4\gamma[x(t)]k_B T \Delta t}}}{2\sqrt{\pi\gamma[x(t)]k_B T \Delta t}} \ . \tag{2.74}$$

The computation of physical observables requires to perform integrations over stochastic variables ($\Delta W[x(t),t]$). This introduces issues related to the arbitrariness in partitioning the integration interval. In fact, for stochastic differentials, the integral value depends on the choice of the intermediate points of the interval. There exists two important integration methods, called *Itô* integration:

$$\int f(t)\, dW(t) = \lim_{\Delta t \to 0} \sum_i f(t_i)\, [W(t_i + \Delta t) - W(t_i)] \tag{2.75}$$

and *Stratonovich* integration:

$$\int f(t) \circ dW(t) = \lim_{\Delta t \to 0} \sum_i \frac{f(t_i) + f(t_i + \Delta t)}{2}\, [W(t_i + \Delta t) - W(t_i)] \ , \tag{2.76}$$

where we use the notation "$\circ$" to denote Stratonovich integral.

In the evaluation of dissipated work (heat) we follow the derivation suggested by Sekimoto [57]. The heat differential $đQ$ is computed as a Stratonovich product, leading to the first law of thermodynamics:

$$\begin{aligned} đQ &= \left(-\gamma[x(t)]\frac{dx(t)}{dt} + \xi[x(t),t]\right) \circ dx \\ &= \left(\frac{dp}{dt} + \frac{\partial V[x(t),t]}{\partial x}\right) \circ dx \\ &= \frac{dp}{dt} \circ dx + dV - \frac{\partial V[x(t),t]}{\partial t}\, dt \\ &= \frac{dp}{dt}\frac{p}{m}\, dt + dV - \frac{\partial V[x(t),t]}{\partial t}\, dt \\ &= d\left(\frac{p^2}{2m}\right) + dV - \frac{\partial V[x(t),t]}{\partial t}\, dt \\ &= dE - đ\mathcal{W} \ . \end{aligned} \tag{2.77}$$

The cumulative work done on the system by the external deterministic force is:

$$\mathcal{W}(t) = \int_0^t dt\, \frac{\partial V[x(t),t]}{\partial t} \ . \tag{2.78}$$

The heat instead is evaluated in the following way:

$$\begin{aligned} đQ &= \left(-\gamma[x(t)]\frac{dx(t)}{dt} + \xi(t)\right) \circ dx \\ đQdt &= -\gamma[x(t)]\frac{p(t)}{m}dt \circ dx + dW(t) \circ dx \\ đQ &= -\gamma[x(t)]\left(\frac{p(t)}{m}\right)^2 dt + \frac{p(t)}{m} \circ dW(t)\ . \end{aligned} \tag{2.79}$$

We have now to take care in calculating the second term $\frac{p(t)}{m} \circ dW(t)$. According to Stratonovich integration, the discrete case it would be:

$$\begin{aligned} \frac{p(t)}{m} \circ dW(t) &= \frac{p(t_i) + p(t_i + \Delta t)}{2m}\left[W(t_i + \Delta t) - W(t_i)\right] \\ &= \frac{p(t_i) + p(t_i) + F(t_i)\Delta t - \gamma[x(t)]\frac{p(t)}{m} + \Delta W(t_i)}{2m}\Delta W(t_i) \end{aligned} \tag{2.80}$$

In the latest expression, almost all terms average to zero because of uncorrelation, except $\frac{\Delta W(t_i)^2}{2m}$. Hence we obtain:

$$đQ = -\gamma[x(t)]\left[\frac{p(t)}{m}\right]^2 dt + \frac{[\Delta W(t)]^2}{2m}\ , \tag{2.81}$$

$$\begin{aligned} Q &= \int_0^t dt\left(-\gamma[x(t)]\left[\frac{p(t)}{m}\right]^2\right) + \frac{1}{2m}\int_0^t (dW(t))^2 \\ &= \int_0^t dt\left(-\gamma[x(t)]\left[\frac{p(t)}{m}\right]^2 + \frac{\gamma[x(t)]k_BT}{m}\right) \\ &= \int_0^t dt\frac{\gamma[x(t)]}{m}\left(-\frac{[p(t)]^2}{m} + k_BT\right)\ , \end{aligned} \tag{2.82}$$

where we can appreciate the fact that at equilibrium, when $\frac{\langle mv^2\rangle}{2} = \frac{k_BT}{2}$, the net transferred heat vanishes.

2.3 Results

The quantum simulation has been performed through a quantum master equation (Eq. 2.26), while the Langevin equation (Eq. 2.67) was used for the classical simulation.

The parameters used in our simulations assume a particle with the mass M of ^{171}Yb, and a lattice spacing $a = 500$ nm. The lattice potential is taken to be $U_0 = 38.5\,E_R$, in terms of the recoil energy $E_R = \pi^2\hbar^2/(2Ma^2)$. The corrugation parameter $\eta = (\omega_l/\omega_0)^2$, defined [62] as the confinement ratio of the lattice intra-well vibrational frequency $\omega_l = 2\sqrt{U_0\,E_R}/\hbar$ to the harmonic trap (the optical tweezer pulling spring) vibrational frequency $\omega_0 = a\sqrt{2kE_R}/\pi\hbar$, is set equal to $\eta = 4$, so that the overall potential energy has just two minima. This automatically

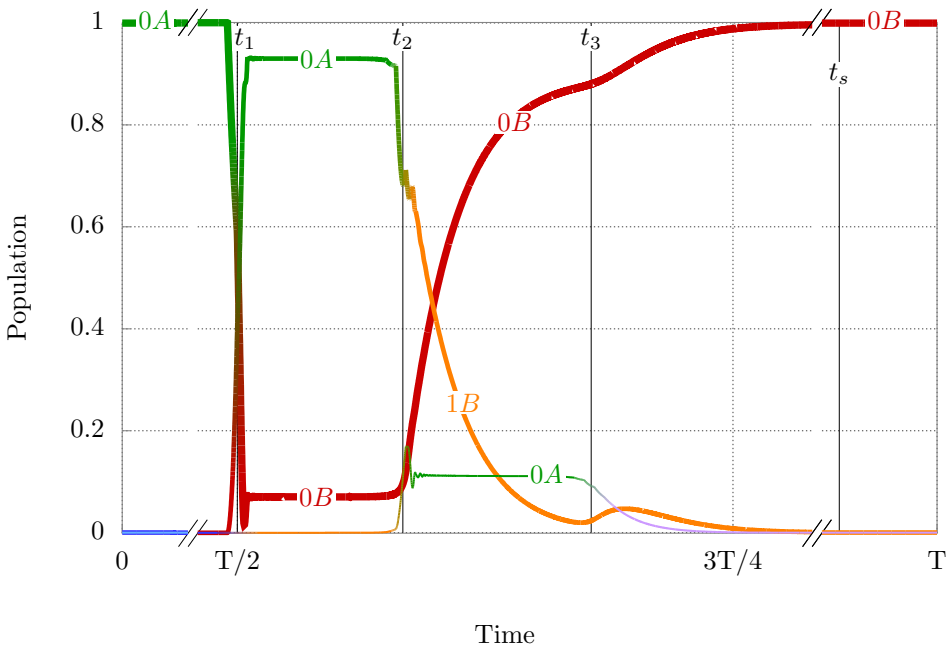

Figure 2.9: Time-dependent population of instantaneous eigenstates. Lines of decreasing thickness are used for higher eigenstates. Notice the cuts in time axis.

sets the value of the optical tweezer spring constant at $k = 190\,E_R/a^2$. Finally, the assumption of weakly coupled Ohmic environment, with $\alpha = 0.002$ and $\omega_c = 12\,E_R/\hbar$, necessary for a consistent perturbative theory, can be realized by a judicious choice of cooling strengths. The values adopted for α and ω_c correspond to a cooling rate $\gamma_c \approx 0.018\,E_R/\hbar$. In order to make the bath effective during the dynamics, the condition on the optical tweezer velocity $v < \gamma_c\, a$ must be satisfied, leading to a time-scale of the optical tweezer motion much larger than the period of vibrations in the lattice well: $v/a \ll \omega_l$.

Figure 2.9 shows the time-dependent population probability of the first three instantaneous eigenstates, $P_k(t) = \langle\psi_k(t)|\hat{\rho}_Q|\psi_k(t)\rangle$, over one period of forced particle motion in the $v_{0\to1} \ll v \ll v_{1\to2}$ regime. As qualitatively sketched, despite the slow motion the probability of the $0A \to 0B$ adiabatic transition to the right well ground state at $t_1 = \mathrm{T}/2$ is already very small, and LZ dominates this first level crossing keeping diabatically the particle in the left A well. At the second $1 \to 2$ crossing where the gap Δ_{12} is much larger, $P_{1\to2}$ is suppressed, and the 1^{st} excited level of the right well ($1B$) becomes strongly populated. Following that, the bath exponentially relaxes $P_k(t)$ down to the right well ground state.

The mechanism just described predicts an advancement of the average position of the particle, as well as a corresponding onset of dissipated power, very different from those of ordinary Langevin frictional dynamics [54], which, with all parameters except $\hbar$ the same as in the quan-

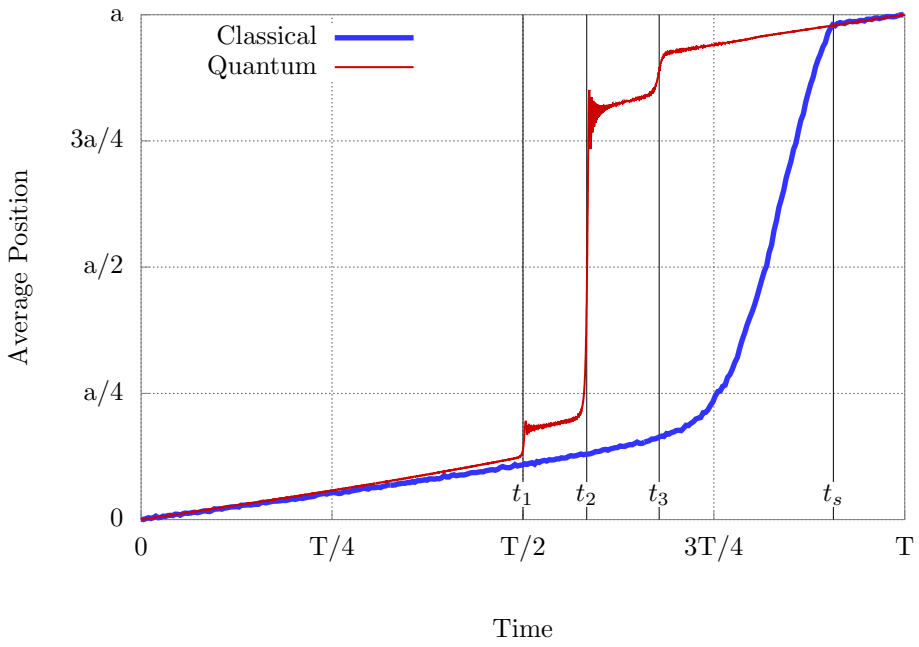

Figure 2.10: Average position of the particle versus time, in the quantum and classical cases. Most of the "slip" of the quantum particle goes through the excited-state resonant tunnelling, taking place at t_2 beyond the symmetric moment $t_1 = \mathrm{T}/2$ between the two potential wells. The dashed line shows the position of the classical "spinodal" moment t_s, where the $x = 0$ local potential minimum disappears and the particle is forced to slip.

tum case, describes the classical forced sliding of the same particle. Figure 2.10 compares the average particle position versus time in the quantum and classical cases. The "quantum slips" occur rather suddenly, reflecting the abruptness of level crossing events and connected barrier passage. In particular, the main quantum slip occurs, for the parameters used in Fig. 2.10, precisely when the instantaneous Wannier ground level the left well is resonantly aligned with the first excited Wannier level in the neighboring well.

Because it occurs at a lower spring loading, the resonant barrier permeation strongly reduces the overall mechanical friction work exerted by the pulling spring. Figure 2.11 shows the amount of energy absorbed by the bath (friction) at the end of each period as a function of velocity. In the classical case the dissipated work (more precisely what we called heat Q in Section 2.2) grows logarithmically with speed, due to thermally activated slip, as is well known for stick-slip at finite temperature [58–61]

$$W_{cl} = a + b \, \ln^{2/3}(c\, v)\,. \tag{2.83}$$

with constants $a = 42.5\, E_R$, $b = 6.11\, E_R$ and $c = 5.92 \cdot 10^3\, \hbar/E_R a$ providing the best fit in our case.

The dissipated work in the quantum case (obtained by taking the difference between the work

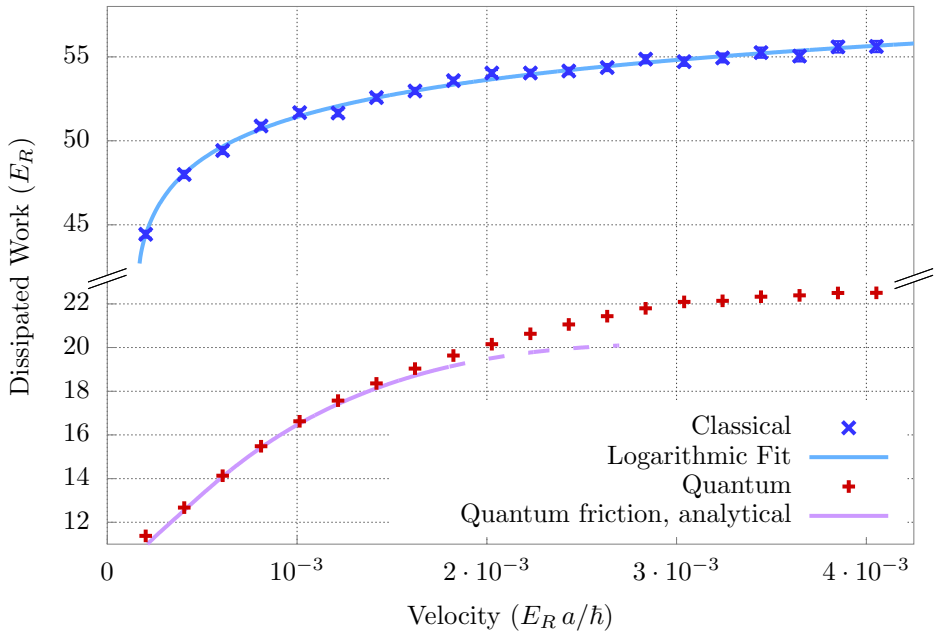

Figure 2.11: Frictional dissipated work for classical and quantum sliding vs driving velocity. Note the large reduction of dissipation induced by the resonant quantum tunneling: quantum lubricity.

made by the spring and the total energy) is by comparison smaller by a factor ~ 3. It is well approximated through the Landau-Zener probabilities Eq. (2.23) of transition from the n^{th} to the $(n+1)^{\text{th}}$ eigenstate:

$$W_q(v) \approx P_{0\to1}(v)\left[(1-P_{1\to2}(v))\,(E_1-E_0)+\right.$$
$$\left.P_{1\to2}(v)\,(1-P_{2\to3}(v))\,(E_2-E_1)\right]\,, \tag{2.84}$$

with $\Delta_{01} = 5.19\cdot10^{-2}\,E_R$, $\Delta_{12} = 3.03\cdot10^{-1}\,E_R$, $\Delta_{23} = 8.83\cdot10^{-1}\,E_R$; $\alpha_{01} = 1.43\cdot10^{2}\,E_R/a$, $\alpha_{12} = 1.38\cdot10^{2}\,E_R/a$, $\alpha_{23} = 1.46\cdot10^{2}\,E_R/a$; $v_{0\to1} = 2.96\cdot10^{-5}\,E_Ra/\hbar$, $v_{1\to2} = 1.05\cdot10^{-3}\,E_Ra/\hbar$, $v_{2\to3} = 8.40\cdot10^{-3}\,E_Ra/\hbar$. Dissipation requires in fact, to start with, that the system does not LZ tunnel, so that $P_{0\to1} > 0$. The amount of power absorbed by the bath equals the probability to populate the first and higher excited states times their energy difference with the ground state. Eq. (2.84) is approximate first of all because it does not include higher excited states. Moreover, it is only valid when velocity is low enough that the cooling rate $\gamma_c \gg v/a$, and the particle loses all its kinetic energy before encountering the subsequent slip, which is not satisfied for the larger velocities. It is clear that, unless temperature is too high, quantum tunnelling through the barrier always preempts classical negotiation of the barrier, causing friction to be necessarily smaller than classical friction. In this sense we can speak of *quantum lubricity*. Despite its

conceptual simplicity, this form of quantum lubricity has not been addressed experimentally but should be well within experimental reach for cold atoms/ions in optical lattices.

2.4 Conclusions

In summary, comparison of classical and quantum stick-slip friction for a particle sliding in a periodic potential reveals major differences. A classical particle slides from a potential well to the next by overcoming the full potential barrier. A quantum particle can permeate the barrier by resonant tunnelling to an excited state, a process suddenly and narrowly available at a well defined position of the harmonic trap, leading to discontinuous transfer to the next well, as shown in Fig. 2.10. This quantum slip preempts the classical slip, giving rise to quantum lubricity. The potential energy accumulated by the particle during sticking, and frictionally dissipated at the quantum slip, is just the amount sufficient to reach the resonant condition with the excited state in the next well. Conversely, the classical potential energy increases necessary for classical slip is close to the top of the barrier, with a correspondingly larger amount of dissipated energy during and after the slip. In addition to this quantum lubricity effect, a regime of quantum superlubricity is in principle expected at sufficiently low temperatures, where the friction growth with velocity should begin non-analytically, with all derivatives vanishing. The natural extension of these predictions to many-particle system will be of interest in the future.

Chapter 3

Conclusions and perspectives

In this thesis we presented two different out-of-equilibrium quantum problems whose dynamics is based on Landau-Zener processes. The first problem, concerning a closed system, is the annealing of an Ising chain for ordered and disordered realizations in both classical and quantum versions. An equal-footing comparison of the dynamics, based on deterministic evolutions, shows a quadratic speedup of the quantum dynamics over the classical one in both ordered and disordered cases. The technique used to diagonalize the problem allows us to perform quantum annealing also in imaginary-time, revealing an exponential speedup, that could inspire new optimization algorithms. The important question regarding the crossover between adiabaticity and non-adiabaticity regimes can be predicted by Landau-Zener theory, from the knowledge of the minimal gap that separates the ground state from the first excited state. For simulated annealing it is not possible to make the same considerations since the critical point occurs at the end of the dynamics, with an exponentially fast decreasing of the gap with temperature. This makes the classical dynamics close to the critical point different from the standard Landau-Zener process.

The second problem is an open system that models the quantum effects of nanofriction. It is a quantum version of the classical Prandtl-Tomlinson, where the dissipation is introduced by the interaction of the particle with a large number of harmonic oscillators forming a bosonic bath. Landau-Zener theory can predict a drop in frictional force due to resonant tunneling between adjacent wells, that we called quantum lubricity. Moreover, a regime of superlubricity is obtained for very low velocities of the dragging spring, when the evolution is adiabatic and the frictional force vanishes non-analytically in the velocity. The quantum nature of the sliding process affects also the position, leading to a discontinuous transfer of the particle to the next well.

In both of the studied problems we provide useful benchmarks for possible future developments: in quantum annealing, the possibility to determine the role of thermal effects, or the comparison with QA simulated by path-integral. Regarding the quantum nanofriction model, we provide useful physical parameters for experiments that aim at chasing quantum effects in sliding physics. One possible extension of the present study is to use Floquet techniques to di-

rectly approach the periodic steady states attained after a transient. A second extension might be to pursue effects due to the interaction in cold trapped ion systems with more than one particle.

Appendix A

Landau-Zener problem

In this appendix we revise the Landau-Zener problem. Since LZ is the basic mechanism in the dynamics of quantum annealing and quantum nanofriction, this discussion is useful to have a clearer picture of the two problems we deal.

The model is presented in the first section, where we show the Hamiltonian and its analytical solution. The second section presents a simple alternative derivation for the asymptotic solution. Finally, in the third section, we discuss numerical solutions of the problem.

A.1 The model

The Landau-Zener problem [1,2] is a coherently driven two-state quantum problem described by the following Schrödinger equation:

$$i\hbar\frac{\partial}{\partial t}\begin{pmatrix} c_1(t) \\ c_2(t) \end{pmatrix} = \begin{bmatrix} at & b \\ b^* & -at \end{bmatrix}\begin{pmatrix} c_1(t) \\ c_2(t) \end{pmatrix}, \tag{A.1}$$

where $c_1(t)$ and $c_2(t)$ are the probability amplitudes of the *diabatic* states $|\psi_1\rangle$ and $|\psi_2\rangle$, defined as the eigenstates at $t \to \infty$, while a and b are constants[1]. Approaching $t = 0$, the instantaneous eigenstates, that we call *adiabatic* states, become a linear combination of $|\psi_1\rangle$ and $|\psi_2\rangle$. Fig. A.1 shows the energy levels for both diabatic and adiabatic bases. The minimum energy gap between the two adiabatic states at $t = 0$ is $\Delta = 2\,|b|$.

The Schrödinger equation A.1 translates into a system of two coupled first order differential equations:

$$\begin{cases} i\hbar\,\dot{c}_1(t) = at\,c_1(t) + b\,c_2(t) \\ i\hbar\,\dot{c}_2(t) = b^*\,c_1(t) - at\,c_2(t) \end{cases} \tag{A.2}$$

[1] The dimensions of a and b are: $[a]$ = [Energy]/[Time], $[b]$ = [Energy].

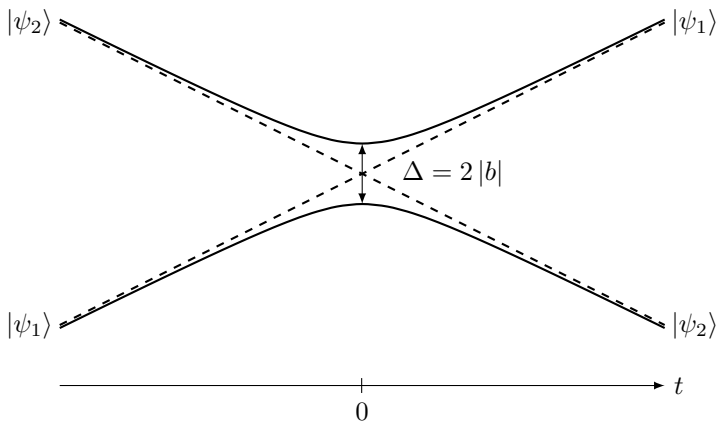

Figure A.1: Adiabatic (solid line) and diabatic (dashed) energies.

Solving Eq. A.2 for c_1(t) leads to the following second order differential equation:

$$\ddot{c}_1 + \left[\frac{|b|^2}{\hbar^2} + \frac{ia}{\hbar} + \frac{a^2t^2}{\hbar^2}\right] c_1(t) = 0 \tag{A.3}$$

Solutions of Eq. A.3 are given in terms of parabolic cylinder functions $D_\nu(z)$ [63]. Starting from $t \to -\infty$ in the ground state $|\boldsymbol{\psi}_1\rangle$, correspondent to $c_1 = 1$, the probability of remaining in the state $|\boldsymbol{\psi}_1\rangle$, called *diabatic transition*, at an arbitrary time t is given by $|c_1(t)|^2$:

$$P_{|\boldsymbol{\psi}_1\rangle}(t) = 1 - \frac{|b|^2}{2\hbar a}\mathrm{e}^{-\pi|b|^2/4\hbar a}\left|D_{-1+\,i|b|^2/2\hbar a}\left(\sqrt{\frac{2a}{\hbar}}\,\mathrm{e}^{3i\pi/4}\,t\right)\right|^2 . \tag{A.4}$$

Eq. A.4 takes a simpler expression for probability at $t \to +\infty$, known as *Landau-Zener formula*:

$$P_{|\boldsymbol{\psi}_1\rangle}(t \to +\infty) = \mathrm{e}^{-\pi|b|^2/\hbar a} . \tag{A.5}$$

Since $|\boldsymbol{\psi}_1\rangle$ coincides with the excited state at $t \to +\infty$, this corresponds to the probability of finding the system in the excited state at the end of the evolution. For $P_{|\boldsymbol{\psi}_1\rangle} \approx 0$ the evolution is called *adiabatic*.

A.2 Derivation of Landau-Zener formula

Now we derive the LZ formula in a simple and elegant way suggested by Curt Wittig [64], without solving directly the usual second-order differential equation.

First rewrite the coefficient $c_1(t)$ separating the out-of-diagonal contribution, embedded in $g(t)$, from the pure rotating phase given by diagonal elements:

$$c_1(t) = g(t)\,\mathrm{e}^{-\frac{i}{\hbar}\int_{t_0}^{t} dt'\,at'} . \tag{A.6}$$

Notice that $g(t)$ is constant during the evolution if we set $b = 0$. We are interested in finding the probability of having the system in the excited state at the end of the evolution, that corresponds to $|c_1(t \to +\infty)|^2$. It is clear from Eq. A.6 that $|g(t)|^2 = |c_1(t)|^2$. We substitute $c_1(t)$ with $g(t)$ in Eq. A.3 and we get:

$$\ddot{g}(t) - \frac{2iat}{\hbar}\,\dot{g}(t) + \frac{|b|^2}{\hbar^2}\,g(t) = 0\ . \tag{A.7}$$

Zener manipulated Eq. A.7 into the form of the Weber equation [1], whose asymptotic solution yields $g_f \equiv g(t \to +\infty)$ for an initial condition $g = 1$. This procedure implies to deal with parabolic cylinder functions involving tricky steps. Here instead we show that Eq. A.7 yields g_f in just a few steps that involve contour integrations, obviating the need to solve the second-order differential equation directly.

Let us consider first the limit $t \to +\infty$: the terms $\ddot{g}$ and $\dot{g}$ must vanish since the two energy levels separate indefinitely and the interaction ceases, while g tends to a constant value g_f. In order to balance the equation, the second term must be finite, leading to $\dot{g}(t) \sim 1/t$. Hence the second order derivative can be neglected:

$$2iat\,\dot{g}(t) = \frac{|b|^2}{\hbar}\,g(t)\ . \tag{A.8}$$

Integration of Eq. A.8 yields

$$g(t) = g(t_0)\,\mathrm{e}^{-\frac{i|b|^2}{2a\hbar}\ln\frac{t}{t_0}}\ , \tag{A.9}$$

where t_0 is an arbitrary beginning of t but restricted to the large time regime. Differentiation of Eq. A.9 shows the $1/t$ and $1/t^2$ behaviors of $\dot{g}$ and $\ddot{g}$:

$$\dot{g}(t) = \frac{-i\,|b|^2\,g(t_0)}{2a\hbar\,t}\,\mathrm{e}^{-\frac{i|b|^2}{2a\hbar}\ln\frac{t}{t_0}}\ , \tag{A.10}$$

$$\ddot{g}(t) = \left(i - \frac{|b|^2}{2a\hbar}\right)\frac{|b|^2\,g(t_0)}{2a\hbar\,t^2}\,\mathrm{e}^{-\frac{i|b|^2}{2a\hbar}\ln\frac{t}{t_0}}\ . \tag{A.11}$$

The asymptotic behavior of $\ddot{g}(t)/g(t)$ will be useful later to show that an integral vanishes:

$$\frac{\ddot{g}(t)}{g(t)} = \left(i - \frac{|b|^2}{2a\hbar}\right)\frac{|b|^2}{2a\hbar\,t^2}\ . \tag{A.12}$$

At $t = 0$ instead Eq. A.7 takes the simple form

$$\frac{\ddot{g}(0)}{g(0)} = -\frac{|b|^2}{\hbar^2}\ . \tag{A.13}$$

Eqs. A.13 will be used shortly to carry out the contour integration.

Dividing Eq. A.7 by g yields an equation that is well behaved with respect to g. In general, g is complex, and its magnitude does not go to zero as a function of t in the complex t-plane. It

only approaches zero as the result of one (or more) of the parameters of the model being assigned an extreme value that is unrealistic within the context of the model, e.g., $|b| \to +\infty$.

Multiplying then Eq. A.7 by dt/t and taking the principal value integral from $t = -\infty$ to $+\infty$ we get:

$$\fint_{-\infty}^{\infty} dt\, \frac{\ddot{g}(t)}{t\, g(t)} - \frac{2ia}{\hbar} \fint_{-\infty}^{\infty} dt\, \frac{\dot{g}(t)}{g(t)} + \frac{|b|^2}{\hbar^2} \fint_{-\infty}^{\infty} \frac{dt}{t} = 0 \,. \tag{A.14}$$

The first and second integrals are straightforward:

$$\fint_{-\infty}^{\infty} dt\, \frac{\dot{g}(t)}{g(t)} = \ln g_f \,, \tag{A.15}$$

$$\fint_{-\infty}^{\infty} \frac{dt}{t} = 0 \,, \tag{A.16}$$

where we used the initial condition $g(t \to -\infty) = 1$, yielding

$$\ln g_f = -\frac{i\hbar}{2a} \fint_{-\infty}^{\infty} dt\, \frac{\ddot{g}(t)}{t\, g(t)} \,. \tag{A.17}$$

By closing a contour in the complex t-plane, the integral in Eq. A.17 can be expressed in terms of the $t = 0$ residue. It is assumed that $\ddot{g}(t)/g(t)$ (Eq. A.12), which is well-behaved on the real axis, is analytic in the complex plane, enabling the residue theorem to be applied. The fact that $\ddot{g}(t)/g(t)$ has no exponential dependence enables us to analytically continue this function into the complex plane without dealing with exponential growth when t becomes complex and $|t| \to +\infty$. The integration contour Γ is chosen as follows (Fig. A.2):

i) from $-R$ to $-\varepsilon$;

ii) semicircle of radius ε above the real axis ;

iii) from ε to R ;

iv) semicircle of radius R above the real axis .

Taking the limits $\varepsilon \to 0^+$ and $R \to +\infty$, the contour integral is

$$\oint_{\Gamma} dt\, \frac{\ddot{g}(t)}{t\, g(t)} = \fint_{-\infty}^{\infty} dt\, \frac{\ddot{g}(t)}{t\, g(t)} + \int_{\varepsilon \to 0^+} dt\, \frac{\ddot{g}(t)}{t\, g(t)} + \int_{R \to +\infty} dt\, \frac{\ddot{g}(t)}{t\, g(t)} \,. \tag{A.18}$$

Since the contour Γ does not contain any singularity, its integral vanishes. Integral on the R semicircle vanishes as well, since the integrand decays as $1/t^3$. Finally the integral on ε semicircle is computed through the residue at $t = 0$;

$$\int_{\varepsilon \to 0^+} dt\, \frac{\ddot{g}(t)}{t\, g(t)} = -i\pi \,\mathrm{Res}\left(\frac{\ddot{g}(t)}{t\, g(t)}, t = 0 \right) = \frac{i\pi\, |b|^2}{\hbar^2} \,, \tag{A.19}$$

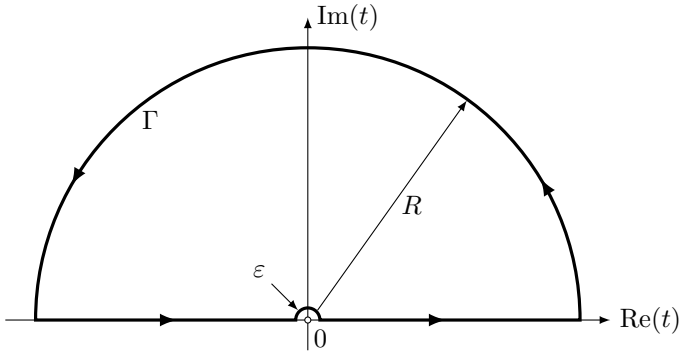

Figure A.2: Integration contour Γ.

where we used Eq. A.13 to compute the residue. Eq. A.18 reduces to

$$\int_{-\infty}^{\infty} dt\, \frac{\ddot{g}(t)}{t\, g(t)} = -\frac{i\pi\, |b|^2}{\hbar^2}\ . \tag{A.20}$$

Substituting this result in Eq. A.17 we obtain the value of g_f:

$$g_f = \mathrm{e}^{-\pi |b|^2 / 2\hbar a}\ . \tag{A.21}$$

Finally we recover the Landau-Zener formula:

$$P_{|\psi_1\rangle}(t \to +\infty) = |g_f|^2 = \mathrm{e}^{-\pi |b|^2 / \hbar a}\ . \tag{A.22}$$

A.3 Numerical solutions

In this last section we show the possible difficulties in simulating a LZ process. Numerical integration of Schrödinger Eq. A.1 is not a trivial problem, particularly when high accuracy is required, since the detuning term (at) is linear in time and changes very slowly. The standard way to compute the LZ probability is to start at a large negative time t_i and propagate the solution to positive times. However, due to finite time t_i, spurious oscillations with amplitude proportional to $\sqrt{\hbar a/(a^2 t_i^2 + |b|^2)}$ [65, 66] appear and it is necessary to start at earlier time t_i in order to achieve a good accuracy, which is computationally very expensive. These deviations from the exact solution are visible in Fig. A.3(a) for starting time $t_i = -10\,\hbar/|b|$. Anticipating the starting time at $t_i = -40\,\hbar/|b|$ the deviations reduce, as shown in Fig. A.3(b).

An alternative and much more efficient solution to this problem has been proposed by Vitanov and Garraway [65, 66]: after a rescaling of physical quantities $\tau = t\sqrt{a/\hbar}$ and $\omega = |b|/\sqrt{\hbar a}$, the transition probability is derived from the equation for the population inversion $u(\tau) \equiv 2P_{|\psi_1\rangle}(\tau) - 1$ (derived from the optical Bloch equations [67]):

$$\tau u''' - u'' + 4\tau\left(\omega^2 + \tau^2\right) u' - 4\omega^2 u = 0\ . \tag{A.23}$$

The integration starts at $\tau = 0$ and the solution is propagated towards the desired – positive or negative – time. The initial conditions are found by identifying the terms in the Taylor expansion of $P_{|\psi_1\rangle}(\tau)$ around $\tau = 0$.

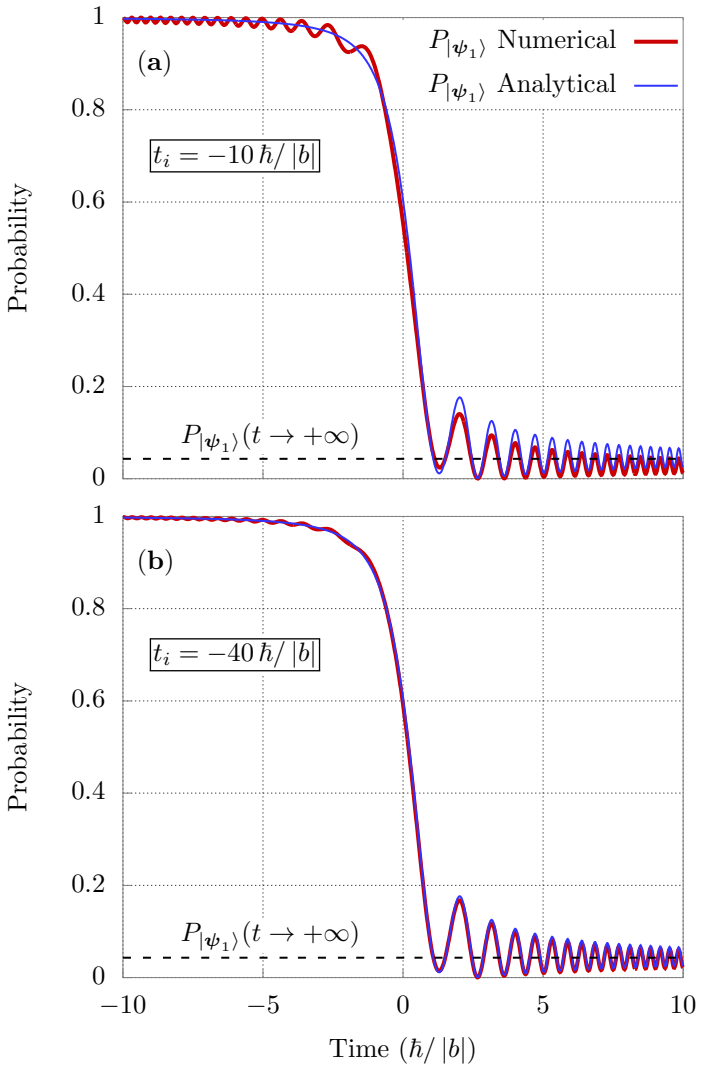

Figure A.3: Diabatic transition probability $P_{|\psi_1\rangle}$ for parameter choice $a = |b|^2/\hbar$, computed by Runge-Kutta method (red thick line) and compared with the analytical solution (blue thin line). The dashed lines represent the asymptotic value of the transition probability (Eq. A.5). The integration in (**a**) starts at $t = -10\,\hbar/\,|b|$, while in (**b**) it starts at $t = -40\,\hbar/\,|b|$. Notice the increased spurious oscillations at negative time and shifted asymptotic limit in (**a**).

Appendix B

Computation of observables

In this appendix we derive the expressions of the average density of defects ρ_{def} and average residual energy ϵ_{res} in terms of the variables λ_k.

B.1 Ordered case

The density of defects is defined as the number of adjacent spin pairs that are antiparallel per unit of length:

$$\hat{\rho}_{\text{def}} = \frac{1}{L}\sum_j \frac{1-\hat{\sigma}_j^z\hat{\sigma}_{j+1}^z}{2} \ . \tag{B.1}$$

The term $-\frac{1}{2}\sum_j \hat{\sigma}_j^z\hat{\sigma}_{j+1}^z$ coincides with the term multiplied by $\Gamma^{(1)}$ in the heat-bath Hamiltonian (Eq. 1.28), hence we can immediately write:

$$\hat{\rho}_{\text{def}} = \frac{1}{2} + \frac{1}{L}\sum_{k>0}^{\text{ABC}} \left[\sin k \left(\hat{c}_k^\dagger\hat{c}_{-k}^\dagger + \hat{c}_{-k}\hat{c}_k\right) - \cos k \left(\hat{c}_k^\dagger\hat{c}_k - \hat{c}_{-k}\hat{c}_{-k}^\dagger\right)\right] \ . \tag{B.2}$$

The average defects density is, by definition:

$$\langle\hat{\rho}_{\text{def}}\rangle = \frac{\langle\psi(t)|\hat{\rho}_{\text{def}}|\psi(t)\rangle}{\langle\psi(t)|\psi(t)\rangle} = \frac{1}{2} + \frac{1}{L}\sum_{k>0}^{\text{ABC}} \left[\sin k \left(\langle\hat{c}_k^\dagger\hat{c}_{-k}^\dagger\rangle + \langle\hat{c}_{-k}\hat{c}_k\rangle\right) - \cos k \left(\langle\hat{c}_k^\dagger\hat{c}_k\rangle - \langle\hat{c}_{-k}\hat{c}_{-k}^\dagger\rangle\right)\right] \ . \tag{B.3}$$

Let us start from the evaluation of $\langle\hat{c}_k^\dagger\hat{c}_k\rangle$. The operator $\hat{c}_k^\dagger\hat{c}_k$ affects only the k-subspace, hence we can write:

$$\begin{aligned}
\langle\psi(t)|\hat{c}_k^\dagger\hat{c}_k|\psi(t)\rangle &= \langle\psi_k(t)|\hat{c}_k^\dagger\hat{c}_k|\psi_k(t)\rangle \\
&= \frac{1}{1+|\lambda_k|^2}\ \langle 0|\left(1-\lambda_k^*\hat{c}_{-k}\hat{c}_k\right)\hat{c}_k^\dagger\hat{c}_k\left(1-\lambda_k\hat{c}_k^\dagger\hat{c}_{-k}^\dagger\right)|0\rangle \\
&= \frac{|\lambda_k|^2}{1+|\lambda_k|^2} \ ,
\end{aligned} \tag{B.4}$$

where the time dependence is embedded in λ_k. Similar calculations lead to the following relations:

$$\langle\psi_k(t)|\hat{c}_{-k}\hat{c}^{\dagger}_{-k}|\psi_k(t)\rangle = \frac{1}{1+|\lambda_k|^2}\ , \tag{B.5}$$

$$\langle\psi_k(t)|\hat{c}^{\dagger}_{k}\hat{c}^{\dagger}_{-k}|\psi_k(t)\rangle = \frac{-\mathrm{Re}\,(\lambda_\mathrm{k})}{1+|\lambda_k|^2}\ , \tag{B.6}$$

$$\langle\psi_k(t)|\hat{c}_{-k}\hat{c}_{k}|\psi_k(t)\rangle = \frac{-\mathrm{Re}\,(\lambda_\mathrm{k})}{1+|\lambda_k|^2}\ . \tag{B.7}$$

Collecting the different terms we obtain:

$$\begin{aligned}\langle\hat{\rho}_{\mathrm{def}}\rangle &= \frac{1}{2} - \frac{2}{L}\sum_{k>0}^{\mathrm{ABC}} \frac{1}{1+|\lambda_k|^2}\left(|\lambda_k|^2\cos k + \mathrm{Re}\,(\lambda_\mathrm{k})\sin\mathrm{k}\right) \\ &= \frac{2}{L}\sum_{k>0}^{\mathrm{ABC}} \frac{\left|\lambda_k \sin\left(\frac{k}{2}\right) - \cos\left(\frac{k}{2}\right)\right|^2}{1+|\lambda_k|^2}\ .\end{aligned} \tag{B.8}$$

The residual energy is given by:

$$\begin{aligned}\epsilon_{\mathrm{res}} &\equiv -J\sum_j \hat{\sigma}^z_j\hat{\sigma}^z_{j+1} + JL \\ &= 2JL\left(\frac{1}{2} - \sum_j \frac{\hat{\sigma}^z_j\hat{\sigma}^z_{j+1}}{2L}\right) \\ &= 2JL\,\langle\hat{\rho}_{\mathrm{def}}\rangle\ .\end{aligned} \tag{B.9}$$

B.2 Disordered case

In the general disordered case with *open* boundary conditions, the density of defects operator is:

$$\hat{\rho}_{\mathrm{def}} = \frac{1}{2\,(L-1)}\sum_{j=1}^{L-1}\left(1-\hat{\sigma}^z_j\hat{\sigma}^z_{j+1}\right)\ , \tag{B.10}$$

and the corresponding expectation value takes the form:

$$\begin{aligned}\rho_{\mathrm{def}} &= \langle\psi(t)|\hat{\rho}_{\mathrm{def}}|\psi(t)\rangle \\ &= \frac{1}{2\,(L-1)}\sum_{j=1}^{L-1}\left[1-\left(\langle\hat{c}^{\dagger}_j\hat{c}_{j+1}\rangle + \langle\hat{c}_{j+1}\hat{c}_j\rangle + c.\,c.\right)\right]\ ,\end{aligned} \tag{B.11}$$

where $c.\,c.$ stands for *complex conjugate*. Writing in terms of $\mathbf{G}$ and $\mathbf{F}$ we have:

$$\begin{aligned}\rho_{\mathrm{def}} &= \frac{1}{2\,(L-1)}\sum_{j=1}^{L-1}\left[1-\left(G_{j+1,j}+F_{j,j+1}+c.\,c.\right)\right] \\ &= \frac{1}{2} - \frac{1}{2\,(L-1)}\sum_{j=1}^{L-1}\left(G_{j+1,j}+F_{j,j+1}+c.\,c.\right)\ .\end{aligned} \tag{B.12}$$

Regarding the residual energy, we obtain:

$$\begin{aligned} E_{\text{res}} &= -\sum_{j=1}^{L-1} J_j \langle\psi(t)|\hat{\sigma}_j^z \hat{\sigma}_{j+1}^z|\psi(t)\rangle + \sum_{j=1}^{L-1} J_j \\ &= -\sum_{j=1}^{L-1} J_j \left(\langle \hat{c}_j^\dagger \hat{c}_{j+1}\rangle + \langle \hat{c}_{j+1}\hat{c}_j\rangle + c.\,c.\right) + \sum_{j=1}^{L-1} J_j \\ &= \sum_{j=1}^{L-1} J_j \left[1 - (G_{j+1,j} + F_{j,j+1} + c.\,c.)\right] \ . \end{aligned} \tag{B.13}$$

In case of *closed* boundary conditions (*anti-periodic*, since we are dealing with an even number of fermions) the density of defects and residual energy are modified into:

$$\rho_{\text{def}} = \frac{1}{2} - \frac{1}{2L}\left[\left(\sum_{j=1}^{L-1} G_{j+1,\,j} + F_{j,\,j+1}\right) - G_{1,\,L} - F_{L,\,1} + c.\,c.\right] \ , \tag{B.14}$$

$$E_{\text{res}} = \left(\sum_{j=1}^{L-1} J_j \left[1 - (G_{j+1,j} + F_{j,j+1} + c.\,c.)\right]\right) + J_L \left[1 + (G_{1,\,L} + F_{L,\,1} + c.\,c.)\right] \ . \tag{B.15}$$

Appendix C

The BCS-form of the ground state.

The problem we would like to solve is how to write the Bogoliubov vacuum $|\emptyset\rangle_\gamma$ in terms of the $\hat{c}_j^\dagger$ in the general non-homogeneous case, in a way that generalizes the simple BCS form we have in k-space:

$$|\emptyset\rangle_\gamma^{\mathrm{ABC}} = \prod_{k>0}^{\mathrm{ABC}} \left(u_k + v_k \hat{c}_k^\dagger \hat{c}_{-k}^\dagger\right)|0\rangle \ . \tag{C.1}$$

For that purpose, let us make the *Ansatz* that $|\emptyset\rangle_\gamma$ can be written as a Gaussian state of the form:

$$|\emptyset\rangle_\gamma = \mathcal{N}\ \mathrm{e}^{\mathcal{Z}}\ |0\rangle = \mathcal{N}\ \mathrm{e}^{\frac{1}{2}(\hat{\mathbf{c}}^\dagger)^T\cdot\mathbf{Z}\cdot(\hat{\mathbf{c}}^\dagger)}\ |0\rangle = \mathcal{N}\ \exp\left(\frac{1}{2}\sum_{j_1 j_2} Z_{j_1 j_2}\hat{c}_{j_1}^\dagger \hat{c}_{j_2}^\dagger\right)|0\rangle \ , \tag{C.2}$$

where $\mathcal{Z}$ will be our shorthand notation for the quadratic fermion form we exponentiate. Clearly, since $\hat{c}_{j_1}^\dagger \hat{c}_{j_2}^\dagger = -\hat{c}_{j_2}^\dagger \hat{c}_{j_1}^\dagger$ we can take the matrix $\mathbf{Z}$ to be *antisymmetric* (but complex, in general): any symmetric part of $\mathbf{Z}$ would give 0 contribution. The conditions that $\mathbf{Z}$ has to satisfy should be inferred from the fact that we pretend that, $\forall\mu$, we must have $\hat{\gamma}_\mu|\emptyset\rangle_\gamma = 0$, which read:

$$\mathcal{N}\sum_{j=1}^{L}\left(U_{j\mu}^*\hat{c}_j + V_{j\mu}^*\hat{c}_j^\dagger\right)\mathrm{e}^{\mathcal{Z}}\ |0\rangle = 0 \qquad \forall\mu \ . \tag{C.3}$$

Since $\mathcal{Z}$ is made of *pairs* of $\hat{c}^\dagger$s, it commutes with $\hat{c}_j^\dagger$, hence, $\hat{c}_j^\dagger \mathrm{e}^{\mathcal{Z}}|0\rangle = \mathrm{e}^{\mathcal{Z}}\hat{c}_j^\dagger|0\rangle$. The first term, containing $\hat{c}_j \mathrm{e}^{\mathcal{Z}}|0\rangle$, is more problematic. We would like to commute $\hat{c}_j$ through $\mathrm{e}^{\mathcal{Z}}$ to bring it towards the $|0\rangle$, where it annihilates. To do so, let us start calculating:

$$\left[\hat{c}_j, \mathcal{Z}\right] = \frac{1}{2}\left[\hat{c}_j, \sum_{j_1 j_2} Z_{j_1 j_2}\hat{c}_{j_1}^\dagger \hat{c}_{j_2}^\dagger\right] = \sum_{j'} Z_{jj'}\hat{c}_{j'}^\dagger \ , \tag{C.4}$$

where we have used the antisymmetry of $\mathbf{Z}$. We see, therefore, that $[\hat{c}_j, \mathcal{Z}]$, being a combination of $\hat{c}^\dagger_{j'}$ commutes with $\mathcal{Z}$ and with any function of $\mathcal{Z}$. It takes then little algebra [1] to show that:

$$\left[\hat{c}_j, \mathrm{e}^{\mathcal{Z}}\right] = \left[\hat{c}_j, \mathcal{Z}\right] \mathrm{e}^{\mathcal{Z}} = \mathrm{e}^{\mathcal{Z}} \left[\hat{c}_j, \mathcal{Z}\right] \quad \Rightarrow \quad \hat{c}_j \mathrm{e}^{\mathcal{Z}} = \mathrm{e}^{\mathcal{Z}} \left(\hat{c}_j + [\hat{c}_j, \mathcal{Z}]\right) . \tag{C.5}$$

The conditions in Eq. (C.3) therefore read:

$$\mathcal{N}\, \mathrm{e}^{\mathcal{Z}} \sum_{j=1}^{L} \left[U^*_{j\mu}\Big(\hat{c}_j + [\hat{c}_j, \mathcal{Z}]\Big) + V^*_{j\mu}\hat{c}^\dagger_j\right] |0\rangle = 0 \qquad \forall \mu \, . \tag{C.6}$$

Noticing that $\hat{c}_j|0\rangle = 0$, substituting Eq. (C.4), and omitting irrelevant prefactors we therefore have:

$$\Big[\sum_{jj'} U^*_{j'\mu} Z_{j'j} \hat{c}^\dagger_j + \sum_j V^*_{j\mu}\hat{c}^\dagger_j\Big] |0\rangle = 0 \qquad \forall \mu \, , \tag{C.7}$$

where we have exchanged the dummy indices j and j' in the first term. Next, we collect the two terms by writing:

$$\sum_j \Big[(\mathbf{U}^\dagger \cdot \mathbf{Z})_{\mu j} + (\mathbf{V}^\dagger)_{\mu j}\Big] \hat{c}^\dagger_j |0\rangle = 0 \quad \Rightarrow \quad \mathbf{Z} = -(\mathbf{U}^\dagger)^{-1} \cdot \mathbf{V}^\dagger \, . \tag{C.8}$$

This is the condition that $\mathbf{Z}$ has to verify in order for the state $|\emptyset\rangle_\gamma$ to be annihilated by all $\hat{\gamma}_\mu$. This is the so-called *Thouless formula*. Observe that such a form of $\mathbf{Z}$ is *antisymmetric*:

$$\mathbf{Z}^T = -(\mathbf{V}^\dagger)^T \cdot \big[(\mathbf{U}^\dagger)^{-1}\big]^T = -\mathbf{V}^* \cdot \big[(\mathbf{U}^\dagger)^T\big]^{-1} = -\mathbf{V}^* \cdot (\mathbf{U}^*)^{-1} \, . \tag{C.9}$$

[1] Simply expand the exponential in the usual way, realize that

$$[\hat{c}_j, \mathcal{Z}^n] = n\, [\hat{c}_j, \mathcal{Z}]\, \mathcal{Z}^{n-1} \, ,$$

because $[\hat{c}_j, \mathcal{Z}]$ commutes with all powers of $\mathcal{Z}$, and reconstruct the exponential to get the result.

Appendix D

Derivation of the Green's functions

The physics of a system described by a BCS state is totally encoded in the antisymmetric matrix $\mathbf{Z}$. We now show how to calculate the observables of the system from $\mathbf{Z}$. First we note that any antisymmetric matrix can always be reduced to a standard "canonical block form" [68] by applying a unitary matrix $\mathbf{D}$ as follows:

$$\mathbf{Z} = \mathbf{D}\mathbf{\Lambda}\mathbf{D}^T \tag{D.1}$$

$$\text{with} \qquad \mathbf{\Lambda} = \left[\begin{array}{cc|cc|c} 0 & \lambda_1 & 0 & 0 & \cdots \\ -\lambda_1 & 0 & 0 & 0 & \cdots \\ \hline 0 & 0 & 0 & \lambda_2 & \cdots \\ 0 & 0 & -\lambda_2 & 0 & \cdots \\ \hline \vdots & \vdots & \vdots & \vdots & \vdots \end{array}\right]_{L\times L} . \tag{D.2}$$

The λ_p are in general complex, but it is always possible to reabsorb their phase-factor by a "canonical transformation", i.e., we can deliver the phase to the unitary matrix $\mathbf{D}$. If L is even, there are $\frac{L}{2}$ blocks 2×2 with some λ_p, while if L is odd, Λ has an extra row/column of zeroes. The matrix $\mathbf{D}$ allows us to define combinations of the fermions $c_j^\dagger$ which form natural "BCS-paired" orbitals,

$$\hat{d}_p^\dagger = \sum_j [\mathbf{D}^T]_{pj}\hat{c}_j^\dagger = \sum_j D_{jp}\hat{c}_j^\dagger \, . \tag{D.3}$$

Labelling the consecutive columns of $\mathbf{D}$ as 1, $\overline{1}$, 2, $\overline{2}$, $\cdots$, p, $\overline{p}$, $\cdots$, with p up to $L/2$, one can readily check that in terms of the $d^\dagger$s the BCS state reads:

$$|\psi\rangle = \mathcal{N}\ \exp\Big(\frac{1}{2}\sum_{pp'}^{L}\Lambda_{pp'}\hat{d}_p^\dagger\hat{d}_{p'}^\dagger\Big)\,|0\rangle = \mathcal{N}\ \exp\Big(\sum_{p=1}^{L/2}\lambda_p\hat{d}_p^\dagger\hat{d}_{\overline{p}}^\dagger\Big)\,|0\rangle = \mathcal{N}\ \prod_{p=1}^{L/2}\Big(1+\lambda_p\hat{d}_p^\dagger\hat{d}_{\overline{p}}^\dagger\Big)\,|0\rangle \, . \tag{D.4}$$

The requirement of a normalized state $|\psi\rangle$ defines the value of $\mathcal{N}$:

$$1 = \langle\psi|\psi\rangle = |\mathcal{N}|^2 \langle 0| \prod_{p=1}^{L/2} \left(1 + \lambda_p^* \hat{d}_{\overline{p}} \hat{d}_p\right) \left(1 + \lambda_p \hat{d}_p^\dagger \hat{d}_{\overline{p}}^\dagger\right) |0\rangle = |\mathcal{N}|^2 \prod_{p=1}^{L/2} \left(1 + |\lambda_p|^2\right) \tag{D.5}$$

$$\Rightarrow |\mathcal{N}| = \Big[\prod_{p=1}^{L/2} \left(1 + |\lambda_p|^2\right) \Big]^{-1/2} . \tag{D.6}$$

The calculation of the observables of the system reduces to the evaluation of the following Green's functions:

$$[\mathbf{G}(t)]_{j'j} = G_{j'j}(t) \equiv \langle\psi(t)|\hat{c}_j^\dagger \hat{c}_{j'}|\psi(t)\rangle \tag{D.7}$$

$$[\mathbf{F}(t)]_{j'j} = F_{j'j}(t) \equiv \langle\psi(t)|\hat{c}_j \hat{c}_{j'}|\psi(t)\rangle . \tag{D.8}$$

We can express $\hat{c}_j$ and $\hat{c}_j^\dagger$ in terms of the new fermionic operators $\hat{d}_j$ and $\hat{d}_j^\dagger$:

$$\hat{c}_j^\dagger = \sum_p D_{jp}^* \hat{d}_p^\dagger \qquad \text{and} \qquad \hat{c}_j = \sum_p D_{jp} \hat{d}_p ,$$

leading to

$$G_{j'j}(t) = \sum_{p,p'} [\mathbf{D}]_{j'p'} [\mathbf{D}^*]_{jp} \langle\psi(t)|\hat{d}_p^\dagger \hat{d}_{p'}|\psi(t)\rangle \tag{D.9}$$

$$F_{j'j}(t) = \sum_{p,p'} [\mathbf{D}]_{j'p'} [\mathbf{D}]_{jp} \langle\psi(t)|\hat{d}_p \hat{d}_{p'}|\psi(t)\rangle . \tag{D.10}$$

The relevant expectation values take the form:

$$\langle\psi(t)|\hat{d}_p^\dagger \hat{d}_{p'}|\psi(t)\rangle = \left([\mathbf{1} + \mathbf{\Lambda}\mathbf{\Lambda}^\dagger]^{-1}\right)_{p'p'} [\mathbf{\Lambda}\mathbf{\Lambda}^\dagger]_{p'p} , \tag{D.11}$$

$$\langle\psi(t)|\hat{d}_p \hat{d}_{p'}|\psi(t)\rangle = \left([\mathbf{1} + \mathbf{\Lambda}\mathbf{\Lambda}^\dagger]^{-1}\right)_{p'p'} [\mathbf{\Lambda}]_{p'p} . \tag{D.12}$$

The Green's function rewritten in terms of $\mathbf{D}$ and $\mathbf{\Lambda}$ are

$$G_{j'j}(t) = \left[\mathbf{D}(\mathbf{1} + \mathbf{\Lambda}\mathbf{\Lambda}^\dagger)^{-1} \mathbf{\Lambda}\mathbf{\Lambda}^\dagger \mathbf{D}^\dagger\right]_{j'j} \tag{D.13}$$

$$F_{j'j}(t) = \left[\mathbf{D}(\mathbf{1} + \mathbf{\Lambda}\mathbf{\Lambda}^\dagger)^{-1} \mathbf{\Lambda}\mathbf{D}^T\right]_{j'j} . \tag{D.14}$$

The last step is to rewrite $\mathbf{G}$ and $\mathbf{F}$ in terms of $\mathbf{Z}$. In order to do this, note that if $f(\cdot)$ is any operator function that can be Taylor expanded, then $f(\mathbf{Z}\mathbf{Z}^\dagger) = \mathbf{D} f(\mathbf{\Lambda}\mathbf{\Lambda}^\dagger)\mathbf{D}^\dagger$. From this we can finally express $\mathbf{G}$ and $\mathbf{F}$ in terms of $\mathbf{Z}$:

$$\mathbf{G} = \mathbf{D}(\mathbf{1} + \mathbf{\Lambda}\mathbf{\Lambda}^\dagger)^{-1} \mathbf{D}^\dagger \mathbf{D}\mathbf{\Lambda}\mathbf{\Lambda}^\dagger \mathbf{D}^\dagger = (\mathbf{1} + \mathbf{Z}\mathbf{Z}^\dagger)^{-1} \mathbf{Z}\mathbf{Z}^\dagger , \tag{D.15}$$

$$\mathbf{F} = \mathbf{D}(\mathbf{1} + \mathbf{\Lambda}\mathbf{\Lambda}^\dagger)^{-1} \mathbf{D}^\dagger \mathbf{D}\mathbf{\Lambda}\mathbf{D}^T = (\mathbf{1} + \mathbf{Z}\mathbf{Z}^\dagger)^{-1} \mathbf{Z} . \tag{D.16}$$

Appendix E

Quantum master equation

Here we present a derivation of the quantum Master equation (QME), closely following the treatment of Gaspard and Nagaoka [69], except for a generalization to the time-dependent case.

Imagine that our system, $\mathcal{A}$, governed by a quantum Hamiltonian $\hat{H}_A(t)$ and with associated Hilbert space $\mathcal{H}_A$ is in contact with a thermal bath $\mathcal{B}$, whose Hamiltonian is $\hat{H}_B$ and the corresponding Hilbert space $\mathcal{H}_B$. For later use, we denote by $\{|\Phi_b\rangle\}$ an orthonormal basis of $\mathcal{H}_B$ — which we take to be the basis of the eigenstates of $\hat{H}_B$ with eigenvalues E_b —, while $\{|\phi_a\rangle\}$ is an orthonormal basis set of $\mathcal{H}_A$, which we need not to specify further. Notice that b typically runs over the very large set of quantum numbers of the bath, while a might run over a (small) finite-dimensional Hilbert space. The Hamiltonian of the combined *system plus bath* is written as:

$$\hat{H}(t) = \hat{H}_A(t) + \hat{H}_B + \hat{V} \ , \tag{E.1}$$

where $\hat{V}$ describes the interation between the system and the bath, which we can imagine to be of the general form

$$\hat{V} = \lambda \sum_\nu \hat{A}_\nu \hat{B}_\nu \ ,$$

$\hat{A}_\nu$ and $\hat{B}_\nu$ being suitable system and bath operators, which can be taken to be Hermitean, [1] and λ a coupling constant that will help in keeping track of the order of the perturbative expansion in later developments. A few comments: we have considered a general situation in which $\hat{H}_A(t)$

[1] If they are not, simply define the four Hermitean combinations

$$\begin{aligned} \hat{A}'_\nu &= \frac{1}{\sqrt{2}}\left(\hat{A}_\nu + \hat{A}^\dagger_\nu\right) \quad \text{and} \quad \hat{A}''_\nu = +\frac{i}{\sqrt{2}}\left(\hat{A}_\nu - \hat{A}^\dagger_\nu\right) \\ \hat{B}'_\nu &= \frac{1}{\sqrt{2}}\left(\hat{B}_\nu + \hat{B}^\dagger_\nu\right) \quad \text{and} \quad \hat{B}''_\nu = -\frac{i}{\sqrt{2}}\left(\hat{B}_\nu - \hat{B}^\dagger_\nu\right) \end{aligned}$$

and the interaction term will simply read:

$$\hat{V} = \lambda \sum_\nu \left(\hat{A}_\nu \hat{B}_\nu + \hat{A}^\dagger_\nu \hat{B}^\dagger_\nu\right) = \lambda \sum_\nu \left(\hat{A}'_\nu \hat{B}'_\nu + \hat{A}''_\nu \hat{B}''_\nu\right) .$$

depends on time, because we have in mind situations in which the system $\mathcal{A}$ is *driven* by some external perturbation. Obviously, nowhere else we have described the Hamiltonian that produces such external driving field. Next, we will always assume that the $\hat{B}_\nu$ have *vanishing diagonal matrix element* on every bath state $|\Phi_b\rangle$, i.e.,

$$\langle\Phi_b|\hat{B}_\nu|\Phi_b\rangle = 0 \; . \tag{E.2}$$

This is certainly appropriate when the $\hat{B}_\nu$ operators are "position operators" of the bath harmonic oscillator, but might otherwise seem a loss of generality: in the end is not really so, but these terms certainly are at the origin of *shifts* of the system energy levels; for instance, the well known *Lamb shift* of atomic physics between $2p$ and $2s$ hydrogen levels is, in the end, due to such effects.

The *interaction* representation is defined in terms of the "non-interacting" Hamiltonian $\hat{H}_0(t) = \hat{H}_A(t) + \hat{H}_B$. The corresponding evolution operator is

$$\hat{U}_0(t,0) = \mathrm{Texp}\left(-\frac{i}{\hbar}\int_0^t dt' \; \hat{H}_0(t')\right) = \hat{U}_{0A}(t,0) \otimes \hat{U}_{0B}(t,0) \; ,$$

since bath and system operators commute. A density matrix $\hat{\rho}(t) = \sum_\mu p_\mu |\Psi_\mu(t)\rangle\langle\Psi_\mu(t)|$ of the whole system obeys the full Liouville-van Neumann equation

$$\frac{d}{dt}\hat{\rho}(t) = \frac{1}{i\hbar}\left[\hat{H}(t), \hat{\rho}(t)\right] = \hat{\mathcal{L}}(t) \circ \hat{\rho}(t) \tag{E.3}$$

where $\hat{\mathcal{L}}(t)$ denotes the so-called *Liouvillian super-operator*: super-operator means that it is an operator that acts on operators, like $\hat{\rho}(t)$, rather then on states of the Hilbert space; in this case by simply taking the commutator with the Hamiltonian: $\hat{\mathcal{L}}(t) \circ \hat{O} \stackrel{def}{=} \frac{1}{i\hbar}\left[\hat{H}(t), \hat{O}\right]$. We observe that when $\hat{H}$ does not depend on time, then $\hat{\mathcal{L}}$ also does not depend on time and we can write, at least formally, a solution of the Liouville-van Neumann equation in the form: $\hat{\rho}(t) = \mathrm{e}^{\hat{\mathcal{L}}t} \circ \hat{\rho}(0)$. In the time-dependent case, we do not even write the equivalent form, although in principle possible.

As it is often the case, it is useful to switch to the interaction representation for $\hat{\rho}(t)$ by defining:

$$\hat{\rho}_I(t) = \hat{U}_0^\dagger(t,0)\hat{\rho}(t)\hat{U}_0(t,0) \; ,$$

which obeys a Liouville-van Neumann equation of the form:

$$\frac{d}{dt}\hat{\rho}_I(t) = \frac{1}{i\hbar}\left[\hat{V}_I(t), \hat{\rho}_I(t)\right] \; , \tag{E.4}$$

where $\hat{V}_I(t) = \hat{U}_0^\dagger \hat{V} \hat{U}_0$ is the system-bath Hamiltonian in interaction representation:

$$\hat{V}_I(t) = \lambda \sum_\nu \hat{A}_{\nu I}(t)\hat{B}_{\nu I}(t) \; .$$

Integrating Eq. (E.4) in the interval $(t, t+\Delta t)$ we have:

$$\hat{\rho}_I(t+\Delta t) = \hat{\rho}_I(t) + \frac{1}{i\hbar}\int_t^{t+\Delta t} dt_1 \left[\hat{V}_I(t_1), \hat{\rho}_I(t_1)\right] \; .$$

Iterating, we get:

$$\hat{\rho}_I(t+\Delta t) = \hat{\rho}_I(t) \quad + \quad \frac{1}{i\hbar}\int_t^{t+\Delta t} dt_1 \left[\hat{V}_I(t_1), \hat{\rho}_I(t)\right] \\ + \quad \frac{1}{(i\hbar)^2}\int_t^{t+\Delta t} dt_1 \int_t^{t_1} dt_2 \Big[\hat{V}_I(t_1), \Big[\hat{V}_I(t_2), \hat{\rho}_I(t_2)\Big]\Big] \ . \tag{E.5}$$

So far, everything is exact. To proceed further we have to make approximations, motivated by some assumptions regarding the bath and the initial conditions, which we now discuss.

E.0.1 Assumptions regarding the Bath

Consider the bath density matrix, obtained by partial trace over the system $\mathcal{A}$ Hilbert-space: $\hat{\rho}_B = \mathrm{Tr}_A\, \hat{\rho}$. A crucial assumption is that the system *perturbs very little the bath*, which we imagine to be very large, as a thermostat should be, so that the density matrix of the bath is simply the one we would have in absence of $\hat{H}_A$, i.e.,

$$\hat{\rho}_{BI}(t) = \mathrm{Tr}_A\, \hat{\rho}_I(t) \approx \hat{\rho}_B = \sum_b p_b |\Phi_b\rangle\langle\Phi_b| \ ,$$

where $p_b = e^{-E_b/k_B T}/Z$ is the Boltzmann factor, while E_b and $|\Phi_b\rangle$ are eigenvalues and eigenstates of $\hat{H}_B$. We assume that the first-order effect of $\hat{B}$ is zero:

$$\mathrm{Tr}_B[\hat{\rho}_B \hat{B}_{\nu I}(t)] = 0 \ . \tag{E.6}$$

This assumption is not crucial at all, and we might even relax it. But we notice that there is no real loss of generality in doing so, as we have discussed before, because such terms amount to rather innocuous *shifts* of the unperturbed energy levels.

Concerning the initial condition, it is reasonable to assume that the system and bath come into contact at $t = 0$ so that the initial density matrix is factorized at $t = 0$:

$$\hat{\rho}(0) = \hat{\rho}_A(0) \otimes \hat{\rho}_B \ . \tag{E.7}$$

The final ingredients we will need are the bath correlation functions:

$$C_{\nu\nu'}(t,t') = \mathrm{Tr}_B[\rho_B \hat{B}_{\nu I}(t)\hat{B}_{\nu' I}(t')] = C_{\nu\nu'}(t-t') = C_{\nu\nu'}(\tau) \ , \tag{E.8}$$

where $\tau = t - t'$ and we have used time-translation invariance for the bath. The evaluation of $C_{\nu\nu'}(\tau)$ requires in principle:

$$C_{\nu\nu'}(\tau) = \mathrm{Tr}_B[\hat{\rho}_B \hat{B}_{\nu I}(\tau)\hat{B}_{\nu' I}(0)] = \sum_{bb'} p_b (\hat{B}_\nu)_{bb'} (\hat{B}_{\nu'})_{b'b} e^{i\omega_{bb'}\tau} \ , \tag{E.9}$$

where $(\hat{B}_\nu)_{bb'} = \langle\Psi_b|\hat{B}_\nu|\Phi_{b'}\rangle$ and $\hbar\omega_{bb'} = (E_b - E_{b'})$. Notice that $C^*_{\nu\nu'}(\tau) = C_{\nu'\nu}(-\tau)$ if the bath operators are Hermitean, $\hat{B}_\nu = \hat{B}^\dagger_\nu$, as we have assumed. An explicit calculation can be

carried out if some assumptions concerning the bath Hamiltonian $\hat{H}_B$ and the explicit form of the operators $\hat{B}_\nu$ are made: for instance, one often assumes that $\hat{H}_B$ is a collection of harmonic oscillators,

$$\hat{H}_B = \sum_\nu \sum_k \omega_{k\nu} \left(\hat{b}^\dagger_{k\nu} \hat{b}_{k\nu} + \frac{1}{2} \right) , \tag{E.10}$$

(perfectly legitimate to describe, for instance, the electromagnetic radiation field), and that $\hat{B}_\nu$ is essentially an appropriate linear combination of the "position operators" of the ν-th Harmonic bath $\hat{b}_{k\nu} + \hat{b}^\dagger_{k\nu}$:

$$\hat{B}_\nu = \sum_k \lambda_{k\nu} \left(\hat{b}_{k\nu} + \hat{b}^\dagger_{k\nu} \right) \tag{E.11}$$

We will further assume that $C_{\nu\nu'}(\tau)$ tends rapidly to 0 for $\tau >> \tau_B$, where τ_B is a characteristic small time-scale of the fluctuations of the bath. Notice that, strictly speaking, the harmonic bath case fails this test, as the correlation functions decay only as power laws for large τ.

E.0.2 A perturbative derivation of the quantum Master equation.

We now proceed with the perturbative derivation of the QME, following Ref. [69]. We first write a perturbative expansion in λ, by writing Eq. (E.5) in the interval $(0, t)$ (i.e., taking $t = 0$ and $\Delta t \to t$), but approximating $\hat{\rho}_I(t_2) \to \hat{\rho}_I(0)$ in the second term:

$$\begin{aligned} \hat{\rho}_I(t) = \hat{\rho}_I(0) \quad &+ \quad \frac{1}{i\hbar} \int_0^t dt_1 \left[\hat{V}_I(t_1), \hat{\rho}_I(0) \right] \\ &+ \quad \frac{1}{(i\hbar)^2} \int_0^t dt_1 \int_0^{t_1} dt_2 \Big[\hat{V}_I(t_1), \Big[\hat{V}_I(t_2), \hat{\rho}_I(0) \Big] \Big] + O(\lambda^3) . \end{aligned} \tag{E.12}$$

Starting from Eq. (E.12) we take a partial trace over the bath B to get an equation for the system A only:

$$\hat{\rho}_{AI}(t) = \hat{\rho}_A(0) - \frac{1}{\hbar^2} \int_0^t dt_1 \int_0^{t_1} dt_2 \, \mathrm{Tr}_B \left[\hat{V}_I(t_1), \Big[\hat{V}_I(t_2), \hat{\rho}_I(0) \Big] \right] + O(\lambda^3) , \tag{E.13}$$

where we have dropped the first-order term in view of Eq. (E.6). Taking the derivative with respect to t and explicitly evaluating the trace over the bath we get:

$$\begin{aligned} \frac{d}{dt} \hat{\rho}_{AI}(t) &= -\frac{1}{\hbar^2} \int_0^t dt_2 \, \mathrm{Tr}_B \left[\hat{V}_I(t), \Big[\hat{V}_I(t_2), \hat{\rho}_I(0) \Big] \right] + O(\lambda^3) \\ &= -\frac{\lambda^2}{\hbar^2} \sum_{\nu_1} \Big\{ \Big[\hat{A}_{\nu_1 I}(t), \hat{S}_{\nu_1 I}(t) \hat{\rho}_A(0) \Big] + \mathrm{H.c} \Big\} + O(\lambda^3) \end{aligned} \tag{E.14}$$

where we have defined the convoluted and integrated system operators:

$$\hat{S}_{\nu_1 I}(t) \stackrel{def}{=} \sum_{\nu_2} \int_0^t dt_2 \, C_{\nu_1 \nu_2}(t - t_2) \, \hat{A}_{\nu_2 I}(t_2) . \tag{E.15}$$

Now switch to the Schrödinger representation, recalling that $\hat{\rho}_A(t) = \hat{U}_0(t,0)\hat{\rho}_{AI}(t)\hat{U}_0^\dagger(t,0)$. The equation for $\hat{\rho}_A(t)$ will read:

$$\frac{d}{dt}\hat{\rho}_A(t) = \frac{1}{i\hbar}\left[\hat{H}_A(t), \hat{\rho}_A(t)\right] - \frac{\lambda^2}{\hbar^2}\sum_{\nu_1}\left\{\left[\hat{A}_{\nu_1}, \hat{S}_{\nu_1}(t)\hat{\rho}_A^0(t)\right] + \text{H.c}\right\} + O(\lambda^3) \tag{E.16}$$

where we have introduced the unperturbed propagation of the density matrix $\hat{\rho}_A^0(t) = \hat{U}_0(t,0)\hat{\rho}_A(0)\hat{U}_0^\dagger(t,0)$, and the Schrödinger representation of the operator $\hat{S}_{\nu_1 I}(t)$:

$$\hat{S}_{\nu_1}(t) \stackrel{def}{=} \hat{U}_0(t,0)\hat{S}_{\nu_1 I}(t)\hat{U}_0^\dagger(t,0) = \sum_{\nu_2}\int_0^t dt_2\; C_{\nu_1\nu_2}(t-t_2)\;\hat{U}_0(t,t_2)\hat{A}_{\nu_2}\hat{U}_0^\dagger(t,t_2)\;. \tag{E.17}$$

The first term describes the unperturbed evolution of $\hat{\rho}_A(t)$: without the λ^2 term, it would be solved by $\hat{\rho}_A^0(t) = \hat{U}_0(t,0)\hat{\rho}_A(0)\hat{U}_0^\dagger(t,0)$. Hence, up to terms of order $O(\lambda^3)$ we can effectively substitute $\hat{\rho}_A^0(t) \to \hat{\rho}_A(t)$ in the second term, obtaining the final form:

$$\frac{d}{dt}\hat{\rho}_A(t) = \frac{1}{i\hbar}\left[\hat{H}_A(t), \hat{\rho}_A(t)\right] - \frac{\lambda^2}{\hbar^2}\sum_{\nu_1}\left\{\left[\hat{A}_{\nu_1}, \hat{S}_{\nu_1}(t)\hat{\rho}_A(t)\right] + \text{H.c}\right\} + O(\lambda^3)\;. \tag{E.18}$$

Bibliography

[1] Clarence Zener. Non-adiabatic crossing of energy levels. *Proceedings of the Royal Society of London A: Mathematical, Physical and Engineering Sciences*, 137(833):696–702, 1932.

[2] Lev D Landau. Zur theorie der energieubertragung. II. *Phys. Z. Sowjetunion*, 2(46):1–13, 1932.

[3] Andrew Lucas. Ising formulations of many NP problems. *Frontiers in Physics*, 2, 2014.

[4] A.B. Finnila, M.A. Gomez, C. Sebenik, C. Stenson, and J.D. Doll. Quantum annealing: A new method for minimizing multidimensional functions. *Chemical Physics Letters*, 219(5-6):343–348, mar 1994.

[5] Tadashi Kadowaki and Hidetoshi Nishimori. Quantum annealing in the transverse ising model. *Physical Review E*, 58(5):5355–5363, nov 1998.

[6] J. Brooke. Quantum annealing of a disordered magnet. *Science*, 284(5415):779–781, apr 1999.

[7] Giuseppe E Santoro, Roman Martoňák, Erio Tosatti, and Roberto Car. Theory of quantum annealing of an ising spin glass. *Science*, 295(5564):2427–2430, 2002.

[8] R. Harris, M. W. Johnson, T. Lanting, A. J. Berkley, J. Johansson, P. Bunyk, E. Tolkacheva, E. Ladizinsky, N. Ladizinsky, T. Oh, F. Cioata, I. Perminov, P. Spear, C. Enderud, C. Rich, S. Uchaikin, M. C. Thom, E. M. Chapple, J. Wang, B. Wilson, M. H. S. Amin, N. Dickson, K. Karimi, B. Macready, C. J. S. Truncik, and G. Rose. Experimental investigation of an eight-qubit unit cell in a superconducting optimization processor. *Physical Review B*, 82(2), jul 2010.

[9] M. W. Johnson, M. H. S. Amin, S. Gildert, T. Lanting, F. Hamze, N. Dickson, R. Harris, A. J. Berkley, J. Johansson, P. Bunyk, E. M. Chapple, C. Enderud, J. P. Hilton, K. Karimi, E. Ladizinsky, N. Ladizinsky, T. Oh, I. Perminov, C. Rich, M. C. Thom, E. Tolkacheva, C. J. S. Truncik, S. Uchaikin, J. Wang, B. Wilson, and G. Rose. Quantum annealing with manufactured spins. *Nature*, 473(7346):194–198, may 2011.

[10] Giuseppe E Santoro and Erio Tosatti. Optimization using quantum mechanics: quantum annealing through adiabatic evolution. *Journal of Physics A: Mathematical and General*, 39(36):R393–R431, aug 2006.

[11] Arnab Das and Bikas K. Chakrabarti. Colloquium: Quantum annealing and analog quantum computation. *Reviews of Modern Physics*, 80(3):1061–1081, sep 2008.

[12] Amit Dutta, Gabriel Aeppli, Bikas K Chakrabarti, Uma Divakaran, Thomas F Rosenbaum, and Diptiman Sen. *Quantum Phase Transitions in Transverse Field Spin Models: From Statistical Physics to Quantum Information*. Cambridge University Press, 2015.

[13] S. Suzuki. Performance of quantum annealing in solving optimization problems: A review. *The European Physical Journal Special Topics*, 224(1):51–61, feb 2015.

[14] Sergio Boixo, Troels F. Rønnow, Sergei V. Isakov, Zhihui Wang, David Wecker, Daniel A. Lidar, John M. Martinis, and Matthias Troyer. Evidence for quantum annealing with more than one hundred qubits. *Nature Physics*, 10(3):218–224, feb 2014.

[15] T. Lanting, A. J. Przybysz, A. Yu. Smirnov, F. M. Spedalieri, M. H. Amin, A. J. Berkley, R. Harris, F. Altomare, S. Boixo, P. Bunyk, N. Dickson, C. Enderud, J. P. Hilton, E. Hoskinson, M. W. Johnson, E. Ladizinsky, N. Ladizinsky, R. Neufeld, T. Oh, I. Perminov, C. Rich, M. C. Thom, E. Tolkacheva, S. Uchaikin, A. B. Wilson, and G. Rose. Entanglement in a quantum annealing processor. *Physical Review X*, 4(2), may 2014.

[16] Sergio Boixo, Vadim N. Smelyanskiy, Alireza Shabani, Sergei V. Isakov, Mark Dykman, Vasil S. Denchev, Mohammad H. Amin, Anatoly Yu Smirnov, Masoud Mohseni, and Hartmut Neven. Computational multiqubit tunnelling in programmable quantum annealers. *Nature Communications*, 7:10327, jan 2016.

[17] KS Kirkpatrick, CD Gelatt, and MP Vecchi. Science 220 671 kirkpatrick ks 1984. *J. Stat. Phys*, 34:975, 1983.

[18] Victor Bapst, Laura Foini, Florent Krzakala, Guilhem Semerjian, and Francesco Zamponi. The quantum adiabatic algorithm applied to random optimization problems: The quantum spin glass perspective. *Physics Reports*, 523(3):127–205, 2013.

[19] Helmut G Katzgraber, Firas Hamze, and Ruben S Andrist. Glassy chimeras could be blind to quantum speedup: Designing better benchmarks for quantum annealing machines. *Physical Review X*, 4(2):021008, 2014.

[20] Sergey Knysh. Computational bottlenecks of quantum annealing. *arXiv preprint arXiv:1506.08608*, 2015.

[21] Demian A Battaglia, Giuseppe E Santoro, and Erio Tosatti. Optimization by quantum annealing: Lessons from hard satisfiability problems. *Physical Review E*, 71(6):066707, 2005.

[22] Roman Martoňák, Giuseppe E Santoro, and Erio Tosatti. Quantum annealing by the path-integral monte carlo method: The two-dimensional random ising model. *Physical Review B*, 66(9):094203, 2002.

[23] Roman Martoňák, Giuseppe E Santoro, and Erio Tosatti. Quantum annealing of the traveling-salesman problem. *Physical Review E*, 70(5):057701, 2004.

[24] Lorenzo Stella, Giuseppe E Santoro, and Erio Tosatti. Monte carlo studies of quantum and classical annealing on a double well. *Physical Review B*, 73(14):144302, 2006.

[25] Bettina Heim, Troels F Rønnow, Sergei V Isakov, and Matthias Troyer. Quantum versus classical annealing of ising spin glasses. *Science*, 348(6231):215–217, 2015.

[26] Florian R. Krajewski and Martin H. Müser. Quantum creep and quantum-creep transitions in 1d sine-gordon chains. *Phys. Rev. Lett.*, 92:030601, Jan 2004.

[27] Florian R. Krajewski and Martin H. Müser. Quantum dynamics in the highly discrete, commensurate frenkel kontorova model: A path-integral molecular dynamics study. *The Journal of Chemical Physics*, 122:124711, 2005.

[28] A. I. Volokitin and B. N. J. Persson. Quantum friction. *Phys. Rev. Lett.*, 106:094502, Mar 2011.

[29] Immanuel Bloch, Jean Dalibard, and Sylvain Nascimbene. Quantum simulations with ultracold quantum gases. *Nat Phys*, 8(4):267–276, 04 2012.

[30] Leon Karpa, Alexei Bylinskii, Dorian Gangloff, Marko Cetina, and Vladan Vuletić. Suppression of ion transport due to long-lived subwavelength localization by an optical lattice. *Phys. Rev. Lett.*, 111:163002, Oct 2013.

[31] Jacek Dziarmaga. Dynamics of a quantum phase transition: Exact solution of the quantum ising model. *Physical review letters*, 95(24):245701, 2005.

[32] Wojciech H Zurek, Uwe Dorner, and Peter Zoller. Dynamics of a quantum phase transition. *Physical review letters*, 95(10):105701, 2005.

[33] Jacek Dziarmaga. Dynamics of a quantum phase transition in the random ising model: logarithmic dependence of the defect density on the transition rate. *Physical Review B*, 74(6):064416, 2006.

[34] Tommaso Caneva, Rosario Fazio, and Giuseppe E Santoro. Adiabatic quantum dynamics of a random ising chain across its quantum critical point. *Physical Review B*, 76(14):144427, 2007.

[35] Tom WB Kibble. Some implications of a cosmological phase transition. *Physics Reports*, 67(1):183–199, 1980.

[36] Wojciech H Zurek. Cosmological experiments in superfluid helium? *Nature*, 317(6037):505–508, 1985.

[37] Wojciech H Zurek. Cosmological experiments in condensed matter systems. *Physics Reports*, 276(4):177–221, 1996.

[38] Anatoli Polkovnikov, Krishnendu Sengupta, Alessandro Silva, and Mukund Vengalattore. Colloquium: Nonequilibrium dynamics of closed interacting quantum systems. *Reviews of Modern Physics*, 83(3):863, 2011.

[39] Roy J Glauber. Time-dependent statistics of the ising model. *Journal of mathematical physics*, 4(2):294–307, 1963.

[40] Hidetoshi Nishimori, Junichi Tsuda, and Sergey Knysh. Comparative study of the performance of quantum annealing and simulated annealing. *Physical Review E*, 91(1):012104, 2015.

[41] NV Vitanov. Transition times in the landau-zener model. *Physical Review A*, 59(2):988, 1999.

[42] Tommaso Caneva, Rosario Fazio, and Giuseppe E Santoro. Adiabatic quantum dynamics of the lipkin-meshkov-glick model. *Physical Review B*, 78(10):104426, 2008.

[43] Lorenzo Stella, Giuseppe E Santoro, and Erio Tosatti. Optimization by quantum annealing: Lessons from simple cases. *Physical Review B*, 72(1):014303, 2005.

[44] Satoshi Morita and Hidetoshi Nishimori. Mathematical foundation of quantum annealing. *Journal of Mathematical Physics*, 49(12):125210, 2008.

[45] Claudia De Grandi, Anatoli Polkovnikov, and AW Sandvik. Universal nonequilibrium quantum dynamics in imaginary time. *Physical Review B*, 84(22):224303, 2011.

[46] Daniel S Fisher. Critical behavior of random transverse-field ising spin chains. *Physical review b*, 51(10):6411, 1995.

[47] AP Young and H Rieger. Numerical study of the random transverse-field ising spin chain. *Physical Review B*, 53(13):8486, 1996.

[48] Sei Suzuki. Cooling dynamics of pure and random ising chains. *Journal of Statistical Mechanics: Theory and Experiment*, 2009(03):P03032, 2009.

[49] David A Huse and Daniel S Fisher. Residual energies after slow cooling of disordered systems. *Physical review letters*, 57(17):2203, 1986.

[50] Matteo M Wauters, Rosario Fazio, Hidetoshi Nishimori, and Giuseppe E Santoro. Direct comparison of quantum and simulated annealing on a fully connected ising ferromagnet. *Physical Review A*, 96(2):022326, 2017.

[51] Sergei V. Isakov, Guglielmo Mazzola, Vadim N. Smelyanskiy, Zhang Jiang, Sergio Boixo, Hartmut Neven, and Matthias Troyer. Understanding quantum tunneling through quantum monte carlo simulations. *Physical Review Letters*, 117(18), oct 2016.

[52] EM Inack and S Pilati. Simulated quantum annealing of double-well and multiwell potentials. *Physical Review E*, 92(5):053304, 2015.

[53] R. P. Feynman and F. L. Vernon. The theory of a general quantum system interacting with a linear dissipative system. *Annals of Physics*, 24:118–173, 1963.

[54] U. Weiss. *Quantum dissipative systems*. World Scientific, second edition, 1999.

[55] Luca Arceci, Simone Barbarino, Rosario Fazio, and Giuseppe E. Santoro. Dissipative landau-zener problem and thermally assisted quantum annealing. *Phys. Rev. B*, 96:054301, Aug 2017.

[56] Makoto Yamaguchi, Tatsuro Yuge, and Tetsuo Ogawa. Markovian quantum master equation beyond adiabatic regime. *Phys. Rev. E*, 95:012136, Jan 2017.

[57] Ken Sekimoto. *Stochastic energetics*, volume 799. Springer, 2010.

[58] E. Gnecco, R. Bennewitz, T. Gyalog, Ch. Loppacher, M. Bammerlin, E. Meyer, and H.-J. Güntherodt. Velocity dependence of atomic friction. *Phys. Rev. Lett.*, 84:1172–1175, Feb 2000.

[59] Yi Sang, Martin Dubé, and Martin Grant. Thermal effects on atomic friction. *Phys. Rev. Lett.*, 87:174301, Oct 2001.

[60] O. K. Dudko, A. E. Filippov, J. Klafter, and M. Urbakh. Dynamic force spectroscopy: a Fokker-Planck approach. *Chemical Physics Letters*, 352:499–504, 2002.

[61] Andrea Vanossi, Nicola Manini, Michael Urbakh, Stefano Zapperi, and Erio Tosatti. Colloquium. *Rev. Mod. Phys.*, 85:529–552, Apr 2013.

[62] Alexei Bylinskii, Dorian Gangloff, and Vladan Vuletic. Tuning friction atom-by-atom in an ion-crystal simulator. *Science*, 348:1115–1118, 2015.

[63] Milton Abramowitz and Irene A Stegun. *Handbook of mathematical functions: with formulas, graphs, and mathematical tables*, volume 55. Courier Corporation, 1964.

[64] Curt Wittig. The Landau-Zener formula. *The Journal of Physical Chemistry B*, 109(17):8428–8430, 2005.

[65] NV Vitanov and BM Garraway. Landau-Zener model: Effects of finite coupling duration. *Physical Review A*, 53(6):4288, 1996.

[66] NV Vitanov and BM Garraway. Erratum: Landau-Zener model: Effects of finite coupling duration. *Physical Review A*, 54(6):5458, 1996.

[67] Bruce W Shore. The theory of coherent atomic excitation, volume 1, simple atoms and fields. *The Theory of Coherent Atomic Excitation, Volume 1, Simple Atoms and Fields, by Bruce W. Shore, pp. 774. ISBN 0-471-61398-3. Wiley-VCH, July 1990.*, page 774, 1990.

[68] Peter Ring and Peter Schuck. *The Nuclear Many-Body Problem*. Springer, 2005.

[69] Pierre Gaspard and Masataka Nagaoka. Slippage of initial conditions for the redfield master equation. *The Journal of chemical physics*, 111(13):5668–5675, 1999.